Inverse Problems and Medical Imaging

Lecture Notes

Pedro Serranho

Mathematics Section
Science and Tecnology Department
Universidade Aberta, Portugal

Original version: 2017
Last revised version: 2025

Contents

Chapter 1

Introduction

Inverse Problems are present in several fields of Science, namely in Mathematics, Physics and Engineering. Inverse Problems are usually paired and are defined as follows.

Definition 1.1 (Inverse Problems)**.**
Two problems are called **Inverse Problems** from each other if the solution of one of the problems is part of the formulation of the second one and *vice-versa*. The easier problem is called the **Direct Problem**, the one with the harder solution is called the **Inverse Problem**.

Example 1.2 (Sum and Difference). The first example of mathematical inverse problems that one is introduced to are probably the sum and difference. These are clearly two inverse problems, since if

$$3 + 4 = 7$$

then one knows that

$$7 - 3 = 4,$$

that is, the solution of the sum is part of the formulation of the difference. In other words, if one knows the solutions to all the sums, than one can solve the all differences by exhaustion, that is, by trying every possible solution (if that can be done in finite time). In this case, to find the solution of the subtraction $9 - 4$, I have to find x such that $4 + x = 9$. Also, in this case the sum is usually considered the direct problem since it is easier (one learns to sum before learning to subtract), while the difference would be considered the inverse problem.

Example 1.3 (Jeopardy). Another example of inverse problems gave rise to a popular TV show in the USA called Jeopardy. Usually in TV contests, the participant

is posed a question to which he has to find the correct answer. However, in *Jeopardy*, the participant has to find the correct question for a given answer. These are clearly two inverse problem (finding an answer to a given question and finding a question to a given answer). However, it is easy to see that there are several questions for a same given answer. For instance 2016 is the answer to all the following questions:

- How much is 1000 plus 1016?
- In which year was Marcelo Rebelo de Sousa elected president of Portugal for the first time?
- ...

It is clear that finding a question to a given answer is the inverse problem, since it is more difficult. In particular, it has an additional difficulty, since the solution is not unique. Non-uniqueness arises usually in Inverse Problems.

Example 1.4 (Differentiation and Integration). Differentiation and Integration are also inverse problems of each other. In fact, for a continuous function f if

$$F(t) = \int_0^t f(u)du$$

then

$$F'(t) = f(t).$$

Usually one learns to differentiate before one learns to integrate, but actually differentiation is the inverse problem in the context of applied mathematics. This is well illustrated in figure 1.1. Since in applied mathematics and engineering data is measured and usually corrupted with noise, figure 1.1 illustrates that the finite integrals (area below the curve) of the exact and noisy functions are quite similar. However, the slope of the tangent line (which is by definition the derivative) can be highly affected by noise. In this case, in differentiation, the solution does not depend continuously on the data, which means that small errors in the data may cause huge errors in the solution. This problem is called **ill-conditioning** and leads to **ill-posedness**, which are concepts to which we will come back in the following lines.

In this text, we will focus on the numerical solution of inverse problems and how to overcome their main difficulties. The main difficulties for the inverse problems in the general framework in which we are interested are related with Hadamard's [Hadamard, 1952] definition of well-posed problem.

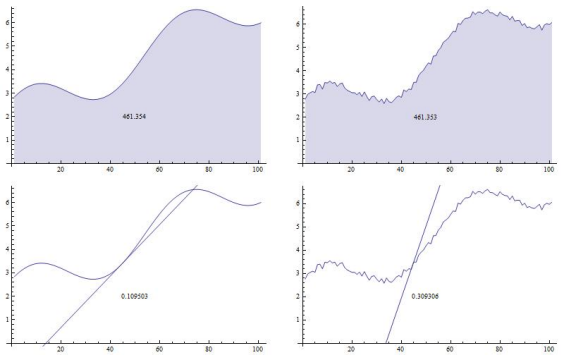

Figure 1.1: *Illustration of the effect of noise in integration (top) and differentiation (bottom).*

Definition 1.5 (Well and ill-posedness)**.**

A problem is called **well-posed** in the sense of Hadamard [Hadamard, 1952] if

(a) **Existence**: It has a solution;

(b) **Uniqueness**: The solution is unique;

(c) **Solution depends continuously on the data**: Small perturbations in the data give rise to small perturbations in the solution;

If one or more of the previous conditions fails, the problem is called **ill-posed**.

The class of inverse problems that we are interested in are usually ill-posed. As we will see throughout this text, the solution does not depend continuously on the data, which means that one needs to find a regularized numerical method to obtain a stable solution. Since measured data is usually affected by noise, this is a key issue that one has to deal with in the context of applied mathematics. Depending on the problem, existence and uniqueness might also be compromised, as we will see. In addition, some of the problems are also non-linear, which means that on top of the regularization to obtain stable solutions, one will also need to consider linearization methods to solve the problem. These issues make inverse problems very challenging to solve.

1.1 Inverse Scattering Problems: General Framework

We are interested in a very specific class of inverse problems, namely inverse scattering problems.

Let us consider an incident wave (or beam) usually denoted by u^i that propagates in free space, governed by some mathematical model that is usually a differential equation. For instance, Maxwell-equations govern electromagnetic wave propagation, while the Helmholtz equation is usually related with acoustic time-harmonic wave propagation. We will also consider a scatterer D (usually an obstacle), with some given properties such as shape, location and the way it interacts with the incident wave. The presence of the obstacle gives rise to the so called scattered wave u^s, being the total field u the sum of the incident and scattered wave, that is, $u = u^i + u^s$.

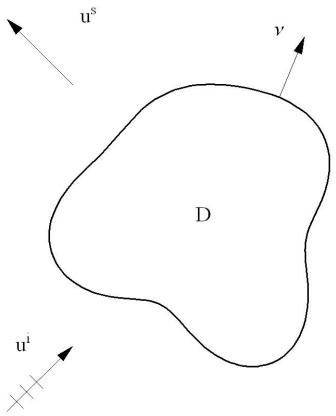

Figure 1.2: *Scheme for scattering problems*

If the obstacle is **impenetrable** the wave does not penetrate the obstacle. In this case one usually considers three possibilities, namely **sound-soft obstacles** which means that

$$u = 0 \text{ in } \Gamma \tag{1.1}$$

where Γ is the boundary of the obstacle D, which means the total field vanishes in the boundary of the obstacle; **sound-hard obstacles** which means that

$$\frac{\partial u}{\partial \nu} = 0 \text{ in } \Gamma \tag{1.2}$$

where ν is the exterior unit normal vector to the boundary of D, which means that the normal derivative of the total field vanishes on the boundary of the obstacle D; or an **impedance condition** given by

$$\frac{\partial u}{\partial \nu} - i\lambda u = 0 \text{ in } \Gamma \tag{1.3}$$

which models a behavior between the sound-soft and sound-hard obstacle. We note that if $\lambda = 0$ one has a sound-hard obstacle, while if $\lambda \to +\infty$ one has a sound-soft one. The impedance condition is the more realistic one, since in reality there are no perfect sound-soft or sound-hard obstacles, however these are useful in some model situations.

If the obstacle is **penetrable** then one has a transmission condition usually of the form

$$\begin{cases} u_1 = \lambda u_2 \\ \dfrac{\partial u_1}{\partial \nu} = \dfrac{\partial u_2}{\partial \nu} \end{cases} \quad \text{in } \Gamma \tag{1.4}$$

which governs the transition between the interior and exterior total field u_1, u_2, respectively, inside and outside the obstacle D.

Another possibility for the model is to consider an inhomogeneous medium, instead of an obstacle. This means that though no obstacle is not present, some coefficients of the governing equations change in some part of the domain, due to a scatterer with different density or electrical properties, amongst others.

At this stage, and focusing on impenetrable obstacles, we are ready to formulate the direct and inverse problem in a general framework for inverse scattering problems.

Direct Problem 1.6 (General direct problem).

Given an incident field u^i and the properties of the scatterer D, determine the scattered field u^s.

Inverse Problem 1.7 (General inverse problem).

Given a set of incident fields $u_1^i, u_2^i, \ldots, u_N^i$ and the corresponding scattered fields $u_1^s, u_2^s, \ldots, u_N^s$, find some properties of the unknown obstacle D, such as shape, location or its physical properties.

Though we are not currently working with any problem in particular, there are some statements that can be formulated right away. The first is that the inverse problem is more difficult to solve than the direct problem. The second, is that the direct problem has a unique solution (the incident field and the scatterer determine a unique scattered field). For the inverse problem this is not quite true. As we will see, this problem usually does not have a unique solution for a finite set of incident and scattered fields, that is, there might be more than one scatterer that would give rise to the same set of scattered fields for the given incident fields. In addition, since the measured scattered fields are affected with noise, in a mathematical sense there might not be even a solution, that is, there

is no scatterer D that would give rise to the (noisy) measured scattered fields. In this sense, existence is not the correct question to ask in terms of inverse scattering problems, and in fact though mathematically challenging, it is not interesting for applied and practical use. Finally, if the presence of two obstacles creates interacting fields between them, the problem is nonlinear, since the scattered field with the two obstacles is not the sum of the scattered fields for each of the obstacles individually. In this text, we will consider a linear problem (computerized tomography in section 4) and a nonlinear problem (Time-harmonic inverse acoustic scatering problems in section 5).

1.2 Relation with Medical Imaging

The relation between medical imaging and inverse scattering problems is quite clear. In fact, inverse scattering problems are the mathematical model for medical imaging. In medical imaging one wants to image the interior of the human body (the scatterer), by applying incident fields (or beams) and measuring the scattered field (or beam).

For instance, Magnetic Resonance Imaging (MRI) relies on the imposition of magnetic fields and the measure of the scattered fields to image the interior of the human body. This works since the different organs have different electrical and magnetic conductivities and permeabilities. In fact, a MRI image is a plot of these coefficients, therefore making it possible for the physician to distinguish the position of the organs and the presence of abnormalities.

Ultrasound relies on incident acoustic waves in different frequencies and their echoes in the interfaces between organs and different propagation properties of acoustic waves within different organs. These echoes are then measured in the probe, making it able to establish from which depth they were send, due to the use of different acoustic frequencies. Again, the produced image is a map of sound echoes.

X-ray imaging is based in the fact the X-rays are more attenuated in bones that in tissue. Therefore, standing in front of an X-ray emission machine, the image obtained is just a map of the different attenuated intensities of the beams that arrives at the film.

Computerized tomography (CT) is based in the same principle as X-ray imaging, but instead of considering one single direction of incident beams, the emissor and receiver rotate along the body on opposite sides, being able to determine an attenuation map in a slice of the human body.

Several other examples could be given, but for now we will focus on the

mathematical background that will allow us to mathematically formulate these inverse problems. This will be the basis for the approaches to numerically solve these models, as we will see in upcoming chapters.

Chapter 2

Functional Analysis Revisited

In this chapter we will revisit some results of functional analysis that are important for what follows. In the majority of cases, we will not show the proofs, since they can be checked in any functional analysis book (e.g. [Schechter, 2001]). In particular, some books in numerical analysis (e.g [Kress, 1998]), also contain the proofs for the following results.

2.1 Normed and Banach Spaces

Let us start with the definition of norm, that will be the basis for the definition of normed space and eventually Banach space.

Definition 2.1 (Norm)**.**
Let X be a linear real (or complex) space. The function $\|.\| : X \to \mathbb{R}$ is called a **norm** if for all $x, y \in X$ and $\alpha \in \mathbb{R}$ (or $\alpha \in \mathbb{C}$) the following hold

(a) Positivity: $\|x\| \geq 0$;

(b) Definitivity: $\|x\| = 0 \Leftrightarrow x = 0$;

(c) Homogeneity: $\|\alpha x\| = |\alpha| \, \|x\|$;

(d) Triangular inequality : $\|x + y\| \leq \|x\| + \|y\|$;

Definition 2.2 (Normed, Complete and Banach space)**.**
A linear real (or complex) space X is called **normed**, if it is equipped with a norm.

A normed space X is called **complete** if every Cauchy sequence$(x_n)_{n\in\mathbb{N}}$ of elements in X, that is,

$$\forall_{\varepsilon>0}\,\exists_{N\in\mathbb{N}}\,\forall_{n,m>N}\,\|x_n - x_m\| < \varepsilon,$$

is convergent for some element $x \in X$.

A complete normed space is called a **Banach space**.

Example 2.3 (Banach Spaces). Some examples of Banach spaces are the following:

(a) The spaces $\mathbb{R}^n$ and $\mathbb{C}^n$ are Banach with the norms

$$\|x\|_p = \sqrt[p]{\sum_{i=1}^{n} |x_i|^p}$$

where $p \in \mathbb{N}$.

(b) The spaces $\mathbb{R}^n$ and $\mathbb{C}^n$ are Banach with the maximum norm

$$\|x\|_\infty = \max_{i=1,\dots,n} |x_i|.$$

(c) The space of real or complex sequences $(x_n)_{n\in\mathbb{N}}$ given by

$$\ell^p = \left\{(x_n)_{n\in\mathbb{N}} : \|x\|_p < \infty\right\}$$

with the norm

$$\|x\|_p = \sqrt[p]{\sum_{i=1}^{\infty} |x_i|^p}$$

for $p \in \mathbb{N}$ are Banach spaces.

(d) The space of real or complex sequences $(x_n)_{n\in\mathbb{N}}$ given by

$$\ell^\infty = \left\{(x_n)_{n\in\mathbb{N}} : \|x\|_\infty < \infty\right\}$$

with the maximum norm

$$\|x\|_\infty = \max_{i\in\mathbb{N}} |x_i|$$

are Banach spaces.

(e) The space of functions

$$L^p = \{f : [a,b] \to \mathbb{R} : \|f\|_p < \infty\}$$

with the norm

$$\|x\|_p = \sqrt[p]{\int_a^b |f(x)|^p dx}$$

are Banach spaces.

(f) more examples of functions spaces will be recalled later in section 2.4.

We also need to recall some results for operators in normed spaces. We start by defining a linear operator.

Definition 2.4 (Linear Operator)**.**
Let $A : X \to Y$ be an operator from space X to the real (or complex) space Y. Then A is called **linear** if

$$A(\alpha x + \beta y) = \alpha Ax + \beta Ay, \tag{2.1}$$

for all $x, y \in X$ and $\alpha, \beta \in \mathbb{R}$ (or $\mathbb{C}$).

We also define as follows the norm of an operator, induced by the norms of the spaces it maps from and into.

Definition 2.5 (Operator Norm, Bounded Operator)**.**
Let X, Y be two normed spaces. We define the operator's **norm** for a linear operator $A : X \to Y$ (induced by the norms $\|.\|_X$ and $\|.\|_Y$ in X and Y, respectively) by

$$\|A\| := \sup_{\|x\|_X = 1} \|Ax\|_Y. \tag{2.2}$$

If $\|A\| < \infty$ the operator A is **bounded**.

To ease the notation, in the following we will drop the indexes X and Y of the norms. We have the following upper bound for bounded operators.

Theorem 2.6.
In the conditions of the previous result, if A is bounded, we have in particular that

$$\|Ax\| \leq \|A\| \, \|x\|, \quad \forall x \in X. \tag{2.3}$$

Similarly, if A and B are bounded operator, then

$$\|ABx\| \leq \|A\| \, \|B\| \, \|x\|, \quad \forall x \in X, \tag{2.4}$$

that is, $\|AB\| \leq \|A\| \, \|B\|$.

Proof. It is shown simply by

$$\|Ax\| = \left\| A\left(\frac{x}{\|x\|}\right)\right\| \|x\| \leq \sup_{\|x\|=1} \|Ax\| \, \|x\| = \|A\| \, \|x\| \, .$$

The proof of (2.4) is now trivial, considering $y = Bx$ and applying (2.3) twice. □

Another important definition is of continuous operator.

Definition 2.7 (Continuous operator)**.**
Let X, Y be two linear normed spaces. The operator $A : X \to Y$ is said to be **continuous at point** x if for every sequence $(x_n)_{n\in\mathbb{N}}$ convergent to x (that is, $x_n \to x$) one has $Ax_n \to Ax$. If A is continuous for all $x \in X$, the operator is said to be **continuous in** X.

For linear operators, one can show that continuous at a point and continuous in X are equivalent.

Theorem 2.8.
Let X, Y be two linear normed spaces and $A : X \to Y$ a linear operator. Then A is continuous at a point $x_0 \in X$ if and only if it is continuous in X.

Proof. Let A continuous in x_0 and let $x_n \to x \neq x_0$. Then for $y_n := x_n - x + x_0$ we have $y_n \to x_0$ and therefore $Ay_n \to Ax_0$. Now, by linearity of the operator, one has

$$Ax_n - Ax = Ay_n - Ax_0 \to 0.$$

so $Ax_n \to Ax$. As x is arbitrary, the result is shown. □

For linear operators, one also has the equivalence between continuous and bounded operators.

Theorem 2.9.
Let X, Y be two linear normed spaces and $A : X \to Y$ a linear operator. Then A is continuous if and only if A is bounded.

Proof. Let A be bounded and $x_n \to 0$. Then

$$\|Ax_n\| \leq \|A\| \, \|x_n\| \to 0$$

so $Ax_n \to 0$ and by theorem 2.8 A is continuous.

Let A be continuous and let us assume that it is not bounded, that is, there exists a sequence $(x_n)_{n\in\mathbb{N}}$ such that $\|x_n\| = 1$ and $\|Ax_n\| > n$. Now, in order to

find a contradiction, we define $y_n = x_n/\|Ax_n\|$. By linearity of the operator, one gets

$$\|Ay_n\| = \frac{1}{\|Ax_n\|}\|Ax_n\| = 1.$$

However, since

$$\|y_n\| \leq \frac{1}{n} \to 0,$$

by continuity of the operator we have $Ay_n \to 0$, which contradicts the previous. Therefore A must be bounded. □

The solution of an operator equation of the form $Ax = b$ is similar to the problem of inverting the operator A. Therefore, we must define an invertible operator.

Definition 2.10 (Invertible Operator)**.**
Let $A : X \to Y$ be bijective, that is, for all $b \in Y$ there exists a unique $x \in X$ such that

$$Ax = b.$$

The operator $A^{-1} : Y \to X$ such that

$$Ax = y \Leftrightarrow A^{-1}b = x,$$

is called the **inverse operator** of A.

If A is a real or complex matrix, we know from linear algebra (see, for instance [Magalhães, 1997]) that A is invertible if and only if

$$\min\{|\lambda| : \lambda \text{ is an eigenvalue of } A\} > 0,$$

or, in other words, if the determinant of A (given by the product of the eigenvalues) is different from zero.

For the case of operators in Banach spaces, there are several results that ensure the invertibility of an operator, such as the following.

Theorem 2.11.
*Let X be a Banach space and $B : X \to X$ a linear operator with norm $\|B\| < 1$. Let $I : X \to X$ be the **identity operator**, that is, $Ix = x$ for all $x \in X$. Then the operator $I - B$ is invertible and its inverse is given by*

$$(I - B)^{-1} = \sum_{n=0}^{\infty} B^n \tag{2.5}$$

with the following upper bound for its norm

$$\|(I-B)^{-1}\| \leq \frac{1}{1-\|B\|}.$$

Proof. We only present the general idea of the proof. For detailsm, we refer to [Kress, 1998]. We start by verifying that the series on the right hand side of (2.5) is convergent. Since $\|B\| < 1$, and from mathematical analysis [Ferreira, 1995] we know that if the series of the norms $\sum_{n=1}^{\infty} \|B^n x\|$ converges, then the series (2.5) also converges. As

$$(I-B)\sum_{n=0}^{\infty} B^n = \sum_{n=0}^{\infty} B^n - \sum_{n=1}^{\infty} B^n = I$$

and

$$\sum_{n=0}^{\infty} B^n(I-B) = \sum_{n=0}^{\infty} B^n - \sum_{n=1}^{\infty} B^n = I,$$

we show that (2.5) represents the inverse of $I-B$. The upper bound for the norm comes from the upper bound of (2.5) by the series of the norms and the expression for the geometric sum. □

2.1.1 Finite Dimensional Banach Spaces

The numerical resolution of model problems in applied mathematics gives usually rise to the solution of linear systems or the use of matrices for the formulation of local linearized approximations of nonlinear problems problems. In this way, it is particularly relevant the study of real and complex vector and matrix spaces. In this section we will recall some results for finite dimensional spaces, in which these are included.

We start by recalling that any normed space of finite dimension is a Banach space. For that, we use the Bolzano-Weierstrass theorem, that will be the ground for the proof.

Theorem 2.12 (Bolzano-Weierstrass)**.**
Any bounded sequence $(x_n)_{n\in\mathbb{N}}$ in $\mathbb{R}^n$, that is, such that it exists a $C > 0$ such that

$$\|x_n\| < C, \forall n \in \mathbb{N},$$

as a convergent subsequence, that is, there exists a $x \in \mathbb{R}^n$ such that

$$x_{n(k)} \to x, \quad k \to \infty.$$

Proof. The proof can be found in any undergraduate level book in mathematical analysis such us [Anton, 1999, Ferreira, 1995]. □

The Bolzano-Weierstrass theorem can be extended for any normed space of finite dimension by the following result.

Theorem 2.13.
In a finite dimensional normed space X, any bounded sequence $(x_n)_{n\in\mathbb{N}}$ has a convergent subsequence.

Proof. Let $\{u_1, u_2, \ldots, u_k\}$ a basis of X and consider the representation

$$x_n = \sum_{i=1}^{k} \alpha_{n,i} u_i.$$

As $(x_n)_{n\in\mathbb{N}}$ is bounded, then every sequence of the vector of coefficients $(\alpha_n)_{n\in\mathbb{N}}$ is bounded in $\mathbb{R}^n$. Then, by the Bolzano-Weierstrass theorem 2.12, there exists $\alpha \in \mathbb{R}^n$ such that

$$\alpha_{n(k)} \to \alpha, \quad k \to \infty.$$

Therefore, as $j \to \infty$ one has

$$x_{n(j)} \to x = \sum_{i=1}^{k} \alpha_i u_i.$$

□

The following result is also a consequence of the Bolzano-Weierstrass theorem.

Theorem 2.14 (Equivalence of norms in finite dimensional spaces)**.**
If X is a normed space with finite dimension, all norms are equivalent, that is,given two norms $\|.\|_1$ and $\|.\|_2$ there exists two constants c_1 and c_2 such that

$$c_1\|x\|_1 \leq \|x\|_2 \leq c_1\|x\|_2 \forall x \in X.$$

Proof. See [Kress, 1998, Thm.3.8]. □

We are now in place to show the following result.

Theorem 2.15.
A normed space X with finite dimension is a Banach space.

Proof. We want to show that every Cauchy sequence $(x_n)_{n\in\mathbb{N}}$ is convergent.

Let $\{u_1, u_2, \ldots, u_k\}$ a basis of X and let us consider the representation of the Cauchy sequence given by

$$x_n = \sum_{i=1}^{k} \alpha_{n,i} u_i.$$

By theorem 2.14, there exists $C > 0$ such that

$$\max_{i=1,\ldots,k} |\alpha_{n,i} - \alpha_{m,i}| \leq C\|x_n - x_m\|, \forall n, m \in \mathbb{N}.$$

Therefore $(\alpha_{n,i})_{n\in\mathbb{N}}$ is a Cauchy sequence in $\mathbb{C}$ (or $\mathbb{R}$) for every $i = 1, \ldots, k,$, so it is convergent, since $\mathbb{C}$ (or $\mathbb{R}$) is complete. Therefore, we have the convergence of x_n to

$$x_n \to x = \sum_{i=1}^{k} \alpha_i u_i.$$

where α_i is the limit of the sequence $(\alpha_{n,i})_{n\in\mathbb{N}}$ for every $i = 1, \ldots, k,$. □

2.2 Hilbert and pre-Hilbert spaces

We now recall the definition of inner product and Hilbert space.

Definition 2.16 (Inner product, pre-Hilbert space)**.**

A function $(.,.) : X \times X \to \mathbb{C}$ (or $\mathbb{R}$) defined for a complex (or real) linear space X is said to be an **inner product** if it satisfies the following properties

(a) Positivity: $(x, x) \geq 0$;

(b) Definitiveness : $(x, x) = 0 \Leftrightarrow x = 0$;

(c) Symmetry: $(x, y) = \overline{(y, x)}$;

(d) Linearity: $(\alpha x + \beta y, z) = \alpha(x, z) + \beta(y, z)$;

for all $x, y, z \in X$ and $\alpha, \beta \in \mathbb{C}$ (or $\mathbb{R}$).

A linear space equipped with an inner product is called a **Pre-Hilbert space**.

We recall also the Cauchy-Schwarz inequality, that will be useful later on.

Theorem 2.17 (Cauchy-Schwarz)**.**
For the inner product we have the following inequality

$$|(x,y)|^2 \leq (x,x)(y,y). \tag{2.6}$$

Proof. For $x = 0$ it is trivial. For $x \neq 0$, one has

$$0 \leq (\alpha x + \beta y, \alpha x + \beta y) = |\alpha|^2(x,x) + 2\mathrm{Re}\Big(\alpha\bar{\beta}(x,y)\Big) + |\beta|^2(y,y).$$

The result now comes from the choice of α as

$$\alpha = -\frac{\overline{(x,y)}}{\sqrt{(x,x)}}, \quad \beta = \sqrt{(x,x)}.$$

□

The Cauchy-Schwartz inequality is the starting point to show that it is always possible to define a norm in a pre-Hilbert space.

Theorem 2.18 (Norm induced by an inner product)**.**
A pre-Hilbert space is always a normed space with the induced norm

$$||x|| = \sqrt{(x,x)}.$$

Proof. It is sufficient to show that this norm satisfies all the properties of the definition 2.1 of a norm. We leave the proof as an exercise, suggesting the use of the Cauchy-Schwartz inequality to show the triangular inequality. □

We also note that using the induced norm, the Cauchy-Schwartz inequality (2.6) can be written as

$$|(x,y)| \leq \|x\| \, \|y\|. \tag{2.7}$$

Moreover, with a norm available, it makes sense to define a complete space in the context of pre-Hilbert spaces.

Definition 2.19 (Hilbert space)**.**
A complete pre-Hilbert space is called a **Hilbert space**.

Also, theorem 2.18 shows that every Hilbert space is a Banach space, so every results shown for Banach spaces is available for Hilbert spaces.

It is also important to introduce the definition of adjoint operator, for what follows.

Theorem 2.20.

*Let X, Y be Hilbert spaces. Let $A : X \to Y$ be a bounded linear operator. Then, there exists a so-called **adjoint operator** $A^* : Y \to X$ such that*

$$(Ax, y)_Y = (x, A^*y)_X, \quad \forall x \in X, y \in Y$$

where $(.,.)_X$ and $(.,.)_Y$ are the inner products in X and Y, respectively.

Proof. See, for instance, [Schechter, 2001].

2.3 Compact Operators

Compact operators will play a key role on the following text, so we will now take some lines to establish its definition and some of its properties. We aim at Fredholm theory, that we will consider in section 2.5. This theory sets the basis for some of the inversion schemes that we will consider throughout the text to solve inverse problems.

We start by characterizing a compact set in a normed space.

Definition 2.21 (Compact set)**.**

A subset U of a normed space X is **compact** if and only if any sequence $(x_n)_n \in U$ has a subsequence with limit in U.

A set is called **relatively compact** if it closure is compact.

Also, we have the following result.

Theorem 2.22.

Let X be a normed space. If a subset $U \subset X$ is compact, then it is bounded and complete.

Let X be an Euclidean space. Then a subset $U \subset X$ being bounded and complete implies also that U is compact.

Proof. We refer to [Bass, 2013].

Let us now define a compact operator.

Definition 2.23 (Compact Operator)**.**

Let X, Y be normed space and $A : X \to Y$ be a linear operator. Then A is called **compact** if the image of any bounded set in X is compact in Y.

There are several important properties of compact operators that we will list now.

Theorem 2.24.
Let $A : X \to Y$ be a compact linear operator. Then A is bounded.

Proof. Let x_n be a bounded sequence in X, such that $\|Ax_n\|_Y \to \infty$. Then $(Ax_n)_n$ could not have a convergent subsequence, so A would not be compact.

From theorem 2.9 and the previous result it is clear that a compact linear operator is also continuous.

Theorem 2.25.
Let X, Y be Hilbert spaces and $A : X \to Y$ be a compact linear operator. Then A^* is compact.

Proof. See for instance [Schechter, 2001].

We also note that the composition of a compact and a continuous operator is a compact operator.

Theorem 2.26.
Let X, Y, Z be Hilbert spaces and $A : X \to Y$ and $B : Y \to Z$ be linear bounded operators. If either A or B is compact, then the operator BA is compact.

Proof. See for instance [Schechter, 2001].

It is also important to look at the eigenvalues of compact operators $A : X \to X$, mapping from X to X. An **eigenvalue** λ is a value such that there exist $x \in X \setminus \{0\}$ such that

$$Ax = \lambda x.$$

Eigenvalues determine whether an operator is easily invertible, or, in other words, whether the image of an operator depends continuously on the object x, in the context of Hadamard ill-posedness 1.5. In this sense, studying the spectral properties of compact operators is important, that is, study how eigenvalues of compact operators behave.

Theorem 2.27 (Spectral theorem for compact operators)**.**
*Let X be a normed space with **infinite dimension** and $A : X \to X$ a compact linear operator. Then*

(a) zero is an eigenvalue of A.

(b) The eigenvalues $\lambda \neq 0$ are at most countable many, each has finite multiplicity, and accumulate only at zero.

If A is also self-adjoint, that is, if $A = A^*$, then all the eigenvalues are real.

Proof. See, for example, [Colton and Kress, 2013, Kress, 1999, Schechter, 2001].

The previous result shows that compact operators are not invertible in infinite dimension. Moreover, even if $Ax = f$ is solvable, the inversion of A is ill-posed, since their eigenvalues accumulate at zero.

We also consider the following result.

Theorem 2.28.

Let X be a normed space and $A : X \to Y$ a linear bounded operator with finite dimensional range, that is, the space

$$R(A) = \{A(x) : x \in X\}$$

has finite dimension. Then A is compact.

Proof. The result follows from the fact that $R(A)$ is complete from theorem 2.15, Bolzano-Weierstrass theorem 2.12 and the definition of compact set 2.21.

2.4 Function spaces

We will recall some function spaces that will be important for us. In what follows, we consider the domain D as a closed bounded domain.

Definition 2.29 (Space of continuously differentiable functions)**.**

The space of functions $C^n(D)$ defines all the **continuously differentiable functions** $f : D \to \mathbb{R}$ up to order n.

Definition 2.30 (Space of Hölder functions)**.**

The space of functions $C^{n,\alpha}(D)$ with $0 < \alpha < 1$ defines all the **Hölder functions** $f : D \to \mathbb{R}$ up to order $n + \alpha$ that are in $C^n(D)$ and that the n^{th}-derivatives satisfies the Hölder condition with index α, that is,

$$|D^j f(x) - D^j f(y)| \leq C|x - y|^\alpha, \quad |j| = n,$$

where $j = (j_1, j_2, \ldots, j_n)$, $|j| = j_1 + j_2 + \cdots + j_n$ and D^j is the derivative of order $|j|$ given by

$$D^j f = \frac{\partial^{|j|} f}{\partial x_1^{j_1} \partial x_2^{j_2} \ldots \partial x_n^{j_n}}. \tag{2.8}$$

Definition 2.31 (L^p Spaces)**.**

The $L^p(D)$ **space** is the space of all the functions that have bounded L^p norm, that is, that

$$L^p(D) = \{f : D \to \mathbb{R} : \|f\|_p < \infty\}$$

with

$$\|f\|_p = \sqrt[p]{\int_D [f(y)]^p dy}. \tag{2.9}$$

For the infinity norm $p = \infty$, one has

$$\|f\|_\infty = \max_{x \in D} |f(x)|.$$

Definition 2.32 (Sobolev Spaces)**.**

The **Sobolev space** $W^{p,k}$ is defined by

$$W^{p,k} = \left\{f : D \to \mathbb{R} : \|D^j f\|_k < \infty, \forall |j| \leq p\right\},$$

with $D^j f$ defined as in (2.8).

For $k = 2$, the Sobolev space is denoted by $H^p(D) := W^{p,2}(D)$. Moreover, $H_0^p(D)$ is the space of functions in $H^p(D)$ with null trace in the boundary of D.

It is no coincidence that we called spaces to the previous sets of functions. It is easy to check in any analysis or mathematical applications book (e.g. [Bass, 2013, Kress, 1998]) that the previous sets are linear spaces. Moreover, all of them can be equipped with a norm. For $L^p(D)$ the norm considered is (2.9), while for instance $C(D)$ can be equipped with $||.||_\infty$ or $||.||_2$. Hölder spaces are usually equiped with the norm

$$\|f\|_{C^{n,\alpha}} = \|f\|_{C^n} + \sup_{|j|=n} |D^j f|_\alpha$$

where

$$\|f\|_{C^{n,\alpha}} = \sup_{x \in D, 0 \leq |j| \leq n} |D^j f(x)|, \quad |f|_\alpha = \sup_{x,y \in D} \frac{|f(x) - f(y)|}{|x - y|^\alpha}.$$

As for Sobolev spaces the norm to consider is

$$\|f\|_{W^{p,k}} = \sum_{0 \leq |j| \leq p} \left\|D^j f\right\|_k$$

while for $H^p(D)$ or $H_0^p(D)$, we consider the norm

$$\|f\|_{H^p} = \sum_{0\leq|j|\leq p} \left\|D^j f\right\|_2 . \tag{2.10}$$

In this sense, these are normed spaces. One can also show that both L^p with the norm $\|.\|_p$ and H^p with the norm $\|.\|_p$ are **complete spaces**, making them **Banach spaces**. As for the space $C^p(D)$ it is in general not complete with the norm $||.||_\infty$ or $||.||_2$.

Considering now the inner product

$$(f,g)_2 = \int_D f(y)\overline{g(y)}dy$$

that gives rise to the norm $\|.\|_2$, the space $L^2(D)$ is a **Hilbert space**,

It is also important to know how these spaces are related between them, namely by checking embedding results between these spaces [Colton and Kress, 2013]. For instance, it is now that $C^{0,\alpha}(D)$ is compactly embedded in $C(D)$. Also, $C^{0,\beta}(D)$ is compactly embedded in $C^{0,\alpha}(D)$ if $0 \leq \alpha \leq \beta \leq 1$. Note that the fact of the embedding is compact means that note only the smaller space is a subpaces of the bigger space, but also it is a compact set in the norm of the bigger space.

Also, Sobolev's embedding theorem states that if

$$\frac{1}{p} - \frac{k}{n} = \frac{1}{q} - \frac{\ell}{n}$$

provided that $p \leq 1$, $q \leq 1$ and $(k-\ell)p < n$, then $W^{k,p}(\mathbb{R}^n)$ is continuously embedded in $W^{\ell,q}(\mathbb{R}^n)$. In particular, for $k = 1, \ell = 0$, one has that $W^{1,p}(\mathbb{R}^n)$ is continuously embedded in $L^q(\mathbb{R}^n)$ for q satisfying $\frac{1}{q} = \frac{1}{p} - \frac{1}{n}$.

2.5 Fredholm-Riesz Theory and Integral Operators

An integral equation is a equation involving an integral of the unknown solution function. The results for existence and uniqueness of solution for an integral equation include the so-called the Fredholm-Riesz theory. Fredholm developed this theory for integral equations with continuous kernels in the early XXth century, while Riesz extended the results for compact operators.

For what follows we will be interested in integral equations of the first kind

$$\int_a^b k(x,y)\varphi(y)dy = f(x), \quad x \in [a,b] \tag{2.11}$$

and second kind

$$\varphi(x) + \int_a^b k(x,y)\varphi(y)dy = f(x), \quad x \in [a,b] \tag{2.12}$$

where $[a,b]$ is clearly a closed set, φ is the unknown, k is the (known) kernel and f is a (known) function.

We first establish the following result, that will be of crucial importance for us.

Theorem 2.33.

*Let $k : [a,b] \times [a,b] \to \mathbb{R}$ be continuous or **weakly singular**, that is, k is defined and continuous for all $x \neq y$ and there exists $M > 0$, $\alpha \in]0,1]$ such that*

$$|k(x,y)| \leq M|x-y|^{\alpha-1}.$$

Then the integral operator $A : C([a,b]) \to C([a,b])$ defined by

$$(A\varphi)(x) = \int_a^b k(x,y)\varphi(y)dy = f(x), \quad x \in [a,b] \tag{2.13}$$

is compact.

Proof. See [Kress, 1999].

Now that we established that this operator is compact, theorem 2.27 establishes that for infinite dimensional spaces, the inversion of A is extremely ill-posed, since there are eigenvalues tending to zero. This means that the solution of equation (2.11) is extremely ill-posed.

As for second kind integral equations the situation is quite different. Fredholm theory shows that if the kernel k and the second member $f$are continuous, then (2.12) has one unique solution in $C([a,b])$. This is based in the so called Fredholm alternative, that can be generalized for compact operators as follows.

Theorem 2.34 (Fredholm alternative)**.**

Let X be normed space. Let $A : X \to X$ be a compact linear operator and I the identity operator. Then $I - A$ satisfies exactly one of the following:

- *$I - A$ is bijective, that is, is injective and surjective;*
- *the dimension of the kernel of $I - A$, that is, the dimension of the space*

$$\{x \in X : (I-A)x = 0\},$$

is greater or equal to one.

Proof. See [Kress, 1999].

Fredholm alternative establishes the equivalence between injectivity and surjectivity for operators of the form $I - A$, with A compact. In this sense, writing (2.12) as

$$(I - A)\varphi = f$$

with A as in (2.13), it is clear that A is compact for a continuous or weakly singular kernel k. Since A is compact, Fredholm alternative is applicable to (2.12), meaning that for the integral equation of the second kind (2.12), uniqueness of solution is equivalent to existence solution. This means, for instance for $K \in C([a,b]) \times C([a,b])$ that if

$$\varphi(x) + \int_a^b k(x,y)\varphi(y)dy = 0, \quad x \in [a,b]$$

has only the trivial solution $\varphi = 0$, the integral equation of the second kind (2.12) is uniquely solvable in $C([a,b])$ for every $f \in C([a,b])$.

Chapter 3

Conditioning

It Mathematics, it is a good practice to study the existence of solution before trying to solve a problem. If it does not exist, it does not make sense to search for it. Moreover, it is also important to know whether the solution is unique. If it is not, though a method might give you a solution, it is important to understand if that solution is the one we are looking for, given the problem at hand. In numerical analysis, usually one looks for an approximation of the exact solution. Therefore, another important problems arises: well-conditioning. As already mentioned in the follow up of definition 1.5, it is important to check if small errors in the data give rise to small errors in the solution. This is of key importance for obtaining approximations of the solution, moreover if one has in mind that in real practical problems data is usually affected by noise.

In the sequence of the definition 1.5 of well-conditioning, it is said that the problem associated with the operator A given by

$$Ax = b \tag{3.1}$$

is well-conditioned at x, if there exists a constant $C \geq 0$ such that

$$\delta_{\tilde{b}} \leq C\delta_x, \forall x \in V_x,$$

where V_x is a neighborhood of x, $\delta_{\tilde{b}} = \frac{\|b-\tilde{b}\|}{\|b\|}$ is the relative error of the second member and δ_x is the relative error of the solution. This means that the relative error of the results is controlled by the relative error in the data, that is, the result depends continuously on the data.

As an introduction to the study of conditioning of linear problems, we start by establishing a norm for the linear operator A. We start by linear operators in finite dimension, that is, that can be represented by a matrix.

3.1 Matrices Norms

In this section, we will consider a real (or complex) matrix A with dimensions $n \times n$ and entries $a_{i,j} \in \mathbb{R}$ (or $\mathbb{C}$) for $i, j = 1, 2, \ldots, n$ and two complex column vectors $x, b \in \mathbb{R}^n$ (or $\mathbb{C}^n$) given by

$$A = \begin{bmatrix} a_{11} & a_{12} & \ldots & a_{1j} & \ldots & a_{1n} \\ a_{21} & a_{22} & \ldots & a_{2j} & \ldots & a_{2n} \\ \vdots & \vdots & \ddots & \vdots & & \vdots \\ a_{i1} & a_{i2} & \ldots & a_{ij} & \ldots & a_{in} \\ \vdots & \vdots & & \vdots & \ddots & \vdots \\ a_{n1} & a_{n2} & \ldots & a_{nj} & \ldots & a_{nn} \end{bmatrix}, \quad x = \begin{bmatrix} x_1 \\ x_2 \\ \vdots \\ x_n \end{bmatrix}, \quad b = \begin{bmatrix} b_1 \\ b_2 \\ \vdots \\ b_n \end{bmatrix}. \tag{3.2}$$

Looking at a matrix $n \times n$ as an operator from the space of column vectors $\mathbb{R}^n$ (or $\mathbb{C}^n$) into itself, it is possible to consider the induced norm (2.2) for the matrices operators space.

Therefore one has the following result, that characterizes some matrix norms.

Theorem 3.1 (Matrix Norms)**.**

The norms in the space of column vectors $\mathbb{R}^n$ (or $\mathbb{C}^n$) given by

$$\|x\|_1 = \sum_{i=1}^{n} |x_i| \tag{3.3}$$

$$\|x\|_\infty = \max_{i=1,\ldots,n} |x_i| \tag{3.4}$$

$$\|x\|_2 = \sqrt{\sum_{i=1}^{n} |x_i|^2} \tag{3.5}$$

induce (in the sense of definition 2.5) the norms in the linear space of real (or complex) matrices of dimensions $n \times n$ given by

$$\|A\|_1 = \max_{j=1,\ldots,n} \sum_{i=1}^{n} |a_{ij}| \tag{3.6}$$

$$\|A\|_\infty = \max_{i=1,\ldots,n} \sum_{j=1}^{n} |a_{ij}| \tag{3.7}$$

$$\|A\|_2 = \sqrt{\rho\left(A^* A\right)} \tag{3.8}$$

*respectively, where A^* is the adjoint matrix given by the (conjugate) transpose matrix of A and the **spectral radius** is given by*

$$\rho(A) := \max_{i=1,\ldots,n} \{|\lambda_i| : \lambda_i \text{ is eigenvalue of} A\}. \tag{3.9}$$

The matrix norm (3.6) *is called* ***columns norm****,while the matrix norm* (3.7) *is called* ***lines norm****.*

If A is hermitian, that is, if $A = A^*$, then

$$\|A\|_2 = \rho(A). \tag{3.10}$$

Proof. Exercise. □

Remark 3.2 (Matrix norms in Octave). In Octave, the command `norm(A,p)` computes the p norm (p=1,2,Inf) of matrix A.

Exercise 3.3. Show that the matrix norm $\|.\|_2$ induced by the euclidean norm for column vectors satisfies

$$\|A\|_2 \leq \sqrt{\sum_{i,j=1}^{n} |a_{ij}|^2}.$$

Solution.

By the Cauchy-Schwartz inequality (2.7) one has

$$\begin{aligned}
\|Ax\|_2^2 &= \sum_{i=1}^{n} \left| \sum_{j=1}^{n} a_{ij} x_j \right|^2 \\
&\leq \sum_{i=1}^{n} \left(\sum_{j=1}^{n} |a_{ij}| \right)^2 \left(\sum_{j=1}^{n} |x_j| \right)^2 \quad \text{(Cauchy-Schwartz (2.7))} \\
&= \left(\sum_{j=1}^{n} |x_j| \right)^2 \sum_{i=1}^{n} \left(\sum_{j=1}^{n} |a_{ij}| \right)^2 \\
&= \left[\sum_{i=1}^{n} \left(\sum_{j=1}^{n} |a_{ij}| \right)^2 \right] \|x\|_2^2
\end{aligned}$$

hence we have the result by the definition of operator norm (2.2).

Theorem 3.4.

For every norm in $\mathbb{C}^n$ and any square matrix A, one has

$$\rho(A) \leq \|A\|. \tag{3.11}$$

On the other hand, for all $\varepsilon > 0$ there exists a norm such that

$$\|A\| \leq \rho(A) + \varepsilon. \tag{3.12}$$

Proof. Let v_m be an eigenvector of A associated to the eigenvalue λ_m such that $|\lambda_m| = \rho(A)$. Without loss of generality, we assume that v_m has unitary norm. Then

$$||A|| = \sup_{||x||=1} \|Ax\| \geq \|Av_m\| = |\lambda_m| = \rho(A).$$

so (3.11) is proven. For the proof of (3.12) we refer for instance to [Kress, 1998, Kincaid and Cheney, 2009]. □

3.2 Conditioning of linear equations

Thought we started focused on linear equations of the form (3.1), where the linear operator A has finite dimension, what follows can also be applied to linear operators with infinite dimension. Therefore, we formulate the results in this section for linear operators A (with possible infinite dimension) as defined in definition 2.4 in normed spaces, since we will need the definition of the norm of A. Obviously, the results are also valid for finite dimensional operators.

The following theorem gives us an upper bound for the conditioning of linear equations. We note that to speak about the conditioning of a linear equation (3.1), we assume that the equation has a unique solution, that is, that the operator A should be invertible in the sense of definition 2.10.

Definition 3.5 (Condition number).

Let $A : X \to Y$ be an invertible operator. We call **condition number** of the operator A to

$$\text{cond}(A) = \|A^{-1}\| \, \|A\|. \tag{3.13}$$

We note that the condition number depends on the norm that one considers.

Remark 3.6 (Conditioning number in Octave). In Octave, one can compute the command `inverse(A)` to compute the inverse matrix of the matrix $A$and the command `cond(A,p)` to compute the condition number of the matrix A in the norm p (p=1,2,Inf).

Independently of the norm considered, we have the lower bound for the condition number given by the following result.

Theorem 3.7.

Let $A : X \to Y$ be an invertible operator. Then

$$\text{cond}(A) \geq 1. \tag{3.14}$$

Proof. We have

$$1 = \|I\| = \|A^{-1}A\| \leq \|A^{-1}\|\|A\| = \text{cond}(A).$$

□

It is also important to establish upper bounds for the error of solution of linear equations of the form

$$Ax = b,$$

when the operator A or the second member b is affected by errors. We have the following results

Theorem 3.8 (Conditioning of linear equations).

Let X and Y Banach spaces and let $A : X \to Y$ be a linear operator with bounded inverse $A^{-1} : Y \to X$. Let also $\tilde{A}$ be a linear operator such that

$$\|A^{-1}\|\|\tilde{A} - A\| < 1$$

and let x and $\tilde{x}$, respectively, be the solutions of the linear equations

$$Ax = b \qquad e \qquad \tilde{A}\tilde{x} = \tilde{b}.$$

Then we have the upper bound for the relative error of the solution

$$\delta_{\tilde{x}} \leq \frac{\text{cond}(A)}{1 - \text{cond}(A)\delta_{\tilde{A}}} (\delta_{\tilde{b}} + \delta_{\tilde{A}}) \tag{3.15}$$

where the relative error is defined by $\delta_{\tilde{x}} = \frac{\|x-\tilde{x}\|}{\|x\|}$.

Proof. We start by noting that by theorem 2.11, the operator $I + A^{-1}(\tilde{A} - A)$ is invertible. Then, the operator $\tilde{A}$ is also invertible, since it can be written by

$$\tilde{A} = A\left(I + A^{-1}(\tilde{A} - A)\right)$$

and his inverse is given by

$$\tilde{A}^{-1} = \left(I + A^{-1}(\tilde{A} - A)\right)^{-1} A^{-1}$$

and has norm bound by

$$\|\tilde{A}^{-1}\| \leq \frac{\|A^{-1}\|}{1 - \|A^{-1}\|\|\tilde{A} - A\|}. \tag{3.16}$$

By the definition of x and $\tilde{x}$ one has

$$\tilde{A}(\tilde{x} - x) = \tilde{b} - b - (\tilde{A} - A)x,$$

therefore applying the inverse of $\tilde{A}$ and getting upper bounds for the norms one has

$$\|\tilde{x} - x\| \leq \|\tilde{A}^{-1}\| \left(\|\tilde{b} - b\| + \|\tilde{A} - A\| \|x\| \right).$$

Applying (3.16), dividing both members by $\|x\|$ and considering the definition of condition number to get $\|\tilde{A}^{-1}\| = \mathrm{cond}(A)/\|\tilde{A}\|$, one gets

$$\frac{\|x - \tilde{x}\|}{\|x\|} \leq \frac{\mathrm{cond}(A)}{1 - \mathrm{cond}(A)\dfrac{\|\tilde{A} - A\|}{\|A\|}} \left(\frac{\|\tilde{b} - b\|}{\|A\|\|x\|} + \frac{\|\tilde{A} - A\|}{\|A\|} \right).$$

and therefore the result, since

$$\|A\|\|x\| \geq \|Ax\| = \|b\|.$$

□

The previous result shows that the higher the condition number, the worst the resolution of the linear equation is conditioned, since the term

$$\frac{\mathrm{cond}(A)}{1 - \mathrm{cond}(A)\delta_{\tilde{A}}} \to \infty$$

when $\mathrm{cond}(A) \to \infty$. This is even more clear where the errors are only in the second member b.

Exercise 3.9. Show that if the linear operator A is invertible and exact (i.e., $\tilde{A} = A$), one has the upper bound.

$$\delta_{\tilde{x}} \leq \mathrm{cond}(A)\delta_{\tilde{b}}. \tag{3.17}$$

Solution.

Comes directly from (3.15) considering $\tilde{A} - A = 0$.

Exercise using Octave 3.10. Consider the norm $\|.\|_2$ and the linear system $Ax = b$ with

$$A = \begin{bmatrix} 3 & 5 & -1 \\ 2 & -4 & 2 \\ 5 & 1 & 1.0001 \end{bmatrix}, \quad b = \begin{bmatrix} 0 \\ 1 \\ 10 \end{bmatrix}.$$

(a) Compute the condition number of A, using Octave.

(b) What can you conclude about the conditioning of the resolution of $Ax = b$.

(c) Consider the approximations

$$\tilde{A} = \begin{bmatrix} 3 & 5 & -1 \\ 2 & -4 & 2 \\ 5 & 1 & 1.00005 \end{bmatrix}, \quad \tilde{b} = \begin{bmatrix} 0 \\ 1 \\ 10.00005 \end{bmatrix}.$$

Compute the relative errors of the matrix $\tilde{A}$ and vector $\tilde{b}$, by its definition, using the command `norm` in Octave.

(d) Verify the conditions of theorem 3.8, using the commands `inv` and `norm` of Octave.

(e) Compute the upper bound for the relative error of the solution of the linear system $\tilde{A}\tilde{x} = \tilde{b}$ with respect to the solution of $Ax = b$.

(f) Compute the exact error.

Answer.

(a) $\text{cond}_2(A) = 1.3831 \times 10^5$.

(b) As the condition number is high, the system is ill-conditioned.

(c) $\delta_{\tilde{A}} = \dfrac{\|\tilde{A} - A\|_2}{\|A\|_2} \approx 6.8778 \times 10^{-6}; \delta_{\tilde{b}} = \dfrac{\|\tilde{b} - b\|_2}{\|b\|_2} = 4.9752 \times 10^{-6}$.

(d) Since we are considering matrices (and therefore linear operators), one just has to verify that A is invertible and

$$\|A^{-1}\|_2 \|\tilde{A} - A\|_2 = 0.95130 < 1,$$

therefore, the hypothesis of the theorem are verified.

(e) From (3.15) we have $\delta_{\tilde{x}} \leq 33.661$, that is the upper bound tells us that the relative error of the solution in less than $3366, 1\%$.

(f) We have the solutions

$$x = [-2.4545, 3.2727, 9]^T \times 10^4; \quad \tilde{x} = [-4.9091, 6.5455, 18]^T \times 10^4$$

and therefore obtain $\delta_{\tilde{x}} = 1$, that is, an error of 100 %.

We will focus in solving linear equations of the form

$$Ax = \tilde{b}$$

where $\tilde{b}$ is a small perturbation of the exact value b, that is, the second member is affected by errors. As we have seen, the conditioning of the equation is related with the condition number of A, by (3.17).

We also note that the condition number is related with the invertibility of A. In particular, if A as eigenvalues close to zero, the invertibility of A is ill-conditioned and the condition number will be high. This claim has its support on the definition of condition number and theorem 3.4. In fact, as the eigenvalues of A^{-1} are the inverse of the eigenvalues of A, so if A has an eigenvalues close to zero (with respect to the other eigenvalues), then A^{-1} has a large eigenvalue in absolute value, so $\rho(A^{-1})$ is large. In this way, by theorem 3.4, whatever the norm considered, we have $\|A^{-1}\|$ very large and therefore the condition number will be very large (supposing that $\|A\|$ is not close to zero, since this would imply that its eigenvalues are close to zero by theorem 3.4).

Therefore, a way to control the ill-conditioning in the resolution of a linear equation $Ax = b$ is to control the eigenvalues of A, that is, solve a similar linear equation where the eigenvalues of the corresponding linear operator are away from zero.

3.3 Regularization

In this section we will focus on some regularization methods for ill-conditioning equations, that is, we will consider processes to stabilize the resolution of linear equations. We start by recalling the concept of singular system, that we will generalize for compact operators. From theorem 2.28, this is also applied to matrices, that are special cases of compact operators.

If A is a compact linear operator, then its adjoint A^* is also compact from theorem 2.25 and therefore the operator AA^* is a self-adjoint compact operator. The spectrum of the operator AA^* is characterized in theorem 2.27 and is the starting point for the singular system that we now describe.

Theorem 3.11 (Singular System).

Let $A : X \to Y$ be a linear compact operator. Then there exists orthonormal systems $u_1, u_2, \ldots, u_n, \cdots \in X$ and $v_1, v_2, \ldots, v_n, \cdots \in Y$ and real values

$$\mu_1 \geq \mu_2 \geq \cdots \geq \mu_n \geq \ldots$$

ordered and repeated by its multiplicity such that

$$Au_j = \mu_j v_j, \qquad A^* v_j = \mu_j u_j, \quad j = 1, 2, \ldots, n, \ldots \tag{3.18}$$

*The system (μ_j, u_j, v_j) is called **singular system** of the compact operator A and the values μ_j are called **singular values** of A.*

Moreover, the linear equation $Ax = b$ has a unique solution if and only if

$$(b, y) = 0, \quad \forall y \in Y : A^* z = 0.$$

In that case, the solution is given by

$$x = \sum_j \frac{1}{\mu_j}(b, v_j)u_j. \tag{3.19}$$

Proof. We refer to [Kress, 1998] for the proof. □

Exercise using Octave 3.12. In Octave, use the command `[V MU U] = svd(A)` to obtain the singular system of $\tilde{A}$ as in exercise 3.10. Verify that (3.18) holds.

Answer.

We obtain the column vectors `U`

$$u_1 = [-0.59153, -0.79603, 0.12814]^T; \quad u_2 = [-0.76710, 0.50670, -0.39347]^T;$$
$$u_3 = [-0.24829, 0.33104, 0.91036]^T;$$

and the column vectors `V`

$$v_1 = [-0.80923, 0.31051 - 0.49872]^T; \quad v_2 = [0.10866, -0.75515, -0.64649]^T;$$
$$v_3 = [-0.57735, -0.57735, 0.57735]^T;$$

that are an orthonormal basis of $\mathbb{R}^3$ and obtain the singular values from the diagonal of `MU` given by

$$\mu_1 = 7.2697; \quad \mu_2 = 5.7577; \quad \mu_3 = 2.6280 \times 10^{-5}.$$

The expression of the solution (3.19) illustrates the relation between the singular values of A and the conditioning of the linear equation $Ax = b$. To simplify the analysis, we will consider A an invertible $n\times$ matrix, which means that all its eigenvalues and singular values are different from zero.

We start by noting that if the singular values μ_j are close to zero, the factor $1/\mu_j$ makes the numerical solution unstable. In fact, as μ_j^2 are the eigenvalues of A^*A since from (3.18) one has

$$A^*Au_j = \mu_j A^* v_j = \mu_j^2 u_j,$$

from (3.10) one gets

$$\mathrm{cond}_2(A) = \frac{\mu_1^2}{\mu_n^2}$$

therefore if the lower eigenvalue μ_n is close to zero, the conditioning of the linear equation $Ax = b$ is compromised.

Finally, we will compare the eigenvalues λ_j of A to their singular values μ_j. We start by noting that the eigenvalues of the adjoint (complex conjugate transpose) matrix A^* are the complex conjugate eigenvalues of A. Therefore, as the determinant of a matrix is the product of its eigenvalues, one gets

$$\prod_{j=1}^{n} \mu_j^2 = \det(A^*A) = \det(A^*)\det(A) = \prod_{j=1}^{n} \bar{\lambda}_j^2 \prod_{j=1}^{n} \lambda_j^2 = \prod_{j=1}^{n} |\lambda_j|^2.$$

In a hand waving argument, if one of the eigenvalues is close to zero (making the inversion of the matrix ill-conditioned), the product of the eigenvalues, and therefore the singular values is close to zero. Therefore, one of the singular values must be close to zero. As seen before, if the eigenvalues are close to zero, the linear equation is ill-conditioned.

3.3.1 Regularization by singular values decomposition

Equation (3.19) illustrates the ill-conditioning associated with singular values μ_j close to zero. On the other hand, it also allows to approximate the solution of the problem in a stable way. Having that in mind, one can truncate the sum, not considering singular values μ_j lower than some given $\varepsilon > 0$. In this way the contribution of the terms $1/\mu_j$ for unstable values disappears. We then get the approximation

$$x_p = \sum_{j=1}^{p} \frac{1}{\mu_j}(b, v_j)u_j,$$

where p is the index such that $\mu_p \geq \varepsilon$ and $\mu_{p+1} < \varepsilon$. The choice of ε or in a similar way, the choice of p is crucial to the quality of the approximation. On the one hand, one wants a stable solution. On the other hand, one does not want to

truncate the sum too much, in order to get a good approximation, since by the triangular inequality one gets

$$\|x - x_p\|_2 \leq \sum_{j=p+1}^{n} \frac{1}{\mu_j} |(b, v_j)|.$$

This error shows us that if b is perpendicular to the space generated by the v_j para $j = p+1, \ldots, n, \ldots$, then $(b, v_j) = 0$ and therefore the error is null. On the other hand, if b belongs to that space, the error might be huge.

Having this in mind, recently some author use the **effective condition number** $\mathrm{cond}_{2,eff}$, instead of the usual condition $\mathrm{cond}_2(A)$ [Chen et al., 2023]. The rationale behing this is that the second member b should also matter to measure the conditioning of a fixed linear equation $Ax = b$, therefore defining

$$\mathrm{cond}_{2,eff} = \frac{||b||}{\mu_n ||x||}.$$

Though it can be shown that $\mathrm{cond}_{2,eff} \leq \mathrm{cond}_2$, and therefore, it illustrates better the conditioning taking into account the second member b, the computation of the effective condition number $\mathrm{cond}_{2,eff}$ relies on knowing the exact solution x of the problem, which is not always the case.

3.3.2 Tikhonov Regularization

The regularization by decomposition in singular values is unpractical, since one needs to compute the singular system of A, which is by itself is time consuming and unstable. In this section, we will consider another method for regularization, namely Tikhonov regularization. The idea is to replace the resolution of the linear equation

$$A\tilde{x} = \tilde{b}$$

by the linear equation

$$(\alpha I + A^* A) x_\alpha = A^* \tilde{b} \tag{3.20}$$

with some regularization parameter $\alpha > 0$. As we will show next, the equation (3.20) has better conditioning than the original equation and its solution x_α is close to x.

Theorem 3.13 (Tikhonov Regularization).

Let (μ_j, u_j, v_j) be the singular system for the compact linear operator A and let $\alpha > 0$ be a real constant.

Then the operator $M = \alpha I + A^*A$ related with the resolution by Tikhonov regularization (3.20) *has condition number*

$$\mathrm{cond}_2(M) \leq \frac{\mu_1^2 + \alpha}{\mu_n^2 + \alpha}. \tag{3.21}$$

Moreover, the solution of (3.20) *can be written in the form*

$$x_\alpha = \sum_j \frac{\mu_j}{\alpha + \mu_j^2} (\tilde{b}, v_j) u_j. \tag{3.22}$$

If x is the solution of the linear equation $Ax = b$ then we have the upper bound for the error

$$\|x - x_\alpha\|_2 \leq \|b\|_2 \sum_j \left| \frac{\alpha}{\mu_j(\alpha + \mu_j^2)} \right| + e_{\tilde{b}} \sum_j \left| \frac{\mu_j}{(\alpha + \mu_j^2)} \right| \tag{3.23}$$

where the absolute error of the second member is given by $e_{\tilde{b}} = \|b - \tilde{b}\|_2$.

Proof. By (3.18) one gets

$$(\alpha I + A^*A) u_j = (\alpha + \mu_j^2) u_j,$$

therefore the eigenvalues of M are given by $(\alpha + \mu_j^2)$. Moreover, since M is hermitian, result (3.21) comes directly from (3.10). The representation (3.22) comes directly form the singular representation (3.19) by noticing that $(\alpha + \mu_j^2, u_j, u_j)$ is a singular system of M and $(A^*\tilde{b}, u_j) = (\tilde{b}, Au_j) = \mu_j(\tilde{b}, v_j)$. Finally, from the representations (3.19) and (3.22) one gets

$$\begin{aligned}
x - x_\alpha &= \sum_{j=1}^{n} \left(\frac{1}{\mu_j}(b, v_j) - \frac{\mu_j}{(\alpha + \mu_j^2)}(\tilde{b}, v_j) \right) u_j \\
&= \sum_{j=1}^{n} \left(\left[\frac{1}{\mu_j} - \frac{\mu_j}{(\alpha + \mu_j^2)} \right] (b, v_j) + \frac{\mu_j}{(\alpha + \mu_j^2)}(b - \tilde{b}, v_j) \right) u_j \\
&= \sum_{j=1}^{n} \left(\frac{\alpha}{\mu_j(\alpha + \mu_j^2)}(b, v_j) + \frac{\mu_j}{(\alpha + \mu_j^2)}(b - \tilde{b}, v_j) \right) u_j
\end{aligned}$$

and from the triangular inequality and Cauchy-Schwartz, one obtains (3.23).

□

The application of Tikhonov regularization as a great advantage with respect to regularization by singular value decomposition: one does not need to compute the singular system. In fact, to apply Tikhonov regularization one only needs to solve (3.20). The major disadvantage of Tikhonov regularization is that one needs to chose the regularization parameter α appropriately, similarly to having to choose the proper index p to truncate the sum in the regularization with singular value decomposition. This is usually not trivial and it most cases, it is still an open problem. On the one hand, α should be small to ensure that the linear equation (3.20) as a similar solution to the original system. This is clear, since the first term in the error estimate (3.23) goes to zero, as α goes to zero. On the other hand, α cannot be too small to ensure that the solution is stable, or in other words, to ensure that the error in the second member $\tilde{b}$ is not amplified. This is clear in the second term of the error estimate (3.23). A similar indication is given by the upper bound for the condition number (3.21), since α must not be too small to ensure well-conditioning of the Tikhonov equation (3.20).

Exercise using Octave 3.14. Consider the matrix A of dimensions $n \times n$, whose entry (j, k) is given by $a_{jk} = \sin(jk/n)$ and the column vector b is such that

$$b_j = \sum_{k=1}^{n} k \sin(kj/n).$$

Consider also $\tilde{b}$ affected by error, such that

$$\tilde{b}_j = b_j + 10^{-12} \cos(2000j/n).$$

The solution of the system $Ax = b$ is given by the vector with components $x_j = j$ for $j = 1, 2, \ldots, N$. Consider $n = 12$ for what follows.

(a) In Octave, define the matrix A and vectors b and $\tilde{b}$.

(b) Compute the relative and absolute error of $\tilde{b}$ in the euclidean norm.

(c) Compute the condition number of A in the euclidean norm.

(d) Compute the relative error of the solution of $A\tilde{x} = \tilde{b}$ obtained by the direct resolution of the linear system in Octave given by the commands xtil = A\ btil with respect to the exact solution x.

(e) Compute an approximation to the solution by regularization by singular value decomposition, using the higher $p = 10$ singular values. Compute the respective relative error.

(f) Compute an approximation to the solution by Tikhonov regularization, using a regularization parameter $\alpha = 10^{-10}$. Compute the respective relative error.

(g) Graphically compare the obtained solutions and draw some comments on the result.

Answer.

(a) In a '.m' file, we write the algorithm:

```
N=12;
b = double(zeros(N,1));
btil = double(zeros(N,1));
A = double(zeros(N,N));
for j= 1:  N
  for k= 1:  N
    A(j,k) = sin(j*k/N);
    b(j) = b(j) + k*sin(k*j/N);
  end
  btil(j)= b(j)+10^(-12)*cos(2000*j/N);
end
```

(b) One gets the absolute $e_{\tilde{b}} = 2.1277 \times 10^{-12}$ and relative $\delta_{\tilde{b}} = 1.9864 \times 10^{-14}\%$ errors in the data, being therefore quite small.

(c) One gets $\mathrm{cond}_2(A) = 1.7470 \times 10^{14}$, therefore the system $Ax = b$ is ill-conditioned.

(d) We have $\tilde{x} = [27.18, -40.25, 47.18, -31.27 \ldots, 12.00]$ therefore

$$\delta_{\tilde{x}} = 312.10\%.$$

This huge error in the results originated from a small error in the data is justified by the ill-conditioning of the system and the lack of regularization in the resolution.

(e) We obtain the regularized solution

$$x_p \approx [1.00, 2.00, 3.00, \ldots, 12.00]^T$$

by writing a '.m' file with the following algorithm:

```
 [v mu u] = svd(A);
p = 10;
xp = zeros(N,1);
for j= 1:  p
  xp = xp + dot(btil,v(:,j))*u(:,j)/mu(j,j);
end
```

The relative error is $\delta_{x_p} = 0.00016850\%$.

(f) We obtain the regularized solution

$$x_\alpha \approx [1.00, 2.00, 3.00, \ldots, 12.00]^T$$

by writing a '.m' file with the following algorithm:

```
alpha = 10^(-10);
MTik = alpha*eye(N) + A'*A;
bTik = (A')*btil;
xTik = MTik\ bTik;
```

The relative error is $\delta_{x_\alpha} = 0.00069637\%$.

(g) The comparison between the three approximate solutions and the exact one is shown in figure 3.1, obtained by the following commands:

```
figure(1)
plot(x,'r-');
hold on;
plot(xtil,'b-');
plot(xp,'g-');
plot(xTik,'c-');
legend('Solucao exata','Solucao com erro','SVD','Tikhonov');
hold off;
```

The instability of the solution by direct solution of the linear system is clear, While the regularized solutions coincide graphically with the exact solution. This illustrates how regularization can be used to solve in a stable way a ill-conditioned system with a smooth solution.

We will now apply the concepts in functional analyisis and conditioning that we have been revising until this moment to two applications. In chapter 4 we will consider a mathematical model for computerized tomography, based on the

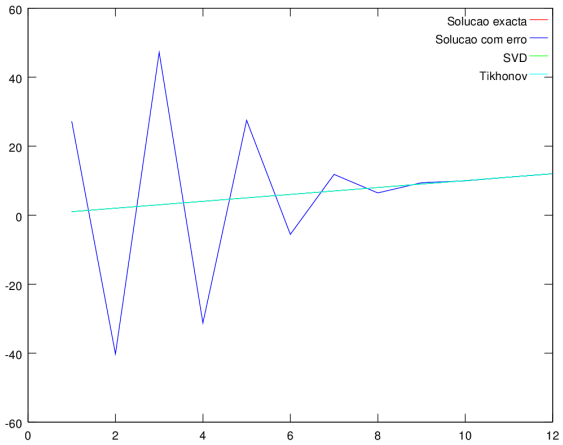

Figure 3.1: *Comparison between the numerical solutions and the exact solution regarding exercise 3.14.*

Radon transform, which inversion is mildly ill-conditioned. Moreover, it is a linear operator, which means that we will consider a mildly ill-posed linear inverse problem. In chapter 5 we will consider the inverse problem of recovering the position and shape of an obstacle given a time-harmonic incident wave and the far-field of the scattered wave. This problem is severly ill-conditioned and nonlinear, posing therefore more difficulties for obtaining a stable solution than in the case of computerized tomography.

Chapter 4

Computerized Tomography

4.1 Introduction

In this chapter, we will focus on the mathematical modelling of **Computerized Tomography** (CT) and some numerical reconstruction algorithms. These lectures notes are based in the lecture notes of Prof. Rainer Kress [Kress, 2005] in *Tomographie* (in german) and the book [Natterer, 2001], so we refer to those for a more detailed version of what we address here.

First, we will focus on the geometrical setting of the problem, and, in particular, how the image of a slice of the body can be obtained in the context of this imaging modality.

Computerized tomography is based on the emission of X-rays through a body of unknown density $f = f(x)$, depending only on the spatial coordinate $x \in \mathbb{R}^2$. The goal is to recover the unknown density f from the knowledge of the intensity of the ray at the source and the measured intensity at the receiver, for a set of rays traveling over different trajectories across the body.

There are several assumptions that one needs to make for the mathematical modeling of computerized tomography. The **first assumption** is that X-rays travel over straight lines, which though not being exactly the case, is a very good approximation. Therefore, one assumes a geometrical setting as in figure 4.1.

In this way, any line L corresponding to the trajectory of a ray can be characterized by a unit vector $\theta \in \mathbb{R}^2$ and a length $s \in \mathbb{R}$, that is

$$L_{s,\theta} = \left\{ s\theta + t\theta^{\perp} : t \in \mathbb{R} \right\} \tag{4.1}$$

where $\theta^{\perp}$ is a unit vector perpendicular to θ.

The **second assumption** for the mathematical modeling of CT is that the loss of energy is proportional to the density itself. In fact, one assumes that the local

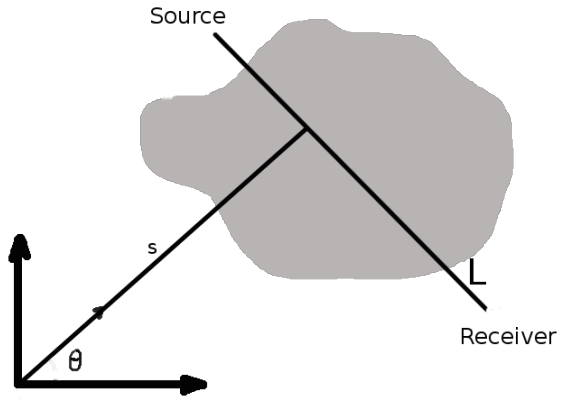

Figure 4.1: *General geometrical setting for a line L corresponding to the trajectory of a ray in CT.*

variation of the intensity ΔI of the ray is proportional to the density f, to the current intensity I and the travelled distance Δx, that is,

$$\Delta I = -\gamma f I \Delta x.$$

Taking the previous assumption as $\Delta x \to 0$, one gets that

$$\frac{dI}{dx} = -\gamma f I,$$

that is

$$\frac{I'(x)}{I(x)} = -\gamma f(x).$$

Integrating the latter in x over the line trajectory L, one gets that

$$\ln(I_{receiver}) - \ln(I_{source}) = -\gamma \int_L f(x)dx$$

that is, taking the parametrization (4.1), one gets

$$\ln\left(\frac{I_{receiver}}{I_{source}}\right) = -\gamma \int_{-\infty}^{\infty} f(s\theta + t\theta^{\perp})dt.$$

For imaging purposes, one can redefine $f = \gamma f$, since the plot of f or γf will only vary by a matter of scale and therefore both will equally distinguish different densities. Therefore, we can simplify the CT mathematical model as

$$\ln\left(\frac{I_{source}}{I_{receiver}}\right) = \int_{-\infty}^{\infty} f(s\theta + t\theta^{\perp})dt. \tag{4.2}$$

We are now in a position to define the Radon transform, that will be of great use throughout this chapter. Before this definition, we also define the Schwarz space of functions, in which the Radon transform is defined.

Definition 4.1 (Schwarz space).
Let $f : \mathbb{R}^2 \to \mathbb{C}$.
Then the **Schwarz space** $S(\mathbb{R}^2)$ is the space of functions $f \in C^{\infty}(\mathbb{R}^2)$ such that both f and all its derivatives decay faster to infinity than any power of x, that is

$$S(\mathbb{R}^2) = \left\{ f \in C^{\infty}(\mathbb{R}^2) : \sup_{x\in\mathbb{R}^2} |x^n D^j f(x)| \leq \infty, \forall n \in \mathbb{N}, \forall j \in \mathbb{N}^2 \right\}$$

with $D^j f$ defined as in (2.8).

The Schwarz space $S(\mathbb{R}^2)$ guarantees that the function f vanishes in an appropriate speed to infinity, so that the line integral is well defined.

Definition 4.2 (Radon Transform).
Let $f \in S(\mathbb{R}^2)$.
Then the **Radon transform** $(Rf) : \mathbb{R} \times \Omega \to \mathbb{C}$ of f is defined as

$$(Rf)(s,\theta) = \int_{-\infty}^{\infty} f(s\theta + t\theta^{\perp})dt, \tag{4.3}$$

where $\Omega = \{\theta : |\theta| = 1\}$ is the unit circumference.

The Radon transform makes the formulation of (4.2) easier, in the sense that it can be written has

$$(Rf)(s,\theta) = \ln\left(\frac{I_{source}}{I_{receiver}}\right),$$

where the right hand side is known for each ray defined by s and θ.

In this way, the direct problem in the context of CT can be formulated as follows.

Direct Problem 4.3. Given the density f, find the Radon transform $(Rf)(s,\theta)$.

However, our interest is the computerized tomography inverse problem, that can be mathematically formulated as follows.

Inverse Problem 4.4 (Computerized tomography with full data). Given the Radon transform $(RF)(s,\theta)$ of f for all $s \in \mathbb{R}$ and $\theta \in \Omega$, determine the unknown density f.

The previous problem will be the basis for the mathematical discussion of the inverse problem in the context of CT in the following sections. However, there is also another problem that is interesting in theory, since in practice sometimes one cannot recover data from a region K. For instance, a prosthesis can ruin the data from lines crossing it, so one needs to recover the density outside that region, form the knowledge of the Radon transform for lines not crossing that region.

Inverse Problem 4.5 (Computerized tomography exterior problem). Given a convex and bounded domain K and the Radon transform $(RF)(s,\theta)$ of f for all $s \in \mathbb{R}$ and $\theta \in \Omega$ such that the line $L_{\theta,s}$ satisfies $L_{\theta,s} \cap K = \emptyset$, determine the unknown density f.

Moreover, it is clear that in real situations one does not have full data, that is, one does not have the value of the Radon transform for all lines, but only for a finite set (s_i,θ_i) for $i = 1, 2, \ldots, n$. There are several possible configuration for the rays. One of them is to use parallel rays and then rotate them, as in the animation in figure 4.2.

Therefore, the numerical methods of interest should consider the following inverse problem.

Inverse Problem 4.6 (Computerized tomography with limited data). Given the Radon transform $(Rf)(s,\theta)$ of f for a finite set $(s_i,\theta_i) \in \mathbb{R} \times \Omega$ for $i = 1, 2, \ldots, n$, determine a (stable) approximation to the unknown density f.

In either case, CT imaging is based on the inversion of the Radon transform. Being the Radon transform based on a integral transformation, we should expect that the inversion of the Radon transform is ill-posed. This statement is supported by theorem 2.33 that makes the integral transformation compact and theorem 2.27 that ensures that the inversion of compact operators is ill-posed. This should be taken into account for the inversion schemes in sections 4.3 and 4.6.

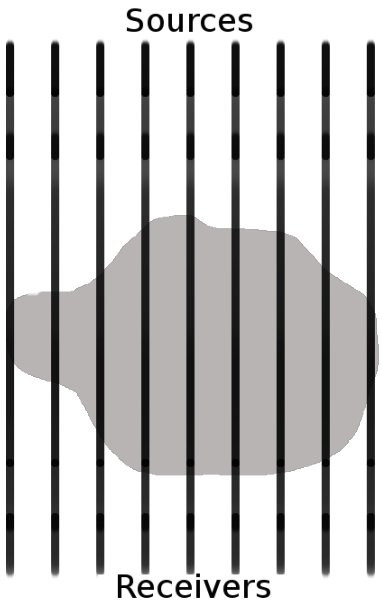

Figure 4.2: Possible configuration of parallel rays for CT imaging (click on the image to animate).

4.2 Fourier Transform

In order to prepare the inversion formulas to the solution of the CT inverse problem 4.4 we will recall the definition and some results on the Fourier transform. Though the definition can be used for higher dimensions, we will focus on the bi-dimensional space $\mathbb{R}^2$, since CT images plane slices.

Definition 4.7 (Fourier Transform).
Let $f \in L^1(\mathbb{R}^m)$.
Then the **Fourier transform** of f is given by

$$\hat{f}(\xi) = \frac{1}{(\sqrt{2\pi})^m} \int_{\mathbb{R}^m} f(x) e^{-i\xi.x} dx, \quad x = (x_1, x_2, \dots x_m)$$

The map

$$\mathcal{F} : f \to \hat{f}$$

is called the **Fourier transformation**.

The Fourier transform has the following properties.

Theorem 4.8 (Properties of the Fourier transform).

Let $f \in L^1(\mathbb{R}^m)$ and $g \in L^1(\mathbb{R}^n)$.

Then,

$$(\mathcal{F}f(x+a))(\xi) = e^{i\xi.a}(\mathcal{F}f)(\xi), \quad \forall a \in \mathbb{R}^m \tag{4.4}$$

$$(\mathcal{F}f(\lambda x))(\xi) = \frac{1}{|\lambda|^m}(\mathcal{F}f)\left(\frac{\xi}{\lambda}\right), \quad \forall \lambda \in \mathbb{R}, \lambda \neq 0 \tag{4.5}$$

$$(\mathcal{F}_{m+n}(f(x)g(y)))(\xi,\eta) = (\mathcal{F}_m f)(\xi)(\mathcal{F}_n g)(\eta) \tag{4.6}$$

Proof. All these proofs are quite trivial, using proper variable changes in the integration. For (4.4), one only needs to take into account that for $y = x + a$ one has

$$\begin{aligned}(\mathcal{F}f(x+a))(\xi) &= \frac{1}{(\sqrt{2\pi})^m}\int_{\mathbb{R}^m} f(x+a)e^{-i\xi.x}dx \\ &= \frac{e^{i\xi.a}}{(\sqrt{2\pi})^m}\int_{\mathbb{R}^m} f(x+a)e^{-i\xi.(x+a)}dx \\ &= \frac{e^{i\xi.a}}{(\sqrt{2\pi})^m}\int_{\mathbb{R}^m} f(y)e^{-i\xi.y}dx \\ &= e^{i\xi.a}(\mathcal{F}f)(\xi).\end{aligned}$$

Similarly, for (4.5) since $y = \lambda x$ implies $dy = |y|^m dx$, one gets

$$\begin{aligned}(\mathcal{F}f(\lambda x))(\xi) =& \frac{1}{(\sqrt{2\pi})^m}\int_{\mathbb{R}^m} f(\lambda x)e^{-i\xi.x}dx \\ =& \frac{1}{(\sqrt{2\pi})^m}\int_{\mathbb{R}^m} f(\lambda x)e^{-i\frac{\xi}{\lambda}.(\lambda x)}dx \\ =& \frac{1}{|\lambda|^m(\sqrt{2\pi})^m}\int_{\mathbb{R}^m} f(y)e^{-i\frac{\xi}{\lambda}.y}dy \\ =& \frac{1}{|\lambda|^m}(\mathcal{F}f)\left(\frac{\xi}{\lambda}\right)\end{aligned}$$

Finally, for (4.5), being $z = (x, y)$, $h(z) = f(x)g(y)$ and $\zeta = (\xi, \eta)$ one gets

$$\begin{aligned}(\mathcal{F}_{m+n}(f(x)g(y)))(\xi,\eta) =&(\mathcal{F}h)(\zeta)\\ =&\frac{1}{\sqrt{2\pi}^{m+n}}\int_{\mathbb{R}^{m+n}} h(z)e^{-i\zeta.z}dz\\ =&\frac{1}{\sqrt{2\pi}^{m+n}}\int_{\mathbb{R}^m}\int_{\mathbb{R}^n} f(x)g(y)e^{-i(\xi.x+\eta.y)}dydx\\ =&\left(\frac{1}{\sqrt{2\pi}^{m}}\int_{\mathbb{R}^m} f(x)e^{-i\xi.x}dx\right)\left(\frac{1}{\sqrt{2\pi}^{n}}\int_{\mathbb{R}^n} g(y)e^{-i\eta.y}dy\right)\\ =&(\mathcal{F}_m f)(\xi)(\mathcal{F}_n g)(\eta)\end{aligned}$$

□

The Fourier transform is, in general, not invertible. However, it would be nice to have a space of functions in which this transform would be invertible. As we will see in the following results, the Fourier transform is invertible in the Schwarz space in definition 4.1. To prepare this result, we will show that the Fourier transform of a derivative of f is related with the Fourier transform of f.

Theorem 4.9.
For $f \in S(\mathbb{R}^m)$ we have that

$$\mathcal{F}(D^j f)(\xi) = (i\xi)^j(\mathcal{F}f)(\xi)$$

with $j \in \mathbb{N}^m$, $\xi^j = (\xi_1^{j_1}, \xi_2^{j_2}, \ldots, \xi_m^{j_m},)$ and $D^j f$ defined as in (2.8).

Proof. In order to use integration by parts and Gauss theorem, we will start by considering the limit of an integral over a bounded domain, namely by

$$(\mathcal{F}f)(\xi) = \frac{1}{(\sqrt{2\pi})^m}\lim_{R\to\infty}\int_{|x|\leq R} f(x)e^{-i\xi.x}dx.$$

In this way, for the derivative of f with respect to x_k, for some $k \in \{1, 2, \ldots, n\}$, by integration by parts one has

$$\begin{aligned}(\sqrt{2\pi})^m\mathcal{F}\left(\frac{\partial f}{\partial x_k}\right)(\xi) =& \lim_{R\to\infty}\int_{|x|\leq R}\frac{\partial f}{\partial x_k}(x)e^{-i\xi.x}dx\\ =& \lim_{R\to\infty}\left[\int_{|x|\leq R}\frac{\partial}{\partial x_k}\left(f(x)e^{-i\xi.x}\right)dx - \int_{|x|\leq R} f(x)\frac{\partial}{\partial x_k}\left(e^{-i\xi.x}\right)dx\right]\end{aligned} \tag{4.7}$$

By Gauss theorem that states that (under some regularity assumptions)

$$\int_D \operatorname{grad} u dx = \int_{\partial D} u.\nu ds,$$

one gets that

$$\int_{|x|\leq R} \operatorname{grad} u dx = \int_{|x|=R} u.\frac{x}{R} ds,$$

and so for the first term on the right hand side of (4.7), one gets

$$\lim_{R\to\infty} \int_{|x|\leq R} \frac{\partial}{\partial x_k} \left(f(x)e^{-i\xi.x}\right) dx = \lim_{R\to\infty} \int_{|x|=R} f(x)e^{-i\xi.x}\frac{x}{R} ds = 0$$

since f is rapidly decaying, since $f \in S(\mathbb{R}^m)$. For the second term on the right hand side of (4.7), one gets

$$\begin{aligned}\lim_{R\to\infty} \int_{|x|\leq R} f(x)\frac{\partial}{\partial x_k} \left(e^{-i\xi.x}\right) dx &= -i\xi_k \lim_{R\to\infty} \int_{|x|\leq R} f(x)e^{-i\xi.x} dx \\ &= -i\xi_k \int_{\mathbb{R}^m} f(x)e^{-i\xi.x} dx \\ &= i\xi_k(\sqrt{2\pi})^m(\mathcal{F}f)(\xi).\end{aligned}$$

Therefore, we have shown that

$$\mathcal{F}\left(\frac{\partial f}{\partial x_k}\right)(\xi) = i\xi_k(\mathcal{F}f)(\xi).$$

The result now follows by repeating the procedure to show that

$$\mathcal{F}\left(\frac{\partial^{j_k} f}{\partial x_k^{j_k}}\right)(\xi) = (i\xi_k)^{j_k}(\mathcal{F}f)(\xi).$$

and then extending the procedure to more than one variable as

$$\mathcal{F}\left(\frac{\partial^{j_1+j_2} f}{\partial x_1^{j_1}\partial x_2^{j_2}}\right)(\xi) = (i\xi_1)^{j_1}(i\xi_2)^{j_2}(\mathcal{F}f)(\xi).$$

□

We are now in the position to show that the Fourier transform is invertible within the Schwarz space. This is the main reason why the Schwarz space is relevant in the context of Fourier transforms.

Theorem 4.10 (Inverse Fourier Transformation).

*The Fourier Transformation $\mathcal{F} : S(\mathbb{R}^m) \to S(\mathbb{R}^m)$ is a bijective map and the **inverse Fourier transformation** is given by*

$$(\mathcal{F}^{-1}g)(x) = \frac{1}{(\sqrt{2\pi})^m} \int_{\mathbb{R}^m} g(\xi) e^{i\xi.x} d\xi, \quad x = (x_1, x_2, \dots x_m) \tag{4.8}$$

Proof. The proof can be found in any harmonic theory book, though it is quite technical. We stress that the proof consists in two steps: $a)$ showing that if $f \in S(\mathbb{R}^m)$ than $\mathcal{F}f \in S(\mathbb{R}^m)$ and $b)$ showing that the inverse operator of $\mathcal{F}$ is given by (4.8). Step $a)$ must be done very carefully since it implies the derivative of an indefinite integral, that are both defined by limits. This creates the additional issue that to interchange the order of the limits one needs to make sure the interchange is legitimate. □

Exercise 4.11. Show that

$$\mathcal{F}^{-1}g = \overline{\mathcal{F}\bar{g}}.$$

Exercise 4.12. Show that

$$D^\alpha_\xi(\mathcal{F}f(x))(\xi) = \mathcal{F}((-ix)^\alpha f(x))(\xi). \tag{4.9}$$

Another important property is the application of the Fourier transformation to the convolution.

Theorem 4.13 (Fourier transform of a convolution).

Let $f, g \in S(\mathbb{R}^m)$.

Then

$$\mathcal{F}(f * g)(\xi) = (\sqrt{2\pi})^m (\mathcal{F}f)(\xi).(\mathcal{F}g)(\xi), \tag{4.10}$$

where the convolution operator $*$ is defined by

$$(f * g)(x) = \int_{\mathbb{R}^m} f(x - y) g(y) dy.$$

Proof. We have that

$$\begin{aligned}
\mathcal{F}(f*g)(\xi) &= \frac{1}{(\sqrt{2\pi})^m}\int_{\mathbb{R}^m} e^{-i\xi.x}\int_{\mathbb{R}^m} f(x-y)g(y)dydx,\\
&= \frac{1}{(\sqrt{2\pi})^m}\int_{\mathbb{R}^m} e^{-i\xi.x}\int_{\mathbb{R}^m} f(x-y)g(y)dydx,\\
&= \frac{1}{(\sqrt{2\pi})^m}\int_{\mathbb{R}^m} g(y)\int_{\mathbb{R}^m} e^{-i\xi.x)}f(x-y)dxdy,\\
&= \frac{1}{(\sqrt{2\pi})^m}\int_{\mathbb{R}^m} g(y)e^{-i\xi.y}\int_{\mathbb{R}^m} e^{-i\xi.(x-y)}f(x-y)dxdy,
\end{aligned}$$

Now, performing the change of variable $\tilde{x} = x - y$ in the inner integral, one gets

$$\begin{aligned}
\mathcal{F}(f*g)(\xi) &= \frac{1}{(\sqrt{2\pi})^m}\int_{\mathbb{R}^m} g(y)e^{-i\xi.y}\int_{\mathbb{R}^m} e^{-i\xi.(x-y)}f(x-y)dxdy,\\
&= \frac{1}{(\sqrt{2\pi})^m}\int_{\mathbb{R}^m} g(y)e^{-i\xi.y}\int_{\mathbb{R}^m} e^{-i\xi.\tilde{x}}f(\tilde{x})d\tilde{x}dy,\\
&= \frac{1}{(\sqrt{2\pi})^m}\int_{\mathbb{R}^m} g(y)e^{-i\xi.y}dy\int_{\mathbb{R}^m} e^{-i\xi.\tilde{x}}f(\tilde{x})d\tilde{x},\\
&= (\sqrt{2\pi})^m(\mathcal{F}f)(\xi).(\mathcal{F}g)(\xi).
\end{aligned}$$

□

Another important property of the Fourier transform is given by Parseval's formulas.

Theorem 4.14 (Parseval's formulas).
For $f, g \in S(\mathbb{R}^m)$ one has ***Parseval's formulas***

$$\int_{\mathbb{R}^m} \hat{f}(\xi)g(\xi)d\xi = \int_{\mathbb{R}^m} f(\xi)\hat{g}(\xi)d\xi, \tag{4.11}$$

$$\int_{\mathbb{R}^m} \hat{f}(\xi)\bar{\hat{g}}(\xi)d\xi = \int_{\mathbb{R}^m} f(\xi)\bar{g}(\xi)d\xi. \tag{4.12}$$

Proof. We leave the proof as an exercise. □

A direct corollary of the previous result is that the Fourier transform $\mathcal{F}$ is an isomorphism, that is,

$$\|\mathcal{F}f\|_{L^2} = \|f\|_{L^2}.$$

This comes directly from (4.12) with $g = f$. To finalize this section, and therefore mention the main tools regarding Fourier transform that we will need for the inversion formulas and reconstruction algorithms in the next sections, we enunciate the Poisson summation formula.

Theorem 4.15 (Poisson summation formula).
For $f \in S(\mathbb{R}^m)$ we have the ***Poisson summation formula***

$$\sum_{j\in\mathbb{Z}^m} \hat{f}\left(\xi - \frac{2\pi j}{h}\right) = \frac{h^m}{(\sqrt{2\pi})^m} \sum_{j\in\mathbb{Z}^m} f(jh)e^{-ih\xi.j}. \tag{4.13}$$

4.3 Inversion Formulas

We are now in a good place to address some inversion formulas for the solution of the Computerized tomography (CT) inversion problem. In the last section, we were introducing some concepts as the Radon transform and the Fourier transform, and some of their properties. We have seen that the Radon transform is clearly related with the solution of the inverse problem 4.4 of CT, since this problem consists in the regularized inversion of the Radon transform. However, the use of the Fourier transform to this end is still to be revealed. To shed some light on this issue, we will start by establishing the Fourier transform of the Radon transform. The following theorem is known has the **Projection theorem** or the **Fourier slice theorem**.

Theorem 4.16 (Projection theorem).
For $f \in S(\mathbb{R}^2)$ one has

$$\hat{f}(r\theta) = \frac{1}{\sqrt{2\pi}}(\widehat{Rf})(\theta, r), \tag{4.14}$$

where one has a 2D Fourier transform on the left-hand side and a 1D Fourier transform (with respect to the second variable s) on the right-hand side.

Proof. The proof comes directly from the definition of Fourier transform, since

$$\begin{aligned}\sqrt{2\pi}(\widehat{Rf})(\theta, r) &= \int_{-\infty}^{\infty} (Rf)(\theta, s)e^{-isr}ds \\ &= \int_{-\infty}^{\infty}\int_{-\infty}^{\infty} f(s\theta + \theta^{\perp}t)e^{-isr}dtds.\end{aligned}$$

Now performing the change of variable $x = s\theta + t\theta^{\perp}$, since $x.\theta = s$, one has

$$\begin{aligned}\sqrt{2\pi}(\widehat{Rf})(\theta, r) &= \int_{-\infty}^{\infty}\int_{-\infty}^{\infty} f(s\theta + \theta^{\perp}t)e^{-irs}dtds \\ &= \int_{\mathbb{R}^2} f(x)e^{-ir\theta.x}dx \\ &= 2\pi\hat{f}(r\theta)\end{aligned}$$

as we intended to proof. □

We now define the Schwarz space in the domain $\Omega\times\mathbb{R}$ of the Radon transform as follows.

Definition 4.17.
We define the Schwarz space in the domain $\Omega \times \mathbb{R}$ as

$$S(\Omega \times \mathbb{R}) := \{g \in C^{\infty}(\Omega \times \mathbb{R}) : g(\theta, .) \in S(\mathbb{R}) \text{ uniformly for all } \theta \in \Omega\}. \quad (4.15)$$

With this definition, we can state the following result for the Radon transform of a function in the Schwarz space.

Corollary 4.18. *If $f \in S(\mathbb{R})$, then $Rf \in S(\Omega \times \mathbb{R})$.*

Proof. Follows directly from theorem 4.10 and 4.16, first to show that $\hat{f} \in S(\mathbb{R})$, than to show that $\widehat{Rf} \in S(\Omega \times \mathbb{R})$ and finally that $Rf \in S(\Omega \times \mathbb{R})$. □

To prepare the first inversion formula, we will first characterize the adjoint operator of the Radon transform.

Theorem 4.19 (Adjoint operator of the Radon Transform).
The operator $R^* : S(\Omega \times \mathbb{R}) \to S(\mathbb{R}^2)$ given by

$$(R^*g)(x) := \int_{\Omega} g(\theta, x.\theta)d\theta \quad (4.16)$$

is the L^2 adjoint of the Radon transform operator R given by (4.3).

Proof. We have to show that for $f \in S(\mathbb{R}^2)$ and $g \in S(\Omega \times \mathbb{R})$ one has

$$\int_{\Omega}\int_{-\infty}^{\infty}(Rf)(\theta, s)g(\theta, s)dsd\theta = \int_{\mathbb{R}^2} f(x)R^*g(x)dx.$$

This can be done, since

$$\begin{aligned}\int_\Omega \int_{-\infty}^{\infty} (Rf)(\theta,s)g(\theta,s)dsd\theta &= \int_\Omega \int_{-\infty}^{\infty}\int_{-\infty}^{\infty} f(s\theta+t\theta^\perp)g(\theta,s)dtdsd\theta \\ &= \int_\Omega \int_{\mathbb{R}^2} f(x)g(\theta,x.\theta)dxd\theta \quad (x = s\theta+t\theta^\perp \Rightarrow x.\theta = s) \\ &= \int_{\mathbb{R}^2} f(x)\int_\Omega g(\theta,x.\theta)d\theta dx \\ &= \int_{\mathbb{R}^2} f(x)(R^*g)(x)dx.\end{aligned}$$

□

In the next subsections, we will consider some inversion formulas for the CT inverse problem 4.4. Some of them will be useful for reconstruction algorithms, while others will only be useful to prove uniqueness of solution.

4.3.1 Radon's Inversion Formula

Radon (1917) developed the next inversion formula for Radon the transform.

Theorem 4.20 (Radon's inversion formula).
*For $f \in S(\mathbb{R}^2)$ one has the **Radon's inversion Formula** given by*

$$f = \frac{1}{4\pi} R^* H \frac{\partial}{\partial s} Rf \tag{4.17}$$

where the Hilbert transform[1] *is defined by*

$$(Hg)(s) := \frac{1}{\pi}\int_{-\infty}^{\infty} \frac{g(t)}{s-t}dt, \quad s \in \mathbb{R}. \tag{4.18}$$

Proof. We start by noting that

$$\begin{aligned} f(x) &= \left(\mathcal{F}^{-1}\hat{f}\right)(x) \\ &= \frac{1}{2\pi}\int_{\mathbb{R}^2} e^{ix.\xi}\hat{f}(\xi)d\xi \end{aligned}$$

[1]The Hilbert transform is well-defined in $S(\mathbb{R})$ as a Cauchy singular value

$$\int_{-\infty}^{\infty}\frac{g(t)}{s-t}dt = \lim_{\varepsilon\to 0}\left[\int_{-\infty}^{s-\varepsilon}\frac{g(t)}{s-t}dt + \int_{s+\varepsilon}^{\infty}\frac{g(t)}{s-t}dt\right].$$

and making the change of variable $\xi = r\theta$, we get from (4.14) that

$$\begin{aligned} f(x) &= \frac{1}{2\pi}\int_{\Omega}\int_{-\infty}^{\infty} e^{irx.\theta}\hat{f}(r\theta)rdrd\theta \\ &= \frac{1}{\sqrt{2\pi}}\frac{1}{2\pi}\int_{\Omega}\int_{0}^{\infty} e^{irx.\theta}\widehat{Rf}(\theta,r)rdrd\theta \end{aligned}$$

Now, noting that

$$\begin{aligned} \widehat{Rf}(-\theta,-r) &= \frac{1}{\sqrt{2\pi}}\int_{-\infty}^{\infty} e^{irs}Rf(-\theta,s)ds \\ &= \frac{1}{\sqrt{2\pi}}\int_{-\infty}^{\infty} e^{-irs}Rf(-\theta,-s)ds \\ &= \frac{1}{\sqrt{2\pi}}\int_{-\infty}^{\infty} e^{-irs}Rf(\theta,s)ds \quad \text{(since } Rf(\theta,s) = Rf(-\theta,-s)\text{)} \\ &= \widehat{Rf}(\theta,r), \end{aligned}$$

we get

$$\begin{aligned} f(x) &= \frac{1}{\sqrt{2\pi}}\frac{1}{2\pi}\int_{\Omega}\int_{0}^{\infty} e^{irx.\theta}\widehat{Rf}(\theta,r)rdrd\theta \\ &= \frac{1}{2}\frac{1}{\sqrt{2\pi}}\frac{1}{2\pi}\int_{\Omega}\int_{-\infty}^{\infty} e^{irx.\theta}\widehat{Rf}(\theta,r)|r|drd\theta. \end{aligned}$$

Defining now

$$h(\theta,r) = \frac{1}{\sqrt{2\pi}}\int_{-\infty}^{\infty} e^{irs}\widehat{Rf}(\theta,r)|r|dr, \tag{4.19}$$

one gets

$$\begin{aligned} f(x) &= \frac{1}{2}\frac{1}{\sqrt{2\pi}}\frac{1}{2\pi}\int_{\Omega}\int_{-\infty}^{\infty} e^{irx.\theta}\widehat{Rf}(\theta,r)|r|drd\theta \\ &= \frac{1}{2}\frac{1}{2\pi}\int_{\Omega} h(\theta,x.\theta)d\theta \\ &= \frac{1}{4\pi}\left(R^{*}h\right)(x). \end{aligned}$$

To complete the proof, we need to show that

$$h(\theta,r) = H\frac{\partial}{\partial s}Rf.$$

To this end, one has

$$\begin{aligned}\frac{\partial}{\partial s}(Rf)(\theta,s) &= \frac{\partial}{\partial s}\left[\mathcal{F}^{-1}\widehat{Rf}(\theta,s)\right]\\ &= \frac{1}{\sqrt{2\pi}}\int_{-\infty}^{\infty} ire^{irs}\widehat{Rf}(\theta,s)dr\end{aligned}$$

which can be shown similarly to (4.9). Using the change of variable $t = s - t$, one can write the Hilbert transform as

$$(Hg)(s) := \frac{1}{\pi}\int_{-\infty}^{\infty}\frac{g(s-t)}{t}dt,$$

while using the change of variable $t = s + t$ one as

$$(Hg)(s) := -\frac{1}{\pi}\int_{-\infty}^{\infty}\frac{g(s+t)}{t}dt.$$

Summing both of the previous equations, one has

$$(Hg)(s) := \frac{1}{2\pi}\int_{-\infty}^{\infty}\frac{g(s-t)-g(s+t)}{t}dt,$$

so, since $e^{ir(s-t)} + e^{ir(s+t)} = -2ie^{irs}\sin(tr)$, one has

$$\begin{aligned}\left(H\frac{\partial}{\partial s}(Rf)\right)(\theta,s) &= H\left(\frac{1}{\sqrt{2\pi}}\int_{-\infty}^{\infty} ire^{irs}\widehat{Rf}(\theta,s)dr\right)\\ &= \frac{1}{\pi\sqrt{2\pi}}\int_{-\infty}^{\infty}\frac{1}{t}r\sin(tr)e^{irs}\int_{-\infty}^{\infty}\widehat{Rf}(\theta,s)drdt\\ &= \frac{1}{\pi\sqrt{2\pi}}\int_{-\infty}^{\infty} re^{irs}\widehat{Rf}(\theta,s)\int_{-\infty}^{\infty}\frac{1}{t}\sin(tr)dtdr.\end{aligned}$$

The result is now proven by noting (by integration by parts several times) that

$$\frac{1}{\pi}\int_{-\infty}^{\infty}\frac{1}{t}\sin(tr)dt = \operatorname{sgn}(r),$$

and therefore, since $|r| = r\operatorname{sgn}(r)$, one gets

$$\begin{aligned}\left(H\frac{\partial}{\partial s}(Rf)\right)(\theta,s) &= \frac{1}{\pi\sqrt{2\pi}}\int_{-\infty}^{\infty} re^{irs}\widehat{Rf}(\theta,s)\int_{-\infty}^{\infty}\frac{1}{t}\sin(tr)dtdr\\ &= \frac{1}{\sqrt{2\pi}}\int_{-\infty}^{\infty} r\operatorname{sgn}(r)e^{irs}\widehat{Rf}(\theta,s)dr\\ &= \frac{1}{\sqrt{2\pi}}\int_{-\infty}^{\infty}|r|e^{irs}\widehat{Rf}(\theta,s)dr\\ &= h(\theta,s)\end{aligned}$$

as defined in (4.19). □

It is clear that Radon's inversion formula (4.17) is useless for numerical reconstruction purposes. Note that the presence of the derivative $\frac{\partial}{\partial s}$ makes the inversion formula highly unstable, as illustrate in example 1.4 of the Introduction. However this inversion formula has importance for uniqueness results, as shown in section 4.4.

4.3.2 Cormack's Inversion Formula

Cormack's inversion formula starts by considering the representation of the solution as a Fourier series in polar coordinates. We will leave most of the details out of this text, and will only show some steps in the long way to show Cormack's inversion formula. We refer to [Kress, 2005, Natterer, 2001] for details.

In polar coordinates, one represents a point $x \in \mathbb{R}^2$ as

$$x = (r\cos\alpha, r\sin\alpha), \quad r \geq 0,\ \alpha \in [0, 2\pi].$$

Then, one represents the density f in Fourier series as

$$f(x) = \sum_{m=-\infty}^{\infty} f_m(r) e^{im\alpha} \tag{4.20}$$

where

$$f_m(r) = \int_0^{2\pi} f(x) e^{-im\alpha} d\alpha.$$

In the same way, the data g (which is the Radon transform of f) would be defined as

$$g(\theta, s) = \sum_{m=-\infty}^{\infty} g_m(s) e^{im\alpha} \tag{4.21}$$

where

$$g_m(s) = \frac{1}{2\pi} \int_0^{2\pi} g\Big((\cos\alpha, \sin\alpha), s\Big) e^{-im\alpha} d\alpha.$$

The idea is to express f_m in terms of g_m and therefore find a way to reconstruct f from the knowledge of $g = Rf$. The first question that one needs to ask is whether the series (4.20) converges.

Theorem 4.21.

Let $f \in S(\mathbb{R}^2)$.

Then the Fourier series (4.20) *converges .*

Proof. The result follows from the fact that if $f \in S(\mathbb{R}^2)$, then $f \in C^\infty(\mathbb{R}^2)$ and therefore the Fourier Series converges. In fact, one can prove a little bit more, since by integration by parts one can gets

$$f_m(r) = \frac{1}{2\pi(im)^k} \int_0^{2\pi} \frac{\partial^k}{\partial \alpha^k} f(r\cos\alpha, r\sin\alpha) e^{-im\alpha} d\alpha$$

and since $f \in S(\mathbb{R}^2)$ one gets that

$$\left| r^n \frac{\partial^k}{\partial \alpha^k} f(r\cos\alpha, r\sin\alpha) \right| \leq C_{n,k}$$

and therefore

$$|r^n f_m(r)| \leq \frac{C_{n,k}}{m^k} dr. \tag{4.22}$$

□

The following theorem relates the Fourier coefficients f_m of the density f (as in (4.20)) with the Fourier coefficients g_m of the data $g = Rf$ (as in (4.21)).

Theorem 4.22.

Let $f \in S(\mathbb{R}^2)$.

Then, the Fourier coefficients (4.20) *of f are related with the Fourier coefficients* (4.21) *of $g = Rf$ by*

$$g_m(s) = 2 \int_s^\infty f_m(r) \frac{T_{|m|}\left(\frac{s}{r}\right)}{\sqrt{1 - \frac{s^2}{r^2}}}, \tag{4.23}$$

for all $m \in \mathbb{Z}$ and $s > 0$, where

$$T_m(r) = \arccos\left(m\cos(r)\right). \tag{4.24}$$

Proof. The result follows (in a non-trivial way) from geometrical arguments and integration by parts by taking the Radon transform of each coefficient f_m of f. We refer to [Kress, 2005] for the complete proof. □

The inversion formula comes now from inverting the integral equation (4.23), in order to obtain f_m in terms of the coefficients g_m and therefore being able to reconstruct f from the coefficients g_m of the data $g = Rf$.

This can be done (see [Kress, 2005]) by the use of the **Mellin transform**

$$(Mf)(s) := \int_0^\infty f(t) t^{s-1} dt, \quad s \in \mathbb{C}$$

which is defined for f such that any restriction of f to a closed interval $[a, b]$ is in $L^1([a, b])$.[2]

The next step is to show (see [Kress, 2005]) from (4.23) and the properties of the Mellin transform that

$$(Mg_m)(s) = M(rf_m)(s)(Mp)(s)$$

for $p = 2\frac{T_{|m|}(t)}{\sqrt{1-t^2}}$. Then one can show that

$$M(rf_m)(s) = \frac{(Mg_m)(s)}{(Mp)(s)} = (Mg_m)(s)(M\tilde{q})(s)$$

for some appropriate $\tilde{q}$. From the fact that (under some assumptions, see [Kress, 2005]) the Mellin transform satisfies

$$(Mg_m)(M\tilde{q}) = M(g_m * \tilde{q})$$

where $*$ is the convolution operator, the inversion formula

$$rf_m = g_m * \tilde{q}$$

now follows from the injectivity of the Mellin transformation for $f \in S([0, \infty])$. Following the previous procedure, one has Cormack's inversion formula.

Theorem 4.23 (Cormack's inversion formula).

Let $f \in S(\mathbb{R}^2)$.

*Then, we have the **Cormack's inversion formula** for the Fourier coefficients*

$$f_m(r) = -\frac{1}{\pi}\int_r^\infty g_m'(s)\frac{T_{|m|}\left(\frac{s}{r}\right)}{\sqrt{s^2-r^2}}ds, \quad r \geq 0, m \in \mathbb{Z} \tag{4.25}$$

Cormack's inversion formula is nor the best way to numerically reconstruct the density f directly, since one can show by the Helgason-Ludwig theorem (See [Kress, 2005, Natterer, 2001]) that g_m is rapidly oscillating. There are ways to stabilize the process, but the main use of this formula is again uniqueness results.

[2]The function space of functions whose restriction to any closed interval $[a, b]$ is in $L^1([a, b])$ is usually denoted by $L^1_{loc}(\mathbb{R}.)$ In this way, the Mellin transform is defined for $f \in L^1_{loc}([0, \infty])$.

4.4 Uniqueness

In this section, we will address some uniqueness results. The first one concerns the inverse problem for full data 4.4.

Theorem 4.24 (Uniqueness for full data).
Let $f_1, f_2 \in S(\mathbb{R}^2)$.
If $g_1 = g_2$ *for* $g_1 := Rf_1$ *and* $g_2 := Rf_2$, *then* $f_1 = f_2$.

Proof. This results comes directly from the Radon's Inversion formula (4.17). □

Another important result, is the uniqueness result for the exterior inverse problem 4.5.

Theorem 4.25 (Uniqueness for the exterior problem).
Let $f_1, f_2 \in S(\mathbb{R}^2)$ *and* $K \subset \mathbb{R}^2$ *a convex and bounded set.*
If $g_1 = g_2$ *for* $g_1 := Rf_1$ *and* $g_2 := Rf_2$ *for all lines* $L_{\theta,s}$ *such that* $L_{\theta,s} \cap K = \emptyset$. *Then* $f_1 = f_2$ *in* $\mathbb{R}^2 \setminus K$.

Proof. If K is a disk of radius $\tilde{r}$, the result comes directly from Cormack's Inversion formula (4.25) using $r \geq \tilde{r}$.

Otherwise, since K is bounded and convex, for every $x \notin K$ there exists a disk $K_{D,x}$ containing K such that $x \notin K_{D,x}$. Therefore, one applies the previous argument to show that $f_1 = f_2$ outside $K_{D,x}$ and therefore $f_1 = f_2$ in K. □

We will now say some words on uniqueness for the case were we do not have full data. We will start by the case where instead of considering all angles θ we only consider a countable (infinite) number of them.

Theorem 4.26 (Uniqueness for countably many θ).
Let $f \in C_0^\infty(\mathbb{R}^2)$, *that is,* $f \in C^\infty(\mathbb{R}^2)$ *and has a compact support*[3].
If $Rf(\theta_n, .) = 0$ *for countably many* $\theta_1, \theta_2, \ldots, \theta_n, \ldots$, *then* $f = 0$.

Proof. We start by reminding that if f has compact support than its Fourier transform $\hat{f}$ is analytic. As $Rf(\theta_n, s) = 0$ then $\widehat{Rf}(\theta_n, r) = 0$. Now from the projection theorem 4.16

$$\hat{f}(r\theta_n) = \frac{1}{\sqrt{2\pi}} \widehat{Rf}(\theta_n, r) = 0$$

for countably many θ_n, $n \in \mathbb{N}$. As $\hat{f}$ is analytic, then $\hat{f} = 0$ so $f = 0$. □

[3]If f has **support** K this means that $f = 0$ outside K.

The uniqueness for a finite number of angles $\theta_1, \theta_2, \ldots, \theta_n$ cannot be proven. However, a question arises of what is the degree of non-uniqueness for the problem with only a finite set of angles. It can be shown (see [Kress, 2005]) that if f a compact support in K_0 then for any compact set $K \subset K_0$, there exists $\tilde{f} \in C^\infty(\mathbb{R}^2)$ with compact support in K_0 such that $\tilde{f} = f$ in K and $R\tilde{f}(\theta_j, .) = 0$ for $j = 1, 2, \ldots, n$. This shows that the density $f + \tilde{f}$ provides the same data for the CT problem then f, since

$$R(f + \tilde{f})(\theta_j, .) = (Rf)(\theta_j, .) + (R\tilde{f})(\theta_j, .) = (Rf)(\theta_j, .), \quad j = 1, 2, \ldots, n.$$

4.5 Shannon's Theorem

Until now, we were focused on the proof of uniqueness. In fact the inversions formulas that we studied so far were more related with uniqueness than with reconstruction algorithms. In this section, we will present a theorem that plants the seed to obtain reconstruction algorithms for band limited functions. We will start by defining this concept.

Definition 4.27 (Band-limited function).

A function $f \in L^1(\mathbb{R}^m)$ is called **band limited** if there exists b such that

$$\hat{f}(\xi) = 0, \forall |\xi| > b.$$

The smaller b with this property is called the **band width** of f.

Remark 4.28. If f is band limited, then by the inverse Fourier transform it is clear that f does not have larger frequencies than b and therefore it does not have smaller periods than $\frac{2\pi}{b}$. In this sense, f does not have smaller oscillations than $\frac{2\pi}{b}$ and therefore the smaller the band width b the larger the details of f, since small details require high frequencies.

Shannon's Sampling theorem determines the degree of detail that a band limited function needs to bew uniquely defined, or in other words, the spacement of a grid of points to uniquely determine a band limited function.

Theorem 4.29 (Shannon's Sampling Theorem).

Let $f, g \in L^2(\mathbb{R}^m)$ be band limited functions with band width b.

Let $h < \frac{\pi}{b}$.

Then f is uniquely determined by its values at equidistant grid points jh with $j \in \mathbb{Z}^m$ and can be given by the series

$$f(x) = \sum_{j \in \mathbb{Z}^m} f(jh) \mathrm{sinc}\left(\frac{\pi}{h}(x - jh)\right), \tag{4.26}$$

which converges in $L^2(\mathbb{R}^m)$ *and where*

$$\operatorname{sinc}(x) = \begin{cases} \frac{\sin(x)}{x}, & x \neq 0 \\ 1, & x = 0 \end{cases}, \quad x \in \mathbb{R},$$

and for $x \in \mathbb{R}^m$ *then* $\operatorname{sinc}(x) = \operatorname{sinc}(x_1) \times \operatorname{sinc}(x_2) \times \cdots \times \operatorname{sinc}(x_m))$.

Moreover, the Fourier transform of f *is determined by*

$$\hat{f}(\xi) = \frac{h^m}{(\sqrt{2\pi})^m} \sum_{j \in \mathbb{Z}^m} f(jh) e^{-i\xi . jh}, \tag{4.27}$$

which converges in $L^2\left(\left[-\frac{\pi}{h}, \frac{\pi}{h}\right]^m\right)$.

Finally, the L^2*-inner product of two band limited functions is determined by*

$$\int_{\mathbb{R}^m} f(x)\bar{g}(x)dx = h^m \sum_{j \in \mathbb{Z}^m} f(jh)\bar{g}(jh). \tag{4.28}$$

Remark 4.30. Shannon's sampling theorem has several implications. The first one is that the Fourier transform and the L^2 inner product of band limited functions can be determined exactly by the trapezoidal rule with appropriate spacement. Moreover, the so called **Nyquist condition** $h < \frac{\pi}{b}$ requires step size $h < \frac{1}{2}\frac{2\pi}{b}$, being $\frac{2\pi}{b}$ the size of the smaller period in f.

To what follows, let us define the operator

$$(S_h f)(x) := \sum_{j \in \mathbb{Z}^m} f(jh) \operatorname{sinc}\left(\frac{\pi}{h}(x - jh)\right). \tag{4.29}$$

It is clear from (4.26) that for band limited functions one has $S_h f = f$.

The importance of Shannon's Sampling theorem to our context of recovering densities $f \in S(\mathbb{R}^2)$ from the data $g = Rf$ starts to be unveiled in the next result, which establishes an upper bound for the error of approximating f by $S_h f$ for a general $f \in S(\mathbb{R}^m)$.

Theorem 4.31.

Let $f \in S(\mathbb{R}^m)$.

Then

$$\|S_h f - f\|_\infty \leq \frac{2}{(\sqrt{2\pi})^m} \int_{|\xi \geq \frac{\pi}{h}|} |\hat{f}(\xi)| d\xi. \tag{4.30}$$

Proof. See [Kress, 2005]. □

Now, from the properties of the Fourier transform (4.10), it is clear that the convolution of a limited band filter with any other function in $S(\mathbb{R}^2)$ is a band limited function. In this way, band limited functions are usually called **low-pass filters**, since the convolution with this functions eliminates the high frequencies. This will be the seed to the first reconstruction algorithm, namely the filtered back projection, where instead of aiming to reconstruct the density f we will aim at reconstructing a low-pass filtered version $W_b * f$, where W_b is an appropriate low-pass filter. We then know that the error with this approximation is bounded by (4.30), that is low, if f has few high frequencies.

Exercise 4.32. Show that sinc is a pass filter, by computing the integral

$$I = \frac{\sqrt{2\pi}}{2} \int_{-1}^{1} e^{i\xi.x} d\xi.$$

Answer.

Since for the function

$$\chi(x) = \begin{cases} \frac{1}{2}, & x \in [-1,1] \\ 0, & x \notin [-1,1] \end{cases}$$

one has

$$\begin{aligned} (\mathcal{F}^{-1}\chi)(x) &= \frac{\sqrt{2\pi}}{2} \int_{-1}^{1} e^{i\xi x} d\xi \\ &= \left[\frac{e^{i\xi x}}{2ix} \right]_{-1}^{1} \\ &= \frac{e^{ix} - e^{-ix}}{2ix} \\ &= \frac{\sin(x)}{x} \\ &= \mathrm{sinc}(x) \end{aligned}$$

one has that $\widehat{\mathrm{sinc}}(\xi) = \chi(\xi)$ and therefore sinc is band limited since $\widehat{\mathrm{sinc}}(\xi) = 0$ for $|\xi| > 1$.

4.6 Reconstructions algorithms

In this section, we will consider some reconstruction methods to numerically recover the density f from the given data $g = Rf$.. We refer, for instance,

to [Kress, 2005, Natterer, 2001] for a theoretical background on the several possibilities. The review paper [Louis, 2006] presents several practical methods and some numerical reconstructions.

4.6.1 Filtered Back projection (FBP)

From the error estimate (4.30) and the following considerations, the main idea of the filtered back projection is to recover a filtered version $W_b * f$ of f, being W_b a low pass-filter. To this end, we will take the Radon inversion formula (4.17) and try to write it as

$$f = \underbrace{R^*}_{\text{Back projection}} \underbrace{\frac{1}{4\pi} H \frac{\partial}{\partial s}}_{\text{Approx. by convolution}} \underbrace{Rf}_{\text{data}}$$

or in other words, try to get a relation of the form

$$W_b * f = R^*(\omega_b * Rf). \tag{4.31}$$

This is possible, due to the following result.

Theorem 4.33.
Let $f_1, f_2 \in S(\mathbb{R}^2)$. Then

$$R(f_1 * f_2) = (Rf_1) * (Rf_2). \tag{4.32}$$

Let $f \in S(\mathbb{R}^2)$ and $g \in S(\Omega \times \mathbb{R})$. Then

$$(R^* g) * f = R^*(g * Rf). \tag{4.33}$$

Proof. The relation (4.32) comes directly from the alternate use of the projection theorem 4.16 and the Fourier transform of a convolution (4.10), namely by

$$\begin{aligned}
\mathcal{F}\left(R(f_1 * f_2)\right)(\theta, s) &= \sqrt{2\pi}\mathcal{F}\left(f_1 * f_2\right)(s\theta) \\
&= (\sqrt{2\pi})^3 \left(\mathcal{F}f_1(s\theta).\mathcal{F}f_2(s\theta)\right) \\
&= \sqrt{2\pi}\left(\mathcal{F}Rf_1(\theta, s).\mathcal{F}Rf_2(\theta, s)\right) \\
&= \mathcal{F}\left(Rf_1(\theta, s) * Rf_2(\theta, s)\right).
\end{aligned}$$

Now the injectivity of the Fourier transform gives the result (4.32). To prove (4.33),

by the definition of convolution and of R^* one has

$$\begin{aligned}(R^*g) * f)(x) &= \int_{\mathbb{R}^2} (R^*g)(x-y)f(y)dy \\ &= \int_{\mathbb{R}^2}\int_{\Omega} g(\theta,(x-y).\theta)f(y)d\theta dy \\ &= \int_{\Omega}\int_{\mathbb{R}^2} g(\theta,(x-y).\theta)f(y)dyd\theta.\end{aligned}$$

Now, by making the change of variable $y = s\theta + t\theta^{\perp}$, that implies $y.\theta = s$, one has

$$\begin{aligned}(R^*g) * f)(x) &= \int_{\Omega}\int_{\mathbb{R}^2} g(\theta,(x-y).\theta)f(y)dyd\theta \\ &= \int_{\Omega}\int_{-\infty}^{\infty}\int_{-\infty}^{\infty} g(\theta,x.\theta-s)f(s\theta+t\theta^{\perp})dtdsd\theta \\ &= \int_{\Omega}\int_{-\infty}^{\infty} g(\theta,x.\theta-s)\underbrace{\int_{-\infty}^{\infty} f(s\theta+t\theta^{\perp})dt}_{=Rf(\theta,s)}dsd\theta \\ &= \int_{\Omega}\int_{-\infty}^{\infty} g(\theta,x.\theta-s)Rf(\theta,s)dsd\theta \\ &= \int_{\Omega} (g*Rf)(\theta,x.\theta)d\theta \\ &= R^*(g*Rf)(x),\end{aligned}$$

as we wanted to prove. □

The identity (4.33) allows our goal of find an identity of the form (4.31), so in this way, (4.33) can be seen as an inversion formula for a filtered solution. In fact, replacing g by ω_b in (4.33), one gets

$$\underbrace{(R^*w_b)}_{=W_b} * f = R^*(\omega_b * \underbrace{Rf}_{g}), \tag{4.34}$$

so our goal now is to find ω_b such that $W_b = (R^*w_b)$ is the optimal low-pass filter. Therefore, in order to guarantee that W_b is band limited, we need to study the behaviour of the Fourier Transform of R^*g, as in the following theorem.

Theorem 4.34.

Let $g \in S(\Omega \times \mathbb{R})$. Then

$$\widehat{R^*g}(\xi) = \frac{\sqrt{2\pi}}{|\xi|}\left[\hat{g}\left(\frac{xi}{|\xi|},|\xi|\right) + \hat{g}\left(-\frac{xi}{|\xi|},-|\xi|\right)\right], \quad \xi \neq 0. \tag{4.35}$$

Proof. For any $w \in C^\infty(\mathbb{R}^2)$, using Parseval's formula (4.11) and the definition of adjoint operator R^*, we have

$$\begin{aligned}\int_{\mathbb{R}^2} \widehat{R^*g}(\xi)w(\xi)d\xi &= \int_{\mathbb{R}^2} R^*g(\xi)\hat{w}(\xi)d\xi \\ &= (R^*g, \hat{w})_{L^2(\mathbb{R}^2)} \\ &= (g, R\hat{w})_{L^2(\Omega\times\mathbb{R})} \\ &= \int_\Omega \int_{\mathbb{R}} g(\theta, s)(R\hat{w})(\theta, s)dsd\theta.\end{aligned}$$

Using Parseval's formula (4.11) in the second variable one has

$$\begin{aligned}\int_{\mathbb{R}^2} \widehat{R^*g}(\xi)w(\xi)d\xi &= \int_\Omega \int_{\mathbb{R}} g(\theta, s)(R\hat{w})(\theta, s)dsd\theta \\ &= \int_\Omega \int_{\mathbb{R}} \hat{g}(\theta, \sigma)(\mathcal{F}^{-1}R\hat{w})(\theta, \sigma)d\sigma d\theta.\end{aligned}$$

Now, by the projection theorem (4.14)

$$\begin{aligned}\mathcal{F}^{-1}R\hat{w}(\theta, \sigma) &= \sqrt{2\pi}\mathcal{F}^{-1}\hat{w}(\sigma\theta) \\ &= \sqrt{2\pi}w(\sigma\theta)\end{aligned}$$

so

$$\begin{aligned}\int_{\mathbb{R}^2} \widehat{R^*g}(\xi)w(\xi)d\xi &= \int_\Omega \int_{\mathbb{R}} \hat{g}(\theta, \sigma)\left(\mathcal{F}^{-1}R\hat{w}\right)(\theta, \sigma)d\sigma d\theta \\ &= \sqrt{2\pi}\int_\Omega \int_{\mathbb{R}} \hat{g}(\theta, \sigma)w(\sigma\theta)d\sigma d\theta \\ &= \sqrt{2\pi}\int_\Omega \left(\int_{-\infty}^0 \hat{g}(\theta, \sigma)w(\sigma\theta)d\sigma + \int_0^{+\infty} \hat{g}(\theta, \sigma)w(\sigma\theta)d\sigma\right) d\theta \\ &= \sqrt{2\pi}\int_\Omega \left(\int_0^{+\infty} \hat{g}(\theta, -\sigma)w(-\sigma\theta)d\sigma + \int_0^{+\infty} \hat{g}(\theta, \sigma)w(\sigma\theta)d\sigma\right) d\theta \\ &= \sqrt{2\pi}\int_\Omega \int_0^{+\infty} \left(\hat{g}(\theta, -\sigma)w(-\sigma\theta) + \hat{g}(\theta, \sigma)w(\sigma\theta)\right) d\sigma d\theta \\ &= \sqrt{2\pi}\int_\Omega \int_0^{+\infty} \frac{1}{\sigma}\left(\hat{g}(\theta, -\sigma)w(-\sigma\theta) + \hat{g}(\theta, \sigma)w(\sigma\theta)\right) \sigma d\sigma d\theta.\end{aligned}$$

Finally, with the change of variable $\xi = \sigma\theta$ which implies that $\theta = \frac{\xi}{|\xi|}$, $\sigma = |\xi|$

and $d\xi = \sigma d\sigma d\theta$, one has

$$\int_{\mathbb{R}^2} \widehat{R^*g}(\xi) w(\xi) d\xi = \int_{\mathbb{R}^2} \frac{\sqrt{2\pi}}{|\xi|} \left[\hat{g}\left(\frac{xi}{|\xi|}, |\xi|\right) + \hat{g}\left(-\frac{xi}{|\xi|}, -|\xi|\right) \right] w(\xi) d\xi,$$

for any $w \in C^\infty(\mathbb{R}^2)$, which concludes the proof. □

The previous result will now help to construct ω_b, since we want $W_b = R^*\omega_b$ to satisfy

$$\hat{W}_b(\xi) = \begin{cases} \frac{1}{2\pi}, & |\xi| \leq b \\ 0, & |\xi| > b \end{cases}$$

but so that ω_b is even and independent of direction, that is $\hat{\omega}_b = \hat{\omega}_b(\sigma)$ independent of θ. From (4.35), one now gets

$$\hat{w}_b(\sigma) = \begin{cases} \frac{|\sigma|}{2\sqrt{2\pi}}, & |\xi| \leq b \\ 0, & |\xi| > b \end{cases} \tag{4.36}$$

From the inverse Fourier transform, one now gets

$$\begin{aligned} \omega_b(s) &= \frac{1}{\sqrt{2\pi}} \int_{-b}^{b} \hat{w}_b(\sigma) e^{is\sigma} d\sigma \\ &= \frac{1}{8\pi^2} \int_{-b}^{b} |\sigma| e^{is\sigma} d\sigma \\ &= \frac{1}{4\pi^2} \int_{0}^{b} \sigma \cos(s\sigma) d\sigma \end{aligned}$$

which after integration is given by

$$\omega_b(s) = \frac{1}{4\pi^2} \begin{cases} \frac{1}{s^2}(\cos(bs) - 1) + \frac{b}{2}\sin(bs), & s \neq 0, \\ \frac{b^2}{2}, & s = 0. \end{cases}$$

With this choice one gets a reconstruction method by (4.31). Other possibilities for ω_b can be found in [Natterer, 2001].

Remark 4.35. The application of (4.31) is not computationally efficient. One needs to take into account that one should have a rectangular grid in order to be able to use Fast Fourier transform in the discretization of the convolution. Details can be seen in [Natterer, 2001].

4.6.2 Fourier method

The Fourier method is based in the direct application of the Projection theorem 4.16. In a brief way, the idea is to follow the next steps:

- **FM1** - Given the data $g(\theta, s) = (Rf)(\theta, s)$ determine the Fourier transform of f by direct application of (4.14) by

$$\hat{f}(s\theta) = \frac{1}{\sqrt{2\pi}}\hat{g}(s, \theta). \tag{4.37}$$

- **FM2** - Since the previous step determines the Fourier transform $\hat{f}$ in polar coordinates, one needs at this intermediate step to determine $\hat{f}$ in a rectangular grid to obtain f in the following step.

- **FM3** - Obtain f by inverse Fourier transform of $\hat{f}$ obtained in the previous step by

$$f(x) = \frac{1}{2\pi}\int_{\mathbb{R}^2} e^{i\xi.x}\hat{f}(\xi)d\xi. \tag{4.38}$$

The key step in this reconstruction method is step FM2. In fact, this is the step that usually turns the reconstructions of the Fourier method to be not that good. Let us consider an example.

Example 4.36. Let us assume the setting of the parallel scanner in figure 4.2. Then our data is given by

$$g(\theta_j, s_\ell), \quad j = 1, \ldots, p, \quad \ell = -q, \ldots, q,$$

with $s_\ell = \ell h$, being h the (uniform) spacing between two following values s_ℓ and $s_{\ell+1}$. Let us also assume that $g(\theta, .)$ as support in $[-1, 1]$. Then, one knows that $\hat{g}$ is band-limited with band width 1, so by Shannon's theorem 4.29 it suffices to sample $\hat{g}$ in a grid of points of spacement π, since the Nyquist condition is

$$h \leq \frac{\pi}{b} = \pi.$$

In this way, considering the points $(\theta_j, r\pi)$, $j = 1, 2, \ldots n$, $r = -q, \ldots, q$ as a grid for $\hat{g}$, one has

$$\hat{g}(\theta_j, r\pi) = \frac{1}{\sqrt{2\pi}}\int_{-1}^{1} e^{-ir\pi s}g(\theta, s)ds,$$

and applying the trapezoidal rule in the known points s_ℓ with spacement h, one gets

$$\hat{g}(\theta_j, r\pi) \approx \underbrace{\frac{h}{\sqrt{2\pi}} \sum_{\ell=-q}^{q} e^{-ir\pi\ell h} g(\theta, s_\ell)}_{:=\tilde{g}_{j,r}},$$

where the values $g(\theta, s_\ell)$ are known, since they are our data. Note that the error given by the previous approximation can be obtained by Poisson summation formula (4.13), since, as $\hat{g}$ is assumed to be band-limited, one has for $\xi = r\pi$ and $m = 1$ that

$$\sum_{j=-\infty}^{\infty} \hat{g}\left(\theta_j, r\pi - \frac{2\pi j}{h}\right) = \underbrace{\frac{h}{(\sqrt{2\pi})} \sum_{j=-q}^{q} g(\theta_j, jh) e^{-ihrj\pi}}_{=\tilde{g}_{j,r}},$$

which can be rewritten as

$$\hat{g}(\theta_j, r\pi) = \tilde{g}_{j,r} - \underbrace{\sum_{\substack{j=-\infty \\ j\neq 0}}^{\infty} \hat{g}\left(\theta_j, r\pi - \frac{2\pi j}{h}\right)}_{\text{error}}.$$

Therefore, if g is essentially band limited, that the error is small. This concludes step FM1.

For step FM2, one aims at approximating the value of $\hat{g}(\xi_k)$ for $\xi_k = kh$ in a rectangular grid with spacing h and $k \in \mathbb{Z}$, using the values $\tilde{g}_{j_k,r_k}$ in polar coordinates from step FM1. One can consider, for instance, a piecewise constant approximation by the nearest neighbour, that is,

$$\hat{g}(\xi_k) \approx \tilde{g}_{j_k,r_k}$$

such that $r_k\theta_{j_k}$ is the closest value to ξ_k.

Having in mind the projection theorem in step FM1, one considers

$$\hat{f}(\xi_k) = \frac{1}{\sqrt{2\pi}}\hat{g}(\xi_k) \approx \frac{1}{\sqrt{2\pi}}\tilde{g}_{j_k,r_k}, \tag{4.39}$$

finalizing step FM3.

Then, in step FM3, having in mind that $\hat{g}(\theta, .)$ is band-limited (and so is $\hat{f}$ by the projection theorem), it suffices to use the Nyquist condition $h = \pi$ and from Shannon's sampling theorem (4.27) (applied to $\hat{f}$ with $m = 2$) one has

$$f(x) = \frac{\pi^2}{2\pi} \sum_{k\in\mathbb{Z}^m} \hat{f}(k\pi) e^{i\pi x.k},$$

that is, the formula

$$f(x) = \frac{\pi}{2} \sum_{k \in \mathbb{Z}^2} \hat{f}(\xi_k) e^{-i\pi x.k}$$

is exact, and therefore, the error of

$$f(x) = \frac{\pi}{2} \sum_{|k| \leq q} \hat{f}(\xi_k) e^{-i\pi x.k}$$

is almost null if f is essentially band limited.

It is clear from the previous example that the errors of steps FM1 and FM3 are small if f is essentially band-limited. Therefore, the interpolation step FM2 is the one responsible for decreasing the quality of the reconstructions of the Fourier method.

4.6.3 Algebraic Reconstruction Technique (ART)

The Algebraic Reconstruction Technique (ART) is a reconstruction method that copes very easily with different setting of CT, in what concerns the lines in which the intensity attenuation is measured. It is based in an algebraic solution using the Kaczmarz's method, that we now introduce. Kaczmarz's method is also know as the method of successive orthogonal projections and was used in the first commercial X-ray scanner in 1972.

Let X and $Y_1, Y_2, \ldots, Y_p$ be Hilbert spaces and let $Y = Y_1 \times Y_2 \times \cdots \times Y_p$. Being an algebraic solver, the Kaczmarz's method wants to find $\varphi \in X$ such that

$$A_j \varphi = f_j, \quad j = 1, 2, \ldots, p,$$

for some given surjective operators $A_j : X \to Y_j$ and $f = (f_1, f_2, \ldots, f_p) \in Y$.

Example 4.37. If we consider $X = \mathbb{R}^p$, $Y_1 = Y_2 = \cdots = Y_p = \mathbb{R}$, and the operators A_j of the form

$$A_j \varphi = \sum_{k=1}^{p} a_{jk} \varphi_k,$$

this corresponds to finding $\varphi \in \mathbb{R}^p$ that belongs to all hyperplanes

$$A_j \varphi = f_j.$$

It is clear that this problem might not always have a solution, so it is important also to characterize what happens with the application of Kaczmarz's method in that case. For the time being, we will define the method.

Definition 4.38 (Kaczmarz's method).

Let X and $Y_1, Y_2, \ldots, Y_p$ be Hilbert spaces and let $A_j : X \to Y_j$ be surjective operators. Let Q_j be the orthogonal projection into the affine spaces

$$U_j = \{\varphi \in X : A_j\varphi = f_j\}$$

for some given $f_j \in Y_j$, $j = 1, 2, \ldots, p$. Let also

$$Q_{j,\omega} := (1-\omega)I + \omega Q_j$$

and

$$Q_\omega = Q_{p,\omega} Q_{p-1,\omega} \ldots Q_{1,\omega}.$$

Then the iteration scheme

$$\varphi_{n+1} = Q_\omega \varphi_n \tag{4.40}$$

is called the **Kaczmarz's method** with relaxation ω.

Remark 4.39 (Relaxation). The use of a relaxation term ω is to try to speed up the convergence of the method.

Theorem 4.40 (Computation of Kaczmarz's method).

One iteration of the Kaczmarz's method (4.40) *has the form*

$$\begin{cases} \varphi^{(0)} = \varphi_n, \\ \varphi^{(j)} = \varphi^{(j-1)} + \omega A_j^* \left[A_j A_j^*\right]^{-1} \left[f_j - A_j \varphi^{(j-1)}\right], \quad j = 1, 2, \ldots, p, \\ \varphi_{n+1} = \varphi^{(p)}. \end{cases} \tag{4.41}$$

Proof. See [Kress, 2005]. □

The ART method comes from applying the Kaczmarz's method in a very specific context of CT. One starts by considering the density f with compact support within a rectangular domain, that one discretizes in K pixels p_k, $k = 1, 2, \ldots, K$. We then consider the approximation $\tilde{f}$ of f as piecewise constant, that is, the density $\tilde{f}$ restricted to the pixel p_k is constant

$$\tilde{f}_{|p_k}(x) = \tilde{f}_k, \quad k = 1, 2, \ldots, K.$$

Therefore, the Radon transform of $\tilde{f}$ can be computed exactly as

$$(Rf)(\theta, s) \approx (R\tilde{f})(\theta, s) = \int_{L_{\theta,s}} \tilde{f}(x)dx = \sum_{k=1}^{K} a_{(\theta,s),k} \tilde{f}_k$$

where $a_{(\theta,s),k} = |L_{\theta,s} \cap p_k|$ is the length of the interception of the line $L_{\theta,s}$ with the pixel p_k. Therefore, if the available data is given by $g_j = g(\theta_j, s_j), j = 1, 2, \ldots, N$, that is, the Radon transform of f over the line $L_j :=_{\theta_j,s_j}$ defined by (θ_j, s_j), one can consider the operators $A_j : \mathbb{R}^K \to \mathbb{R}$ defined by

$$A_j f = \sum_{k=1}^{K} a_{j,k} f_k \tag{4.42}$$

where $a_{j,k} = |L_j \cap p_k|$ and $f = (f_1, f_2, \ldots, f_K) \in \mathbb{R}^K$, wiht each f_k corresponding to the unknown value of the density in each pixel. Therefore, one wants to solve

$$A_j \tilde{f} = g_j, \quad j = 1, 2, \ldots, N, \tag{4.43}$$

to get a piecewise constant approximation $\tilde{f}$ of f and the ART method comes from applying the Kaczmarz's method to the previous operators. We note that in this case, the adjoint operator $A_j^* : \mathbb{R} \to \mathbb{R}^K$ is defined by

$$A_j^* \alpha = \alpha a_{j,\cdot}, \quad \alpha \in \mathbb{R}, \tag{4.44}$$

where $a_{j,\cdot} = (a_{j,1}, a_{j,2}, \ldots, a_{j,K})$ since

$$(A_j f, \alpha)_{\mathbb{R}} = \alpha A_j f = \alpha \sum_{k=1}^{K} a_{j,k} f_k = \sum_{k=1}^{K} \alpha a_{j,k} f_k = (f, \alpha a_{j,\cdot})_{\mathbb{R}^K}.$$

In this way,

$$A_j A_j^* \alpha = A_j(\alpha a_{j,\cdot}) = \alpha \|a_{j,\cdot}\|_2^2.$$

Therefore, applying Kaczmarz's method (4.41) to the operator (4.42) and equation (4.43), one gets the following method.

Theorem 4.41 (Algebraic Reconstruction Technique).

*Given the CT data $g_j = g(\theta_j, s_j), j = 1, 2, \ldots, N$, that is, the Radon transform of f over the line L_j defined by (θ_j, s_j), the **Algebraic Reconstruction Technique** corresponds to iteratively compute*

$$\begin{cases} f^{(0)} = F_n, \\ f^{(j)} = f^{(j-1)} + \frac{\omega}{\|a_{j,\cdot}\|_2^2} \left[g_j - A_j f^{(j-1)} \right] a_{j,\cdot}, \quad j = 1, 2, \ldots, N, \\ F_{n+1} = f^{(N)}. \end{cases} \tag{4.45}$$

If the problem is solvable, the iterations F_n converge to the solution of minimal norm, if $\omega \in [0, 2]$.

If the problem is unsolvable, the method converges to f_ω that, as $\omega \to 0$, converges to the solution of the minimization of the cost function

$$\sum_{j=1}^{N} \frac{1}{\|a_{j,\cdot}\|_2^2} \left| \left(\sum_{k=1}^{M} F_k a_{j,k} \right) - g_j \right|^2 .$$

Proof. See [Kress, 2005]. □

Chapter 5

Acoustic Scattering Theory

In this section, we will introduce a simple model for sound propagation. This will be a simplified approach for another medical imaging modality, namely **ultrasound** imaging. This modality is based on the emission of sound waves and the measurement of the echoes of the reflected waves on the different organs inside the body. Ultrasound is usually modelled by the Westervelt's equation

$$\Delta u = \frac{1}{c^2}\frac{\partial^2 u}{\partial t^2} - \frac{\delta}{c^4}\frac{\partial^3 u}{\partial t^3} - \frac{\beta(u)}{\rho c^4}\frac{\partial^4 u}{\partial t^4},$$

where u is the sound pressure, c is the small signal sound velocity, δ is the sound diffusity, ρ in the medium density and $\beta(u)$ is a nonlinear coeficient, that depends on u. The fact that the previous equation is nonlinear makes its analytical and numerical treatment very difficult for an introduction to inverse scattering problem, so we will simplify the acoustic wave propagation model.

In this way, in order to introduce this topic, we will consider sound waves with fixed frequency ω, which leads to the Helmholtz equation described in a few lines. Though we will focus on mathematical models for wave propagation more than on the reconstruction method for ultrasound imaging, it is important to mention that ultrasound uses more than one frequency for image acquisition. The combination of more than one frequency allows to distinguish the depth were each measured echo is coming from, being this the main principle for ultrasound image acquisition [Ammari, 2011]. In this chapter, we will mostly focus on the propagation and inverse problems relates with acoustic waves with a single frequency, as a simple model for wave propagation.

We will now go back to some of the concepts already discussed in section 1.1, in order to recall the context of inverse scattering problems.

5.1 Scattering theory revisited

Scattering theory has been a matter of interest for scientists over the last century. There is a broad band of applications, such as radar and sonar and, to our special interest, medical imaging. Roughly speaking, scattering theory studies the effect that an obstacle or some inhomogeneity in the propagation medium has on an incident wave or particle. Considering the total field u to be the sum of the incident field u^i and the scattered field u^s, then the direct problem consists of determining u^s from the knowledge of the geometry and properties of the medium and the characteristics of the propagation of the field. In mathematical terms, this means the determination of the scattered field u^s from the knowledge of the obstacle or inhomogeneity (including the boundary condition satisfied at the boundary of the obstacle) and the differential equation that models the propagation of the field. The inverse problem is, however, a much more challenging and interesting problem: Given measured information on the scattered field u^s, one wants to find some unknown properties of the obstacle, such as its location and shape, the boundary condition or some refractive index, for instance. We refer to the monographs Lax and Philips [Lax and Philips, 1967] and Colton and Kress [Colton and Kress, 1983, Colton and Kress, 2019] for further reading on the basic theory of some of these problems.

Our main purpose in this chapter is to focus on the acoustic time-harmonic obstacle scattering problem within an homogeneous background. This is not a good model for ultrasound imaging by two main reasons: a) usually the background is inhomogeneous, since there are several different organs, tissues and bones with different densities; b) we will assume that the obstacle is impenetrable, with is also not the case in many human organs. However, in the context of theis text where we aim to introduce the reader to this topic, we will consider this simpler problem, and say some words on how to extend the problem for inhomogeneous mediums in section 5.7.

In this way we will motivate the **Helmholtz equation** as the model to the inverse obstacle scattering problem in the next section. Then, in the following sections, we will present classical theoretical results for the direct and inverse obstacle scattering problems, including representation formulas and asymptotic behaviours for the scattered field u^s, as well as uniqueness and existence results for the referred problems.

5.2 The Helmholtz Equation

We start by giving a motivation to the **Helmholtz equation**

$$\Delta u + k^2 u = 0$$

for $k > 0$, as being a model to the space dependence of the limit state of a time-harmonic acoustic wave with a point source excitement. We refer to thesis [Grinberg, 2004] or the classical work [Lax and Philips, 1967] for details.

Consider the wave equation with a point source at y. This means that the system is at rest and at $t = 0$ the harmonic excitement is started at the point y in free space. In mathematical terms, this can be formulated in terms of an acoustic wave $U^i(x, t; y)$, depending on the space variable $x \in \mathbb{R}^3$ and the time variable $t \geq 0$, satisfying the **wave equation**

$$\frac{1}{c^2}\frac{\partial^2 U(x,t)}{\partial t^2} - \Delta_x U(x,t) = e^{-i\omega t}\delta(x-y), \quad x \in \mathbb{R}^3, t \geq 0 \tag{5.1}$$

with initial conditions

$$U(x,0) = \frac{\partial U(x,0)}{\partial t} = 0,$$

where c is the speed of sound and ω is the frequency. We are interested in studying the behaviour of the solution as $t \to \infty$. One can show the asymptotic behaviour

$$U^i(x,t) \approx e^{-i\omega t}\Phi(x-y), \quad t \to \infty,$$

where Φ is the **fundamental solution** to the Helmholtz equation in $\mathbb{R}^3$ given by

$$\Phi(x) = \frac{e^{ik|x|}}{4\pi|x|}, \quad x \neq 0 \tag{5.2}$$

where $|.|$ denotes the usual Euclidean norm and $k = \omega/c$ is the wave number.

Let us now consider a bounded and connected obstacle $D \subset \mathbb{R}^3$ and U^i (the solution in free space as) the incident wave. In the context of impenetrable obstacle, we then have an extra condition to be satisfied at the interface between the obstacle and the exterior propagation medium. Therefore, we will consider either a Dirichlet, Neumann or Robin boundary condition at the boundary $\Gamma := \partial D$. In any case, if D has no energy traps, we expect the obstacle to give rise to a scattered wave U^s and therefore the asymptotic behaviour of the solution is given by

$$U(x,t) := U^i(x,t) + U^s(x,t) \approx e^{-i\omega t}\left(\Phi(x-y) + u^s(x)\right), \quad t \to \infty, \tag{5.3}$$

and the scattered field u^s behaves as an outgoing spherical wave, that is, it satisfies the **Sommerfeld radiation condition** (see [Lax and Philips, 1967])

$$\lim_{r\to\infty} r\left(\frac{\partial u^s}{\partial r} - iku^s\right) = 0. \tag{5.4}$$

The physical meaning of this condition is that there are no energy sources at infinity (see the classical work of Sommerfeld [Sommerfeld, 1967]). As the solution U satisfies the wave equation (5.1) in $\mathbb{R}^m\backslash\overline{D}$, by substitution of (5.3) in (5.1) we get that

$$\Delta u^s + k^2 u^s = 0, \quad x \in \mathbb{R}^m\backslash\overline{D},$$

that is, the solution to the Helmholtz equation can be interpreted as the spatial dependence of a time-harmonic acoustic wave as $t \to \infty$. Mathematically, the radiation condition will ensure uniqueness of solution to the Helmholtz equation.

We also note that if the point source y goes to infinity in the direction $-d$, from the asymptotic behaviour of the fundamental solutions, we then get

$$\lim_{r\to\infty} \left(4\pi r e^{-ikr}\Phi(x + rd)\right) = e^{ikx.d}, \tag{5.5}$$

so in this case it makes sense to approximate the point source by an incident plane field $u^i(x) = e^{ikx.d}$ up to some multiplicative constant depending on the distance r between the evaluation point x to the source point y. We also note that defining the total field $u = u^i + u^s$ as the sum of the incident and scattered fields, the boundary conditions on Γ carry over from the total wave U to the total field u. This means that if, for instance, we consider a sound-soft obstacle D, that is, the pressure of the total wave vanishes at the boundary Γ of D, then the boundary condition imposed is

$$U(x,t) = 0, \quad x \in \Gamma, t \geq 0,$$

which implies the Dirichlet boundary condition for u given by

$$u(x) = 0, \quad x \in \Gamma$$

since from (5.3)

$$U(x,t) \approx u(x)e^{-i\omega t}, \quad t \to \infty$$

where again $u = u^i + u^s$. In the same way, for sound-hard obstacles, the normal velocity vanishes on the boundary Γ and so we get the Neumann boundary condition for u

$$\frac{\partial u(x)}{\partial \nu} = 0, \quad x \in \Gamma$$

where ν is the exterior unit normal vector to D. Since there are no perfect sound-soft or sound-hard obstacles in reality, a more realistic situation is the one where the pressure and the normal velocity are proportional at the boundary, that is, an impedance boundary condition

$$\frac{\partial u(x)}{\partial \nu} + i\lambda(x)u(x) = 0, \quad x \in \Gamma,$$

with $\lambda \geq 0$. All these three cases will be addressed during this work.

5.3 The Direct Acoustic Scattering Problem

The main topic of this chapter is to discuss methods to numerically solve the inverse acoustic scattering problem. Therefore, a solid knowledge on the direct problem is needed. In this section we present the basic results on the solutions to the Helmholtz equation and to the direct problem, that will be of crucial importance later on when studying the inverse problem.

We are interested in time harmonic acoustic obstacle scattering. Therefore, as motivated in the previous section, we want to find a solution to the following problem:

Direct Problem 5.1 (Obstacle Scattering). Given an open obstacle D of class C^2 with connected boundary Γ and an incident field u^i we want to find the scattered field $u^s \in C^2(\mathbb{R}^m \backslash \overline{D}) \cap C(\mathbb{R}^m \backslash D)$, for $m = 2,\ 3$ that satisfies

$$\Delta u^s + k^2 u^s = 0, \quad x \in \mathbb{R}^m \backslash \overline{D}, \tag{5.6}$$

$$Bu = 0, \quad x \in \Gamma := \partial D, \tag{5.7}$$

$$\lim_{r\to\infty} r^{\frac{m-1}{2}} \left(\frac{\partial u^s}{\partial r} - iku^s \right) = 0, \tag{5.8}$$

where the total field u is given by the sum of the incident field u^i and the scattered field u^s, that is, $u = u^i + u^s$.

A solution satisfying the Sommerfeld radiation condition (5.8) is called a **radiating** solution. Again we stress the notation Γ for the boundary of D, that will be carried out throughout this work. The differential operator B represents one of the already referred **boundary conditions**, that is,

$$Bu = u\,|_\Gamma \qquad \text{(Dirichlet)}; \tag{5.9}$$

$$Bu = \left(\tfrac{\partial u}{\partial \nu}\right)\,|_\Gamma \qquad \text{(Neumann)}; \tag{5.10}$$

$$Bu = \left(\tfrac{\partial u}{\partial \nu} + i\lambda u\right)\,|_\Gamma \quad \text{(Robin)} \tag{5.11}$$

where $\lambda \geq 0$ is a continuous function defined on Γ and ν is the exterior unit normal to D. All these boundary conditions are to be satisfied in the sense of uniform convergence on Γ. We note that the Neumann case is a particular case of the Robin case for $\lambda = 0$ and that the Dirichlet case can be seen as the limit of the Robin case as $\lambda \to \infty$.

Most results presented in this section on the properties of the solutions to the direct problem have as primary tools the following first and second Green's theorems.

Theorem 5.2 (Green's Theorem). *Let D be a domain of class C^1. Then for $u \in C^1(\overline{D})$ and $v \in C^2(\overline{D})$ we have the first Green's theorem*

$$\int_D (u\,\Delta v + \operatorname{grad} u \cdot \operatorname{grad} v)\,dx = \int_{\partial D} u\,\frac{\partial v}{\partial \nu} ds.$$

Moreover if $u, v \in C^2(\overline{D})$ we have the second Green's theorem

$$\int_D (u\,\Delta v - v\,\Delta u)\,dx = \int_{\partial D} \left(u\,\frac{\partial v}{\partial \nu} - v\,\frac{\partial u}{\partial \nu} \right) ds.$$

Proof. The first theorem is proved by applying the divergence theorem to the vector field $(u \operatorname{grad} v) \in C^1(\overline{D})$. The second is obtained by interchanging the roles of u and v in the first and subtracting both equations. □

Based on these theorems, a classical result for representing the solution can be achieved. For its formulation, we will need the **fundamental solution** to the Helmholtz equation in $\mathbb{R}^m$ given by

$$\Phi(x) = \begin{cases} \frac{i}{4} H_0^{(1)}(k|x|), & m = 2, \\ \frac{e^{ik|x|}}{4\pi|x|}, & m = 3, \end{cases}$$

where $H_0^{(1)}$ is the **Hankel function** of first kind and order zero given by

$$H_0^{(1)}(t) = J_0(t) + iY_0(t), \quad t \in \mathbb{R},$$

where the **Bessel function** of order zero J_0 is analytic for all $t \in \mathbb{R}$ and the **Neumann function** of order zero has a logarithmic singularity at $t = 0$ (see, for instance, [Colton and Kress, 2019, Chap. 3.4.] for details). Therefore both the fundamental solutions have singularities for $m = 2, 3$ at zero, that will need to be taken care of for numerical purposes. We will define

$$\Phi(x, y) := \Phi(|x - y|)$$

to simplify the notation.

We are now in position to present the classical Green's representation formula for exterior radiating solutions to the Helmholtz equation.

Theorem 5.3 (Green's Representation Formula). *Assume the bounded set $D \subset \mathbb{R}^m$ to be the open complement of an unbounded domain of class C^2.*

Let $u^s \in C^2(\mathbb{R}^m \backslash \overline{D}) \cap C(\mathbb{R}^m \backslash D)$ be a radiating solution to the Helmholtz equation (5.6) which possesses a normal derivative on the boundary in the sense that the limit

$$\frac{\partial u^s}{\partial \nu}(x) = \lim_{h \to 0^+} \nu(x) \cdot \operatorname{grad} u^s(x + h\nu(x)), \quad x \in \Gamma,$$

exists uniformly on Γ. Then, we have Green's representation formula

$$u^s(x) = \int_\Gamma \left(u^s(y) \frac{\partial \Phi(x,y)}{\partial \nu(y)} - \frac{\partial u^s}{\partial \nu}(y) \Phi(x,y) \right) ds(y), \quad x \in \mathbb{R}^m \backslash \overline{D}. \tag{5.12}$$

Proof. We will just state a sketch of the proof in [Colton and Kress, 2019, Sec. 3.4.] for the two-dimensional case $m = 2$ and [Colton and Kress, 2019, Thm. 2.4.] for the three-dimensional case $m = 3$, and refer to those for details.

Denoting by $B(x, r)$ the ball with center in x and radius r, let us then define the set $G^* = B(0, R) \backslash (\overline{D \cup B(x, r)})$ with $x \in \mathbb{R}^m \backslash \overline{D}$ and with R sufficiently large and r sufficiently small such that $D \subset B(0, R)$, $B(x, r) \subset B(0, R)$ and $B(x, r) \cap D = \emptyset$. As u^s and Φ satisfy the Helmholtz equation in G^* we have that

$$\int_{G^*} (u^s(y) \Delta_y \Phi(x, y) - \Phi(x, y) \Delta u^s(y))\, dy = 0.$$

By the definition of the fundamental solution, we have

$$\lim_{r \to 0} \int_{\partial B(x,r)} \left(u^s(y) \frac{\partial \Phi(x,y)}{\partial \nu(y)} - \Phi(x,y) \frac{\partial u^s}{\partial \nu(y)}(y) \right) ds(y) = u^s(x),$$

where ν is the exterior unit normal to G^* and therefore the interior unit normal to $B(x, r)$. By the radiation condition, one can also prove that

$$\lim_{R \to \infty} \int_{\partial B(0,R)} \left(u^s(y) \frac{\partial \Phi(x,y)}{\partial \nu(y)} - \Phi(x,y) \frac{\partial u^s}{\partial \nu(y)}(y) \right) ds(y) = 0.$$

The proof is now complete by applying Green's theorem to $u = u^s$ and $v = \Phi(x, .)$ on G^* and let $r \to 0$ and $R \to \infty$. □

From the previous representation, one can conclude [Colton and Kress, 2019, thm.2.2] that if u is a C^2–solution to the Helmholtz equation in $\mathbb{R}^m \backslash \overline{D}$ then u is analytic in $\mathbb{R}^m \backslash \overline{D}$.

Another important theorem for what follows is the following.

Theorem 5.4 (Holmgren's Theorem). *Let D be a bounded domain of class C^2 and $u \in C^2(D) \cap C^1(\overline{D})$ be a solution of the Helmholtz equation in D such that*

$$u = \frac{\partial u}{\partial \nu} = 0 \text{ on } \Gamma$$

for some open set $\Gamma \subset \partial D$. Then $u = 0$ in D.

Proof. Since $u = \frac{\partial u}{\partial \nu} = 0$ on Γ, we can consider Green's representation formula as

$$u(x) = \int_{\partial D \setminus \Gamma} \left(u(y) \frac{\partial \Phi(x,y)}{\partial \nu(y)} - \frac{\partial u}{\partial \nu}(y) \Phi(x,y) \right) ds(y), \quad x \in \mathbb{R}^m \setminus \overline{D}.$$

Now, Green's second theorem applied to u and the fundamental solution Φ tells us that

$$u = 0 \text{ on } \mathbb{R}^m \setminus \overline{D}.$$

Now one consider an open bounded subset A of $\mathbb{R}^m \setminus \overline{D}$ such that $\partial A \cap \Gamma \neq \emptyset$. Now $u = 0$ in D by analytic continuation, since u solves the Helmholtz equation in $A \cup \Gamma \cup D$ and vanishes in A. □

We now introduce the notation Ω_m for the unit spherical surface in $\mathbb{R}^m$, that is,

$$\Omega_m = \{x \in \mathbb{R}^m : |x| = 1\}$$

where as before $|.|$ denotes the usual Euclidean norm.

From the previous theorem one can conclude the following asymptotic behaviour of the solution.

Theorem 5.5 (Far-field pattern). *Every radiating solution u^s to the Helmholtz equation in $\mathbb{R}^m \setminus \overline{D}$ has an asymptotic behaviour of an outgoing spherical wave*

$$u^s(x) = \frac{e^{ik|x|}}{|x|^{\frac{m-1}{2}}} \left(u_\infty(\hat{x}) + O\left(\frac{1}{|x|} \right) \right), \quad |x| \to \infty \tag{5.13}$$

uniformly in all directions $\hat{x} = x/|x| \in \Omega_m$ where the function u_∞ is called the far-field pattern of u. Under the assumptions of theorem 5.3 we have

$$u_\infty(\hat{x}) = \varrho_m \int_\Gamma \left(u^s(y) \frac{\partial e^{-ik\hat{x}\cdot y}}{\partial \nu(y)} - \frac{\partial u^s}{\partial \nu}(y) e^{-ik\hat{x}\cdot y} \right) ds(y) \tag{5.14}$$

where

$$\varrho_m = \begin{cases} \frac{e^{i\pi/4}}{\sqrt{8\pi k}}, & m = 2 \\ \frac{1}{4\pi}, & m = 3. \end{cases} \tag{5.15}$$

Proof. Using the Taylor expansion of the square root function around 1, we get that

$$\begin{aligned} |x-y| &= \sqrt{|x|^2 - 2x\cdot y + |y|^2} \\ &= |x|\sqrt{1 - 2\frac{\hat{x}\cdot y}{|x|} + \frac{|y|^2}{|x|^2}} \\ &= |x| - \hat{x}\cdot y + O\left(\frac{1}{|x|}\right) \end{aligned}$$

as $|x| \to \infty$ uniformly for $y \in \Gamma$. Therefore we derive

$$\begin{aligned} \frac{e^{ik|x-y|}}{|x-y|} &= \frac{e^{ik|x|}}{|x|}\left(e^{-ik\hat{x}\cdot y} + O\left(\frac{1}{|x|}\right)\right), \\ \frac{\partial}{\partial\nu(y)}\frac{e^{ik|x-y|}}{|x-y|} &= \frac{e^{ik|x|}}{|x|}\left(\frac{\partial e^{-ik\hat{x}\cdot y}}{\partial\nu(y)} + O\left(\frac{1}{|x|}\right)\right), \end{aligned}$$

as $|x| \to \infty$ uniformly for $y \in \Gamma$. Replacing this in (5.12) we have the result for $m = 3$. For $m = 2$, the procedure is similar (see [Colton and Kress, 2019, Sec. 3.4.]), using the asymptotics of the Hankel function. □

Remark 5.6. We have seen in section 5.2 that if the source point y is very far in the direction $-d$ from the obstacle, then the point source incident field can be approximated (up to a multiplicative constant depending on the distance $|x-y|$) by a plane wave $u^i(x) = e^{ikx\cdot d}$, with $d \in \Omega_m$. In other words, the asymptotic behaviour (5.5) means that the far-field of a point source is a plane wave, that is,

$$\Phi_\infty(x;y) = \rho_m\, e^{ikx\cdot d}.$$

In the same way, by theorem 5.5 if one measures the scattered wave very far from the obstacle, one can assume that the measured data is the far-field pattern (up to the same multiplicative constant). Both this assumptions will be taken later on for the inverse problem, where we will consider an incident plane wave and the far-field pattern as data.

In this way, we will present a few more properties of the far-field pattern, since it will be important in the forthcoming sections. From the representation (5.14), we see that the far-field pattern u_∞ is analytic on Ω_m. The following result shows us that having an incident field in the direction d and measuring the far-field pattern in the direction $\hat{x}$ is the same as having an incident field in the direction $-\hat{x}$ and measuring the far-field pattern in the direction $-d$. This means that, at large distances from it, the obstacle as mirroring properties.

Theorem 5.7 (Reciprocity relation). *For any of the boundary conditions previously mentioned (5.9)–(5.11), we have that the far-field pattern satisfies*

$$u_\infty(\hat{x}; d) = u_\infty(-d; -\hat{x}), \quad \hat{x}, d \in \Omega_m \tag{5.16}$$

where $u_\infty(.; d)$ denotes the far-field pattern obtained by scattering of a plane wave with incident direction $d \in \Omega_m$.

Proof. Making use of the fact that the incident plane field $u^i(x; d) = e^{ikx\cdot d}$ satisfies the Helmholtz equation inside the obstacle D, by the second Green's theorem applied to $u = u^i(.; d)$ and $v = u^i(.; -\hat{x})$ we get

$$\int_\Gamma \left(u^i(.; d) \frac{\partial u^i(.; -\hat{x})}{\partial \nu} - u^i(.; -\hat{x}) \frac{\partial u^i(.; d)}{\partial \nu} \right) ds = 0.$$

Applying the same tools and procedure for the scattered wave in the exterior domain, making use of the radiation condition we get

$$\int_\Gamma \left(u^s(.; d) \frac{\partial u^s(.; -\hat{x})}{\partial \nu} - u^s(.; -\hat{x}) \frac{\partial u^s(.; d)}{\partial \nu} \right) ds = 0.$$

From (5.14) we get

$$\frac{1}{\varrho_m} u_\infty(\hat{x}; d) = \int_\Gamma \left(u^s(.; d) \frac{\partial u^i(.; -\hat{x})}{\partial \nu} - u^i(.; -\hat{x}) \frac{\partial u^s(.; d)}{\partial \nu} \right) ds$$

and interchanging the roles of d and $\hat{x}$

$$\frac{1}{\varrho_m} u_\infty(-d; -\hat{x}) = \int_\Gamma \left(u^s(.; -\hat{x}) \frac{\partial u^i(.; d)}{\partial \nu} - u^i(.; d) \frac{\partial u^s(.; -\hat{x})}{\partial \nu} \right) ds.$$

Subtracting the last equation from the sum of the previous three, one gets

$$\frac{1}{\varrho_m} \left(u_\infty(\hat{x}; d) - u_\infty(-d; -\hat{x}) \right) = \int_\Gamma \left(u(.; d) \frac{\partial u(.; -\hat{x})}{\partial \nu} - u(.; -\hat{x}) \frac{\partial u(.; d)}{\partial \nu} \right) ds.$$

Making use of the boundary condition $Bu(.; d) = Bu(.; -\hat{x}) = 0$, for any B defined in (5.9)–(5.11), the left hand side of the previous equation vanishes and we get the result. □

The question whether the far-field pattern u_∞ uniquely determines the scattered field u^s is affirmatively answered by Rellich's Lemma. The detailed proof can be found in [Colton and Kress, 2019, thm.2.11].

Lemma 5.8 (Rellich). *Let D be as in theorem 5.3 and $u \in C^2(\mathbb{R}^m \backslash \overline{D})$ be a solution to the Helmholtz equation satisfying*

$$\lim_{r\to\infty} \int_{\{|x|=r\}} |u|^2 ds = 0.$$

Then $u = 0$ in $\mathbb{R}^m \backslash \overline{D}$.

We formulate now the result that establishes the promised unique relation between the far-field pattern and the scattered field as a corollary of the previous result, simply by considering the asymptotic behaviour (5.13) of the scattered field (e.g. [Colton and Kress, 2019, thm. 2.13]).

Corollary 5.9. *Let D be as in theorem 5.3 and $u \in C^2(\mathbb{R}^m \backslash \overline{D})$, $m = 2, 3$, be a radiating solution to the Helmholtz equation for which the far-field pattern u_∞ vanishes on Ω_m. Then $u = 0$ in $\mathbb{R}^m \backslash \overline{D}$.*

5.3.1 Layer Potentials

In this section, we will present the **layer potentials** and basic results on their properties. The layer potentials will be of crucial importance to represent the solution to the direct problem and to numerically solve the inverse problem for methods requiring a forward solver.

Given an integrable function φ, the **single-layer potential** is defined by

$$w(x) = \int_\Gamma \Phi(x, y)\varphi(y) ds(y), \quad x \in \mathbb{R}^m \backslash \overline{D}, \tag{5.17}$$

while the **double-layer potential** is defined by

$$v(x) = \int_\Gamma \frac{\partial \Phi(x, y)}{\partial \nu(y)} \varphi(y) ds(y), \quad x \in \mathbb{R}^m \backslash \overline{D}. \tag{5.18}$$

Explicit computations show that both are solutions to the Helmholtz equation in D and in $\mathbb{R}^m \backslash \overline{D}$ and that they satisfy the Sommerfeld radiation condition. Green's representation theorem 5.3 tells us that any solution to the Helmholtz equation can be represented as a combination of single-and double-layer potentials. We will now state the classical result on the jump relations of these potentials, but similar results can also be shown for densities φ living in Sobolev spaces (see [Kirsch, 1989]).

Theorem 5.10. *Let Γ be of class C^2 and let $\varphi \in C(\Gamma)$. Then the single-layer potential w with density φ is continuous throughout $\mathbb{R}^m$ and satisfies the estimate in the usual maximum norm*

$$||w||_{\infty,\mathbb{R}^m} \leq C||\varphi||_{\infty,\Gamma}$$

for some constant C depending on Γ. On the boundary, we have the representations

$$\begin{aligned} w(x) &= \int_\Gamma \Phi(x,y)\varphi(y)ds(y), \quad x \in \Gamma, \\ \frac{\partial w_\pm}{\partial \nu}(x) &= \mp\frac{\varphi(x)}{2} + \int_\Gamma \frac{\partial \Phi(x,y)}{\partial \nu(x)}\varphi(y)ds(y), \quad x \in \Gamma, \end{aligned}$$

where

$$\frac{\partial w_\pm}{\partial \nu}(x) := \lim_{h\to 0^+} \nu(x) \cdot \operatorname{grad} w(x \pm h\nu(x)), \quad x \in \Gamma,$$

is to be understood in the sense of uniform convergence on Γ and where the integrals exist as improper integrals.

The double-layer potential v with density φ can be continuously extended from D to $\overline{D}$ and from $\mathbb{R}^m\backslash\overline{D}$ to $\mathbb{R}^m\backslash D$ with limiting values

$$v_\pm(x) = \pm\frac{\varphi(x)}{2} + \int_\Gamma \frac{\partial \Phi(x,y)}{\partial \nu(y)}\varphi(y)ds(y), \quad x \in \Gamma,$$

where

$$v_\pm(x) := \lim_{h\to 0^+} v(x \pm h\nu(x)), \quad x \in \Gamma$$

and the integral exists as an improper integral. We also have the estimate

$$||v||_{\infty,\overline{D}} \leq C||\varphi||_{\infty,\Gamma}, \quad ||v||_{\infty,\mathbb{R}^m\backslash D} \leq C||\varphi||_{\infty,\Gamma},$$

for some constant C depending on Γ. The normal derivative has no jump in the sense that

$$\lim_{h\to 0^+} \left(\frac{\partial v}{\partial \nu}(x + h\nu(x)) - \frac{\partial v}{\partial \nu}(x - h\nu(x)) \right) = 0, \quad x \in \Gamma,$$

uniformly in Γ.

Proof. For the proof of these classical results, we refer to theorems 2.12, 2.16, 2.17, and 2.23 in ([Colton and Kress, 1983]). □

Let us now introduce the single-layer operator S given by

$$\big(S\varphi\big)(x) := \int_\Gamma \Phi(x,y)\varphi(y)ds(y), \quad x \in \Gamma, \tag{5.19}$$

and the double-layer operator K given by

$$\big(K\varphi\big)(x) := \int_\Gamma \frac{\partial \Phi(x,y)}{\partial \nu(y)} \varphi(y) ds(y), \quad x \in \Gamma. \tag{5.20}$$

as well as the normal derivative operators

$$\big(K^*\varphi\big)(x) := \int_\Gamma \frac{\partial \Phi(x,y)}{\partial \nu(x)} \varphi(y) ds(y), \quad x \in \Gamma \tag{5.21}$$

$$\big(T\varphi\big)(x) := \frac{\partial}{\partial \nu(x)} \int_\Gamma \frac{\partial \Phi(x,y)}{\partial \nu(y)} \varphi(y) ds(y), \quad x \in \Gamma. \tag{5.22}$$

The previous jump relations can be given in terms of these operators, namely through

$$w(x) = (S\varphi)(x), \qquad \frac{\partial w_\pm}{\partial \nu}(x) = \mp \frac{\varphi(x)}{2} + (K^*\varphi)(x),$$

$$v_\pm(x) = \pm \frac{\varphi(x)}{2} + K\varphi(x), \qquad \frac{\partial v}{\partial \nu}(x) = (T\varphi)(x)$$

for $x \in \Gamma$. We will now state some results on the mapping properties of these four operators. For the proofs, we refer to [Colton and Kress, 1983, thm. 2.31].

Theorem 5.11. *Let Γ be of class C^2. Then*

(a) the operators S, K and K^* are bounded from $C(\Gamma)$ into $C^{0,\alpha}(\Gamma)$,

(b) the operators S and K are also bounded from $C^{0,\alpha}(\Gamma)$ into $C^{1,\alpha}(\Gamma)$,

(c) the operator T is bounded from $C^{1,\alpha}(\Gamma)$ into $C^{0,\alpha}(\Gamma)$.

We also state the following theorem for weak solutions and refer to [Kirsch, 1989] for the proof.

Theorem 5.12. *Let $p \in \mathbb{N} \cap \{0\}$ and $\alpha \in (0,1)$.*

(a) Let Γ be of class $C^{p+2,\alpha}$. Then S and K are bounded from $H^p(\Gamma)$ into $H^{p+1}(\Gamma)$ and T is bounded from $H^{p+1}(\Gamma)$ into $H^p(\Gamma)$.

(b) Let Γ be of class $C^{p+3,\alpha}$. Then K^* is bounded from $H^p(\Gamma)$ into $H^{p+1}(\Gamma)$.

The mapping properties of these operatoirs in the case that Γ is not C^2–smooth can also be obtained (see [McLean, 2000]).

We also introduce the far-field operators

$$(S_\infty\varphi)(\hat{x}) := \varrho_m \int_\Gamma e^{-ik\hat{x}\cdot y}\varphi(y)ds(y), \quad \hat{x}\in\Omega \tag{5.23}$$

$$(K_\infty\varphi)(\hat{x}) := \varrho_m \int_\Gamma \frac{\partial e^{-ik\hat{x}\cdot y}}{\partial\nu(y)}\varphi(y)ds(y), \quad \hat{x}\in\Omega. \tag{5.24}$$

with ϱ_m given as in (5.15). Since their integral kernels are continuous, the previous operators are compact from the space of continuously k-differentiable functions $C^k(\gamma)$ into $C^k(\Omega_m)$ and from the space of Hölder continuously k-differentiable functions $C^{k,\alpha}(\gamma)$ for $\alpha>0$ into $C^{k,\alpha}(\Omega_m)$. By the asymptotics of the layer potentials, one can also prove (see [Colton and Kress, 2019]) that the far-field pattern of the single layer potential (5.17) is given by

$$w_\infty(\hat{x}) = (S_\infty\varphi)(\hat{x}), \quad \hat{x}\in\Omega,$$

and the far-field of the double-layer potential (5.18) is given by

$$v_\infty(\hat{x}) = (K_\infty\varphi)(\hat{x}), \quad \hat{x}\in\Omega.$$

For a combined single-and double-layer potential

$$u(x) = \int_\Gamma \left(\frac{\partial\Phi(x,y)}{\partial\nu(y)} - i\eta\Phi(x,y)\right)\varphi(y)ds(y), \quad x\in\mathbb{R}^m\backslash\Gamma$$

we would obviously get the far-field given by

$$u_\infty(\hat{x}) = \Big((K_\infty - i\eta S_\infty)\varphi\Big)(x), \quad \hat{x}\in\Omega. \tag{5.25}$$

5.3.2 Uniqueness and Existence

We recall that the solution u^s must satisfy

$$\begin{aligned} \Delta u^s + k^2u^s = 0, \quad x \in \mathbb{R}^m\backslash\overline{D},\\ Bu^s = f, \quad x\in\Gamma := \partial D,\\ \lim_{r\to\infty} r^{\frac{m-1}{2}}\left(\frac{\partial u^s}{\partial r} - iku^s\right) = 0. \end{aligned}$$

We consider $f := -Bu^i$, where the incident field u^i is considered to be analytic up to the boundary of D.

We will state the uniqueness and existence results concerning the three boundary conditions (5.9)–(5.11) but the proofs will only be given for some of the cases. We refer to [Colton and Kress, 1983, Colton and Kress, 2019] for the remaining ones.

Theorem 5.13 (Uniqueness). *The exterior Dirichlet, Neumann or Robin problems have at most one solution.*

Proof. We will just give a sketch of the proof for the Dirichlet and Neumann case. For details see [Colton and Kress, 2019, Thm.3.7.]. For the Robin case we refer to [Colton and Kress, 1983, Thm.3.37.].

One has to show that solutions to the homogeneous boundary value problem $Bu^s = 0$ vanish on the domain of definition. From the radiation condition and applying Green's theorem one concludes that

$$\lim_{r\to\infty} \int_{\Omega_r} \left(\left| \frac{\partial u^s}{\partial \nu} \right|^2 + k^2 |u|^2 \right) ds = -2\,k\,\mathrm{Im} \int_\Gamma u^s \frac{\partial \overline{u^s}}{\partial \nu} ds,$$

where $\Omega_r = \{x : |x| = r\}$. As u^s is just assumed to be continuous up to the boundary, for the Dirichlet case the existence of the integral on the right-hand side must be assured. We overcome the problem by considering Γ of class C^2 and u^i to be at least $C^{1,\alpha}$ (see [Levine, 1964]). By the boundary conditions $u^s = 0$ or $\partial u^s/\partial \nu = 0$ on Γ we get that

$$\lim_{r\to\infty} \int_{\Omega_r} |u|^2 ds = 0$$

and by Rellich's lemma 5.8 one gets the result. □

Theorem 5.14 (Existence). *There exists a unique solution to the exterior Dirichlet, Neumann or Robin problem.*

Proof. We first consider the Dirichlet boundary condition. We start by writing a candidate for the solution as a combined single-and double-layer potential representation, that is, let

$$v(x) := \int_\Gamma \left(\frac{\partial \Phi(x,y)}{\partial \nu(y)} - i\eta \Phi(x,y) \right) \varphi(y) ds(y), \quad x \in \mathbb{R}^m \backslash \overline{D}. \tag{5.26}$$

with some coupling parameter $\eta > 0$. By the properties of the layer potentials, we conclude that v satisfies the Helmholtz equation and the radiation condition. By the jump relations, in order to fulfil the boundary equation, we get that

$$\frac{\varphi}{2} + (K - i\eta S)\varphi = f$$

must be satisfied over Γ. The fact that S and K are compact operators from $C(\Gamma)$ into itself (thm. 5.11 combined with the compact embedding of $C^{0,\alpha}(\Gamma)$ in $C(\Gamma)$) and the Fredholm-Riesz theory for equations of the second kind with a compact operator show that the equation has a solution if the operator $I + 2(K - i\eta S)$ is injective. Let us then assume that φ is a solution to the homogeneous equation

$$\varphi + 2(K - i\eta S)\varphi = 0.$$

Then, the potential v given by (5.26) satisfies the exterior homogeneous boundary condition and by uniqueness of this problem we conclude that $v = 0$ on $\mathbb{R}^m \backslash \overline{D}$. The jump relations from theorem 5.10 yield

$$v_- = -\varphi, \quad \frac{\partial v_-}{\partial \nu} = -i\eta\varphi \quad \text{on } \Gamma$$

and from the first Green's theorem applied to v_- and $\overline{v}_-$ in D we get

$$i\eta \int_\Gamma |\varphi|^2 ds = \int_\Gamma \overline{v}_- \frac{\partial v_-}{\partial \nu} ds = \int_D \left(|\operatorname{grad} v|^2 - k^2 |v|^2 \right).$$

Taking the imaginary part of the previous equation we get $\varphi = 0$ and the existence proof is finished.

For the Neumann and Robin cases, the proofs go in a similar way, choosing appropriate combinations of layer potentials. We refer to [Colton and Kress, 2019, thm.3.10] and [Colton and Kress, 1983, thm.3.38], respectively, for details. □

Remark 5.15. The estimates of theorem 5.10, along with the continuous dependence of the density φ on the boundary data f contained in the previous proof as a consequence of the Fredholm-Riesz theory, show continuous dependence of the solution u^s on the boundary data f.

5.4 The Inverse Acoustic Scattering Problem

The inverse problem is a much harder and more exciting problem to solve. It has been studied for the last decades but there are still many rather fundamental open problems, namely uniqueness proofs for a finite number of incident waves. In this section, we will give an overview of the results for the time-harmonic acoustic obstacle scattering problem under consideration.

We formulate the inverse problem we want to solve as follows.

Inverse Problem 5.16. Let u^i be an incident field, usually considered to be a plane wave $u^i(x) = e^{ikx\cdot d}$, with incident direction d such that $|d| = 1$.

Given a far-field pattern u_∞ corresponding to a scattered field u^s satisfying

$$\Delta u^s + k^2 u^s = 0, \quad x \in \mathbb{R}^m \backslash \overline{D}, \tag{5.27}$$

$$B(u^i + u^s) = 0, \quad x \in \Gamma := \partial D, \tag{5.28}$$

$$\lim_{r\to\infty} r^{\frac{m-1}{2}} \left(\frac{\partial u^s}{\partial r} - iku^s \right) = 0, \tag{5.29}$$

where B is known and is one of the operators (5.9)–(5.11) corresponding to a Dirichlet, Neumann or Robin boundary condition, find the position and shape of the obstacle D of class C^2. In the case of the impedance boundary condition (5.11), we also want to find the unknown impedance λ.

Remark 5.17. The latter case is equivalent to recovering the obstacle and the boundary condition, since we recover also the unknown impedance λ. As referred before, both the Dirichlet and Neumann are particular cases of the Robin one. If λ is close to zero we recover the information that the obstacle is sound-hard and if λ is large that it is sound-soft. A coated-obstacle can also be recovered, though in this text we assume λ to be a continuous function.

The problem 5.16 is ill-posed in the sense of Hadamard [Hadamard, 1952] and is also non-linear. The ill-posedness comes from the fact that the determination of D does not depend continuously on the far-field pattern u_∞. In the procedure of decomposition methods (as explained later on in section 5.6.2), this is illustrated in the reconstruction of u^s from the knowledge of u_∞, since it can be seen as the inversion of the integral operator (5.25), which is a compact operator due to its continuous kernel. The non-linearity comes from the fact that the scattered wave does not depend linearly on the obstacle. This can be illustrated as finding the position of the obstacle as the location of the zero level set of Bu not being a linear problem. Moreover, scattering by two different obstacles is different from the sum of scattering by each one of them separately.

5.4.1 Uniqueness

In the context of the inverse scattering problem, the first and only issue that needs to be addressed is uniqueness. Note that existence is a wrong question to ask, since we assume that the given far-field u_∞ corresponds to scattering by the unknown obstacle D. In this case of academic examples, existence is settled. However, if one actually wanted to proof existence of a solution for a general

given far-field pattern u_∞, it would imply that one would be able to characterize whether the zero level set of the scattered field corresponding to the given far-field u_∞ is a union of closed and non self-intersecting curves, which is nowa-days way beyond the capabilities of the available theory. On the other hand, in an applied context where the far-field data contains noise due to measurements, then due to the smoothing properties of the far-field operator, it is clear that the noisy data will fall out of the range of this operator. In this sense, in this case there is no existence. However, and having in mind that the problem is severely ill-posed, we would still want to find a stable approximation of the solution to the inverse problem, despite the noise on the data making it outside the range of admissible far-field data patterns.

Having these aspects in mind, we will proceed by presenting some classical results on the uniqueness of this inverse problem and sketch the proofs. We start by the classical result presented in [Lax and Philips, 1967], based on the ideas of Schiffer.

Theorem 5.18. *Assume that D_1 and D_2 are two sound-soft scatterers such that the far-field patterns coincide for an infinite number of incident plane waves with distinct directions and one fixed wave number. Then $D_1 = D_2$.*

Proof. Let $u_j^s(.,d)$, $j = 1, 2$, be the scattered fields corresponding to scattering by the obstacle D_j with incident direction d and let $u_j(.,d)$, $j = 1, 2$, be the corresponding total field. By Rellich's lemma 5.9, we know that the far-field pattern uniquely determines the scattered filed and so we have that

$$u_1^s(x,d) = u_2^s(x,d), \quad x \in G,$$

where G is the unbounded component of $\mathbb{R}^m \backslash (D_1 \cup D_2)$. Consequently, we get that $u_1(x,d) = u_2(x,d)$ for $x \in G$ and by the boundary condition and continuity of the total fields we get that

$$u_1(x,d) = u_2(x,d) = 0, \quad x \in \partial G.$$

We now assume that $D_1 \neq D_2$ in order to obtain a contradiction. Without loss of generality we can assume that $D^* = (\mathbb{R}^m \backslash G) \backslash \overline{D}_2$ is non-empty. Then $u_2^s(.,d)$ is defined in D^*, since it is describes scattering by D_2. Therefore, $u_2(.,d)$ satisfies the Helmholtz equation in D^* as well as the homogeneous Dirichlet boundary condition on ∂D^*, that is,

$$\begin{cases} \Delta u_2^s(x,d) + k^2 u_2^s(x,d) = 0, & x \in D^*, \\ u_2^s(x,d) = 0, & x \in \partial D^*. \end{cases}$$

Therefore $u_2(.,d)$ is a Dirichlet eigenfunction of the negative Laplacian in D^* with eigenvalue k^2. In this way, considering an infinite number of incident directions $\{d_n\}, n \in \mathbb{N}$, we have an infinite number of Dirichlet eigenfunctions $u_2(.,d_n)$ in D^* for the same eigenvalue k^2. The proof is now finished by showing that the $u_2(.,d_n) \in H_0^1(D^*)$ (e.g. [Colton and Kress, 2019, Lem.3.8]) are linearly independent and that for a fixed eigenvalue there exists only finitely many linearly independent Dirichlet eigenvalues in $H_0^1(D^*)$ (e.g. [Colton and Kress, 2019, proof of thm.5.1]). In this way, we get the desired contradiction and the proof is finished. □

For practical reason, one should be also interested in methods to solve the inverse obstacle scattering problem considering as data the far-field pattern for just one incident direction, or, at most, a finite number of incident directions. In this way, we will proceed by presenting uniqueness results considering just a finite number of incident directions, namely using some *a priori* bounds on the size of the obstacle. The bound on the size of the obstacle was initially proposed by Colton and Sleeman [Colton and Sleeman, 1983] and recently improved by Gintides [Gintides, 2005].

Theorem 5.19. *Let $D_1, D_2 \in \mathbb{R}^3$ be two scatterers which are contained in a ball of radius R, let*

$$N := \sum_{t_{nl}<kR} (2n+1)$$

where t_{nl}, $l \in \mathbb{N}$ are the positive zeros of the spherical Bessel function j_n, $n \in \mathbb{N}$ and let

$$M := \begin{cases} N/2+1, & N \text{ is even} \\ (N+1)/2, & N \text{ is odd.} \end{cases}$$

Assume also that the far-field patterns for both obstacles coincide for one fixed wave number k and for M different incident directions $d_n, n = 1, \ldots, M$, such that $d_n \neq \pm d_{n'}$ for $n \neq n'$. Then $D_1 = D_2$.

Proof. We use the same definition of D^* as used in the previous proof. The Courant maximum-minimum principle for compact symmetric operators implies that the negative Laplacian Dirichlet eigenvalues have the following property (see [Leis, 1986, thm.4.7]): The n–th eigenvalue λ_n ordered by magnitude taking into account its multiplicity for a ball B containing the domains D_1 and D_2 is always smaller than the n–th eigenvalue μ_n for the sub-domain $D^* \subset B$. In particular, for $\lambda_n = k^2$, the multiplicity of λ_n must be less than or equal to the sum of multiplicities of the eigenvalues of the ball B that are smaller than k^2. It is known that the eigenvalues of the ball B are given by $\mu_{nl} = t_{nl}^2/R^2$

(e.g. [Colton and Kress, 2019, pp.57]) and one can show that each has multiplicity $2n+1$ (e.g. [Colton and Kress, 2019, thm.2.6]). Therefore, the multiplicity of λ_n must be smaller or equal to N, by definition of N. Assuming D^* is non-empty, that is, that $D_1 \neq D_2$, similarly to the previous proof, we will be led to a contradition. We have that M incident directions $\{d_n\},\ n = 1, \dots, M$, would lead to M linearly independent eigenfunctions $u_2(., d_n),\ n = 1, \dots, M$ with the same eigenvalue k^2. Moreover, under the assumptions on the incident directions, the conjugate complex total fields $\bar{u}_2(., d_n),\ n = 1, \dots, M$ would be also linearly independent from the previous and would also satisfy the Helmholtz equation in D^* and the homogeneous Dirichlet boundary condition on ∂D^* (see [Gintides, 2005]). Therefore, we would have $2M$ linearly independent eigenfunctions related with the eigenvalue λ_n and so the multiplicity of λ_n is greater or equal to $2M$, which leads to a contradiction because $2M > N$. Therefore $D_1 = D_2$. □

Corollary 5.20. *Let $D_1, D_2 \in \mathbb{R}^3$ be two scatterers which are contained in a ball of radius R such that $kR < t_{10} \approx 4.4939$. Assume also that the far-field patterns coincide for one incident direction. Then $D_1 = D_2$.*

Proof. From $kR < t_{10}$ and the fact that t_{00} is the only positive zero t_{nl} of a Bessel spherical function j_n satisfying $t_{nl} < t_{10}$, we conclude that $N \leq 1$ and so by the previous theorem one incident direction is enough to uniquely determine the obstacle. □

From the previous theorem, we can obtain the size constraint for domains in $\mathbb{R}^3$ that must be satisfied to ensure uniqueness for the far-field data of a single incident direction.

Remark 5.21. A similar result can be obtained in $\mathbb{R}^2$ with the restriction $kR < z_{10}$, where z_{nl} are the positive zeros of the Bessel functions J_n. The proof is identical and relies on the fact that $J_n(kr)e^{\pm ik\phi}$ is an entire solution to the Helmholtz equation in $\mathbb{R}^2$ and therefore $\mu_{nl} = z_{nl}^2/R^2$ are Dirichlet eigenvalues on a circle of radius R. Everything then follows in a similar way.

Note that for the previous uniqueness results no regularity assumption was made on the domains.

For the Neumann and Robin boundary conditions, the same procedure of proof can not be carried out. This is due to the fact that the domain D^* defined as in the previous proofs might have corners or even cusps and the finiteness of the dimensions of the eigenspaces of the Laplace operator with boundary conditions requires the boundary to be sufficiently smooth. This cannot be overcome with requiring more regularity or even analyticity on D_1 and D_2, since this does not

prevent D^* to have corners or cusps. A new idea of proof that could be applicable to these two boundary conditions was suggested by Isakov (e.g. [Isakov, 1998]), who obtained a contradiction on the value of an integral over some appropriate contour when its length went to zero. A much simpler approach was presented by Kirsch and Kress [Kirsch and Kress, 1993], where this contradiction was achieved in a pointwise sense. Moreover, this procedure of proof can be carried out for any of the referred boundary conditions, as mentioned in remark 5.23. We formulate it in the following result.

Theorem 5.22. *Assume that D_1 and D_2 are two sound-hard scatterers such that the far-field patterns coincide for all incident plane waves with incident directions within an open non-empty subset of Ω_m and one fixed wave number. Then $D_1 = D_2$.*

Proof. By reciprocity (5.16) and analyticity of the far-field pattern, we first conclude that the far-field patterns must coincide for all incident directions. Then, as in theorem 5.18, we conclude that $u_1(.,d) = u_2(.,d)$ on the unbounded component G of $\mathbb{R}^m \backslash (\overline{D}_1 \cup \overline{D}_2)$. Let $x_0 \in G$ be fixed and consider the two Neumann problems

$$\Delta w_j^s + k^2 w_j^s = 0 \quad \text{in } \mathbb{R}^m \backslash \overline{D_j}, \tag{5.30}$$

$$\frac{\partial w_j^s}{\partial \nu} = -\frac{\partial \Phi(\,.\,, x_0)}{\partial \nu} \qquad \text{on } \partial D_j \tag{5.31}$$

for $j = 1, 2$. Our first goal is to prove that $w_1^s = w_2^s$ in G.

To this end, we choose a bounded C^2–domain B, such that $\mathbb{R}^m \backslash B$ is connected, the set $(\overline{D}_1 \cup \overline{D}_2) \subset B$, $x_0 \notin B$ and k^2 is not an interior Dirichlet eigenvalue for B, which is possible to achieve with a proper choice of B due to the strong monotonicity properties of the eigenvalues. Then, from the completeness of $\{u^i(.;d) \mid_{\partial B} :\ d \in \Omega_m\}$ in $L^2(\partial B)$ (e.g. [Colton and Kress, 2019, thm.5.5]), there exists a sequence $\{v_n\}$ in span$\{u^i(.;d) : d \in \Omega_m\}$ such that

$$||v_n - \Phi(\,.\,, x_0)||_{L^2(\partial B)} \to 0, \quad n \to \infty.$$

Then as each v_n is a solution to the Helmholtz equation and by the assumption that k^2 is not an eigenvalue for B, we can conclude (e.g. [Colton and Kress, 2019, thm.5.4]) that

$$\operatorname{grad} v_n \to \operatorname{grad} \Phi(\,.\,, x_0), \quad n \to \infty \tag{5.32}$$

uniformly on compact sets of B, in particular, in $\overline{D}_1 \cup \overline{D}_2$. Since the v_n are combinations of plane waves, from the first paragraph of this proof, the corresponding

scattered fields $v^s_{n,j}$ for the obstacles D_j, $j = 1, 2$ must coincide in G. This implies also that

$$\frac{\partial v^s_{n,j}}{\partial \nu} = -\frac{\partial v_n}{\partial \nu} \text{ on } \partial D_j, \quad j = 1, 2$$

so the convergence (5.32) along with the uniqueness and well-posedness of the solution to the exterior Neumann problem show us that

$$v^s_{n,j} \to w^s_j, \quad n \to \infty$$

uniformly in compact sets of $\mathbb{R}^m \backslash \overline{D_j}, j = 1, 2$. Therefore $w^s_1 = w^s_2$ in G, since as already mentioned the fields $v^s_{n,j}$, $j = 1, 2$ coincide in G.

We now assume that $D_1 \neq D_2$ in order to get a contradiction. Without loss of generality, there exists $x^* \in \partial D_1 \backslash \overline{D}_2$. We choose $h > 0$ sufficiently small such that the sequence

$$x_n := x^* + \frac{h}{n}\nu(x^*), \quad n \in \mathbb{N},$$

is contained in G. We now consider $w^s_{n,j}$ as the solutions to the exterior Neumann problems (5.30)–(5.31) with x_0 replaced by x_n. We recall that $w^s_{n,1} = w^s_{n,2} = w^s_n$ in G. On the one hand, we have that the Neumann boundary data over ∂D_2 is uniformly bounded with respect to the maximum norm and along with the well-posedness of the exterior Neumann problem we have that

$$\left| \frac{\partial w^s_n}{\partial \nu}(x^*) \right| \leq C,$$

for some positive constant C and all $n \in \mathbb{N}$. On the other hand, the scattered field corresponding to D_1 must satisfy the boundary condition and so

$$\left| \frac{\partial w^s_j}{\partial \nu}(x^*) \right| = \left| \frac{\partial \Phi(x^*, x_n)}{\partial \nu} \right| \to \infty, \quad n \to \infty$$

This contradiction shows that $D_1 = D_2$. □

Remark 5.23. Note that with proper changes in (5.31) and in the following boundary conditions, this proof works for all boundary conditions (5.9)–(5.11). The only requirement is that

$$|B\Phi(x^*, x_n)| \to \infty, \quad n \to \infty$$

in order to get the contradiction at the end. In particular, it is not needed that the boundary condition imposed for both obstacles D_1 and D_2 is the same.

A similar result can also be proved for the Robin or impedance boundary condition, where the uniqueness is guaranteed not only for the obstacle, but also for the impedance function λ.

Theorem 5.24. *Assume that D_1 and D_2 are two scatterers with continuous impedances λ_1 and λ_2 such that the far-field patterns coincide for all incident plane waves with incident directions within an open non-empty subset of Ω_m and one fixed wave number. Then $D_1 = D_2$ and $\lambda_1 = \lambda_2$.*

Proof. As referred in remark 5.23, with a similar proof to the one of theorem 5.22, one shows that $D_1 = D_2$. Let us assume that $\lambda_1 \neq \lambda_2$. By Rellich's lemma we have that the total fields u_1 and u_2, corresponding to scattering by $D = D_1 = D_2$ with impedances λ_1 and λ_2, respectively, coincide outside $\overline{D}$ and therefore by continuity, one finds that

$$\frac{\partial u}{\partial \nu} + i\lambda_1 u = \frac{\partial u}{\partial \nu} + i\lambda_2 u = 0, \text{ on } \partial D$$

where $u = u_1 = u_2$. Hence $(\lambda_1 - \lambda_2)u = 0$. If the total field would vanish on an open set of ∂D, then, by the boundary condition, the Cauchy data of u would vanish on the same open set of ∂D and by Holmgren's theorem and analyticity of the solution u, the total field u would vanish in $\mathbb{R}^m \backslash \overline{D}$. Therefore, this cannot happen and $\lambda_1 = \lambda_2$ in a L^2-sense. By the continuity of λ_1 and λ_2 we have the result. □

The previous result can also be extended to the case of a point source incident field instead of plane incidence (e.g. [Kress and Rundell, 2001]).

A uniqueness result for both sound-hard or impedance obstacle considering just a finite number of incident directions is still open, even with *a priori* knowledge on the size of the obstacle D (analogous to thm. 5.19 for the sound-soft case). Uniqueness results for a finite number of incident directions with no *a priori* knowledge on the size of the obstacle for the Dirichlet case are also an open problem. However, some work as also been developed in this direction with geometrical restrictions such as the case of balls [Liu, 1997] and, more recently, polygonal obstacles [Alessandrini and Rondi, 2005, Cheng and Yamamoto, 2003]. Uniqueness results for phaseless data (that is, with knowledge of only the absolute value of the far-field pattern) can also be established in some contexts [Sun et al., 2019]. Also, uniqueness for the transmission problem, that is, with transmission condition on a penetrable obstacle, was also be proven [Elschner and Hu, 2011].

In section 5.6, we will be interested in recovering star-shaped obstacles, that is, with boundary of the form

$$\Gamma = \{r(\hat{x})\,\hat{x} : \hat{x} \in \Omega_m\} \tag{5.33}$$

with $r \in C^2(\Omega_m)$. In this way, by a formal algebraic argument, given a complex valued function u_∞ on Ω_m, it makes sense to try to reconstruct one real function r over Ω_m, getting a formally overdetermined problem. In the same way, for a star-shaped domain, the impedance λ defined on the boundary can be seen as $\lambda = \lambda(\hat{x})$, $\hat{x} \in \Omega_m$. Therefore, even for the impedance case it would make sense to try to reconstruct both real functions r and λ from the knowledge of one complex valued function u_∞ over Ω. Having this algebraic formal argument in mind, we will proceed in the next chapter by suggesting methods to numerically solve the inverse scattering problem 5.16 having as data the far-field pattern u_∞ corresponding to one single incident field.

5.5 Numerical methods for the Direct Problem

Usually one needs a deep knowledge of the direct problem, in order to attack the inverse problem. In this way, we will focus on the numerical solution of the direct problem in the following lines, concentrating on the solution in 2D. There are many ways to do it, but we will focus on two approaches: a) the numerical aproximation by appropriate quadrature rules of the integral layer representation; and b) the method of fundamental solutions.

5.5.1 Layer Potential Representation

In this section we will present the numerical procedure to solve the inverse problem 5.16 by the hybrid method in $\mathbb{R}^2$. For simplicity, in this section we will denote the unit sphere by $\Omega := \Omega_2$. We will briefly present the direct problem in order to introduce the quadrature rule to deal with the logarithmic singularities of the fundamental solution in $\mathbb{R}^2$. In this way, we present how the direct problem can be solved in order to generate synthetic far-field data for the inverse problem.

The goal is to compute the far-field pattern u_∞ corresponding to scattering by a given obstacle D with boundary Γ and a given incident field u^i. We represented the scattered field as a combined single-and double-layer potential over Γ

$$u^s(x) = \int_\Gamma \left(\frac{\partial \Phi(x,y)}{\partial \nu(y)} - i\eta \Phi(x,y) \right) \varphi(y) ds(y), \quad x \in \mathbb{R}^m \backslash \Gamma$$

with $\eta > 0$, which is possible to do requiring enough regularity on Γ and on the incident field u^i over the boundary (see [Colton and Kress, 1983]). For each of the boundary conditions (5.9)–(5.11), the scattered field u^s must satisfy

$$Bu^s = -Bu^i \quad \text{on } \Gamma.$$

Considering the layer operators given in section 5.3.1, one is lead to the following integral equation for the Dirichlet boundary condition (5.9)

$$\frac{\varphi}{2} + (K - i\eta S)\varphi = -u^i \quad \text{on } \Gamma, \tag{5.34}$$

making use of the jump relations. Considering φ in the appropriate smooth space, as discussed before due to the comnpacteness of operators S and K, the previous integral equation is of the second kind (e.g. [Colton and Kress, 2019]). Now, assuming the boundary Γ can be parameterized by $z : [0, 2\pi] \to \mathbb{R}^2$, that is,

$$\Gamma = \{z(t) : t \in [0, 2\pi]\}$$

where z is a C^2-smooth $2\pi-$periodic and counter-clockwise oriented parameterization, the next step is to parameterize the previous integral equations. Then, by the Nyström method, one just needs to straightforwardly approximate the integrals by appropriate quadrature rules, and collocate the equation in the quadrature points in order to obtain a linear system.

For the operators S and K we simply apply the quadrature rules for smooth functions and logarithmic singularities in [Colton and Kress, 2019, sec. 3.5.], which are exponentially convergent for analytic boundaries Γ.

Therefore, for the Dirichlet case, we write (5.34) in the parametric form

$$\psi(s) + 2\int_0^{2\pi} M(s,t)\psi(t)dt = 2g(s), \quad s \in [0, 2\pi], \tag{5.35}$$

where $\psi(s) = \varphi(z(s))$ and $g(s) = -u^i(z(s))$ and

$$M(s,t) = M^K(s,t) - i\eta M^S(s,t), \quad s, t \in [0, 2\pi], \tag{5.36}$$

where M^S and M^K are respectively the parametric kernels of the single- and double-layer operators that will be defined in a few lines. The goal is to decompose the parameterized kernel M in the form

$$M(s,t) = M_1(s,t)\ln\left(4\sin^2\frac{s-t}{2}\right) + M_2(s,t), \quad s \neq t \tag{5.37}$$

for $s, t \in [0, 2\pi]$, where M_1 and M_2 are analytic. This can be done by considering the expansion of the fundamental solution $H_0^{(1)} = J_0 + iN_0$ in its power series (e.g. [Colton and Kress, 2019]). The idea is to apply this decomposition to the parametric kernel M^S of the single layer operator S and to the parametric kernel M^K of the double layer operator K and then make use of (5.36) to obtain the decomposition (5.37).

Therefore, following the ideas of [Kussmaul, 1969, Martensen, 1963] described in [Colton and Kress, 2019, sec.3.5], we have that the parametric kernel M^S of the single layer operator S, such that

$$(S\varphi)(z(s)) = \int_0^{2\pi} M^S(s,t)\psi(t)dt, \quad s \in [0, 2\pi]$$

can be decomposed as

$$\begin{aligned} M^S(s,t) &:= \frac{i}{4} H_0^{(1)}(k|z(s) - z(t)|)|z'(t)| \\ &= M_1^S(s,t) \ln\left(4\sin^2\frac{s-t}{2}\right) + M_2^S(s,t) \end{aligned}$$

where

$$M_1^S(s,t) := -\frac{1}{4\pi} J_0(k|z(s) - z(t)|)|z'(t)|, \tag{5.38}$$

$$M_2^S(s,t) := M^S(s,t) - M_1^S(s,t) \ln\left(4\sin^2\frac{s-t}{2}\right) \tag{5.39}$$

are analytic and M_2^S has a diagonal term given by

$$M_2^S(t,t) = \left(\frac{i}{4} - \frac{C}{2\pi} - \frac{1}{4\pi}\ln\left(\frac{k^2}{4}|z'(t)|^2\right)\right)|z'(t)|$$

where $C = 0.5772156649\ldots$ is Euler's constant.

In a similar way the parametric kernel M^K of the double-layer operator K can be decomposed as

$$\begin{aligned} M^K(s,t) &:= \frac{ik}{4}\frac{[(z(s) - z(t)) \cdot \nu(z(t))]}{|z(s) - z(t)|} H_1^{(1)}(k|z(s) - z(t)|)|z'(t)| \\ &= M_1^K(s,t) \ln\left(4\sin^2\frac{s-t}{2}\right) + M_2^K(s,t) \end{aligned}$$

where

$$M_1^K(s,t) := -\frac{k}{4\pi}\frac{[(z(s) - z(t)) \cdot \nu(z(t))]}{|z(s) - z(t)|} J_1(k|z(s) - z(t)|)|z'(t)| \tag{5.40}$$

$$M_2^K(s,t) := M^K(s,t) - M_1^K(s,t) \ln\left(4\sin^2\frac{s-t}{2}\right) \tag{5.41}$$

are also analytic with diagonal term

$$M_2^K(t,t) = \frac{1}{4\pi}\frac{z''(t)\cdot\nu(z(t))}{|z'(t)|}.$$

Note that though M^K is continuous, this decomposition brings advantages since its derivatives are not continuous at $s = t$. We also note that $H_1^{(1)} = -H_0^{(1)'}$ denotes the Hankel function of first kind and order one and $J_1 = -J_0'$ denotes the Bessel function of order one.

For other boundary conditions or layers representations that require the use of operator K^*, the procedures is similar (see [Kress, 1995]), getting

$$\begin{aligned} M^{K^*}(s,t) &:= -\frac{ik}{4}\frac{[(z(s)-z(t))\cdot\nu(z(s))]}{|z(s)-z(t)|}H_1^{(1)}(k|z(s)-z(t)|)|z'(t)| \\ &= M_1^{K^*}(s,t)\ln\left(4\sin^2\frac{s-t}{2}\right) + M_2^{K^*}(s,t) \end{aligned}$$

where

$$M_1^{K^*}(s,t) := \frac{k}{4\pi}\frac{[(z(s)-z(t))\cdot\nu(z(s))]}{|z(s)-z(t)|}J_1(k|z(s)-z(t)|)|z'(t)| \quad (5.42)$$

$$M_2^{K^*}(s,t) := M^K(s,t) - M_1^{K^*}(s,t)\ln\left(4\sin^2\frac{s-t}{2}\right) \quad (5.43)$$

are also analytic with diagonal term

$$M_2^{K^*}(t,t) = \frac{1}{4\pi}\frac{z''(t)\cdot\nu(z(t))}{|z'(t)|}.$$

In this way the logarithmic singularity of these kernels is exposed explicitly. As for the layer operator T in (5.22), due to its hypersingular kernel, the treatment must be different. We refer to [Colton and Kress, 2019] for details.

Going back to the Dirichlet case, having equation (5.35) in mind, one can proceed using the quadrature rule for the equidistant points $t_j := \pi j/N$, $j = 0,\ldots,2N-1$ given by

$$\int_0^{2\pi}\ln\left(4\sin^2\frac{s-t}{2}\right)f(t)dt \approx \sum_{j=0}^{2N-1}R_j^{(N)}(s)f(t_j) \quad (5.44)$$

with weights

$$R_j^{(N)}(s) := -\frac{2\pi}{N}\sum_{l=1}^{N-1}\frac{1}{l}\cos l(s-t_j) - \frac{\pi}{N^2}\cos N(s-t_j)$$

and the trapezoidal rule

$$\int_0^{2\pi} f(t)dt \approx \frac{\pi}{N} \sum_{j=0}^{2N-1} f(t_j). \tag{5.45}$$

Both these quadrature rules are derived by replacing the integrand f by its trigonometric interpolation polynomial and then integrating exactly to determine the quadrature weights.

We end up with an approximated equation of the form

$$\psi(s) + 2 \sum_{j=0}^{2N-1} \left(R_j^{(N)}(s) M_1(s,t_j) + \frac{\pi}{N} M_2(s,t_j) \right) \psi(t_j) = 2g(s), \quad s \in [0, 2\pi].$$

In particular, by the Nyström method, for $\psi_i = \psi(t_i)$, $i = 0, \ldots, 2N-1$ we get the linear system

$$\psi_i + 2 \sum_{j=0}^{2N-1} \left(R_{|i-j|}^{(N)} M_1(t_i,t_j) + \frac{\pi}{N} M_2(t_i,t_j) \right) \psi_j = 2g(t_i), \quad i = 0, \ldots, 2N-1 \tag{5.46}$$

where the quadrature weights can be simplified to the form

$$R_j^{(N)} = -\frac{2\pi}{N} \sum_{l=1}^{N-1} \frac{1}{l} \cos \frac{l\, j\, \pi}{N} - \frac{(-1)^N \pi}{N^2}. \tag{5.47}$$

In this way, one obtains a reconstruction of the density ψ that can be used to obtain the far-field u_∞ from the integral far-field representation of the combined single-and double-layer potential. As the far-field pattern of a combined single- and double-layer potential is given by

$$u_\infty(\hat{x}) = \Big((K_\infty - i\eta S_\infty)\varphi \Big)(x), \quad \hat{x} \in \Omega$$

and both S_∞ and K_∞ defined by (5.23) and (5.24), respectively, have a continuous kernel, we simply use the trapezoidal rule (5.45) to compute the far-field pattern by

$$u_\infty(\hat{x}) \approx \frac{\pi}{N} \sum_{j=0}^{2N-1} M_\infty(\hat{x}, t_j) \psi_j, \quad \hat{x} \in \Omega$$

where $M_\infty(\hat{x}, t)$ is the parametric kernel of the combined single-and double-layer far-field operator given by

$$M_\infty(\hat{x}, t) = \frac{e^{-i\pi/4}}{\sqrt{8\pi k}} \left(k\, \hat{x} \cdot \nu(z(t)) + \eta \right) e^{-ik\hat{x}\cdot z(t)} |z'(t)|.$$

FTjis procedure allows us to compute the far-field pattern for one incident direction at N equidistant points on the unit circle Ω and considered it as the given data for the inverse scattering problem. As suggested in [Kress, 1985] we choose $\eta = k$.

5.5.2 Method of Fundamental Solutions

The **method of fundamental solutions** (MFS) is much easier to implement numerically then the previous representation, but it not always presents the same exponential convergence. It is based on density results in $L^2(\Gamma)$ of a family of fundamental solutions

$$\{\Phi(., s) : s \in \gamma\}$$

where γ is an appropriate curve (or surface) inside of the obstacle D. For details on this method we refer for instance to [António et al., 2008, Barnett and Betcke, 2008, Fairweather et al., 2003, Smyrlis and Karageorghis, 2009, Smyrlis, 2009]. One way that is usually used to determine γ is to define consider the boundary parameterized by $\tilde{z} = \beta z$ where z is the parameterization of the exact boundary Γ and $\beta \leq 1$. Therefore, the idea is to approximate the scattered field by a sum of the form

$$\tilde{u}^s(x) = \sum_{i=1}^{n} a_i \Phi(x, s_i) \tag{5.48}$$

where $s_i \in \gamma$ are the so called **source points**. An approximation of the previous form satisfies the Helmoltz equation in $\mathbb{R}^m \backslash \overline{D}$ and the Sommerfeld radiation condition, so one wants to find the weigths a_i such that the boundary condition is satisfied. Due to the previously mentioned denseness results, one cannot expect to have a solution of the form (5.48), but due to the denseness one can expect to aproximate the solution by a filed of the form (5.48) as well as one desires. For the Dirichlet boundary condition and given the incident field u^i, one way to do this is to use a collocation method, that is, to make that

$$\tilde{u}^s(x_j) = -u^i(x_j), \quad j = 1, 2, \ldots, p$$

and solve the previous equation in terms of the coefficients a_i in a least square sense with $p \geq n$. This can be done by considering the matrix

$$A = \begin{bmatrix} \Phi(x_1, s_1) & \Phi(x_1, s_2) & \ldots & \Phi(x_1, s_n) \\ \Phi(x_2, s_1) & \Phi(x_2, s_2) & \ldots & \Phi(x_2, s_n) \\ \vdots & \vdots & & \vdots \\ \Phi(x_p, s_1) & \Phi(x_p, s_2) & \ldots & \Phi(x_p, s_n) \end{bmatrix}$$

and the second member vector

$$b = \begin{bmatrix} -u^i(x_1) \\ -u^i(x_n) \\ \vdots \\ -u^i(x_p) \end{bmatrix}.$$

If $p = n$, the solution of the linear system $Ax = b$ determines the weights a_i, $i = 1, 2, \ldots, n$. If $p > n$, the solution of the linear system $A^*Ax = A^*b$ determines the weights a_i, $i = 1, 2, \ldots, n$ that best fit (5.48) in a least square sense. For a proper choice of the source points we refer to [Alves, 2009]. As the choice of source points influences the conditioning of the linear system, [Araújo and Serranho, 2019] proposed a method to find equidistant points over a unit sphere to improve the conditioning of the linear system in 3D. More recently, [Chen et al., 2023] proposed an optimization procedure to optimize the pseudo-boundary γin terms of the effective condition number of the linear system (5.48). It should be noticed that the choice of the points s_i are related with the accuracy of the approximation of the scattered field u^s and conditioning of the system. Using fundamental solutions as basis functions, Schaback's uncertainty principle [Schaback, 1995] states that usually one cannot have both accuracy and well-conditioning, so a compromise between conditioning and quality of the approximation must be obtained. Another approach is the one proposed in [Antunes, 2022], where a proper change of basis functions that are close to orthogonal but span the same space as fundamental solutions is considered to overcome the ill-conditioning for the 2D Laplace equation. This work was then generalized to the 3D Laplace equation [Antunes et al., 2025] and the 2D Helmholtz equation [Antunes et al., 2024].

As a standard approach for ill-conditioned system, one can consider regularization. Using Tikhonov's regularization, the previous systems should be replaced by

$$(\alpha I + A^*A)x = A^*b.$$

From the far-field behaviour Φ_∞ of the fundamental solution, one can then reconstruct from the weight's a_i both the scattered field (5.48) and the far-field pattern

$$\tilde{u}_\infty(\hat{x}) = \sum_{i=1}^{n} a_i \Phi_\infty(\hat{x}, s_i), \tag{5.49}$$

where the far-field pattern of the fundamental solution Φ is given in $\mathbb{R}^m$, considering $m = 2, 3$, by

$$\Phi_\infty(\hat{x}, y) = \varrho_m e^{-ik\hat{x}.y},$$

where ϱ_m is defined in (5.15). The MFS is clearly easier to implement numerically, since no quadrature rule is considered. However, the convergence is usually poorer than the layer representation approach. The Layer representation approach guarantees exponetial convergence for C^2-domains in $\mathbb{R}^2$, while MFS only has proven exponetialk convergence for the disk.

5.6 Numerical methods for the Inverse Problem

We recall that we aim to solve the inverse problem 5.16. For simplicity, we will consider in this section that the obstacle is sound-soft, that is, we consider a Dirichlet boundary condition with vanishing total field u in the boundary of D as

$$u^s = -u^i, \quad \text{in } \partial D. \tag{5.50}$$

However, the methods can be extended for other types of boundary conditions. We will also consider the domain to be star-shaped, that is, the boundary of the obstacle is of the form (5.33). Again, the methods can be easily extended for more general parameterizations

$$z : \Omega_m \mapsto \Gamma.$$

5.6.1 Newton-type methods

Newton-type methods appeared in the decade of 1980. They usually consider the far-field operator

$$F : \partial D \mapsto u_\infty$$

that maps the boundary of the obstacle to far-field pattern u_∞ generated by that obstacle, considering that the incident field u^i is fixed. In this way, given the far-field pattern, one wants to find the solution D to

$$F(D) = u_\infty.$$

As mentioned before, the previous equation is ill-posed and nonlinear. In this way, one approach is to linearize the previous equation by Newton's method, and then solve a regularized version of this linear equation iteratively. Therefore, at the n th step one has a domain D_n that is parameterized by the function z_n. In this way, we consider the far-field operator for the parameterization's space

$$F(z) = u_\infty,$$

and linearize the previous equation in z around z_n by the **Newton's method**

$$F(z_n) + F'(z_n)h = u_\infty,$$

which is equivalent to

$$F'(z_n)h = u_\infty - F(z_n), \tag{5.51}$$

and update the new approximation for the parameterization of the boundary of the domain D by $z_{n+1} = z_n + h$. However, this equation is severelly ill-posed, so one should consider a regularized version of it, for instance, by Tikhonov regularization, and solve

$$(\alpha I + F'(z_n)^* F'(z_n))h = F'(z_n)^*(u_\infty - F(z_n)).$$

Moreover, one also needs to characterize the **Fréchet derivative** of the operator F, which by definition is the operator A that satisfies

$$\lim_{h\to 0} \frac{\|F(z) - F(z+h) - Ah\|}{\|h\|} = 0.$$

It can be shown that the Fréchet derivative of F is given by

$$F'(z)\, h = u^\dagger_\infty,$$

where $u^\dagger_\infty$ is the far-field pattern of $u^\dagger$, which is a radiating solution of the Helmholtz equation with boundary condition

$$u^\dagger = -(h \cdot \nu)\frac{\partial u}{\partial \nu} \quad \text{on } \gamma, \tag{5.52}$$

where γ is parameterized by z. This means that is the parameterization space is of dimension n with basis function υ_i, $i = 1, 2, \ldots, n$, one has that

$$h = \sum_{i=1}^{n} \beta_i \upsilon_i,$$

which means that, for each iteration of Newton's method, one needs to solve n direct problems, one for each υ_i in the place of h in equation (5.52). In this way, Newton's method requires a forward solver as described in section 5.5.

Though Newton's methods usually is able to get good reconstructions of the obstacle, the main drawback of this method is that it requires a forward solver to be used n-times at each iteration step, which is costly in terms of computations. A reasonable initial guess is also needed to start the iterations. As for

the theoretical background, the convergence proofs for these methods are not yet completely satisfactory, though there has been some progress in that matter (see [Hohage, 1997, Hohage, 1998, Hohage, 1999, Potthast, 2001]).

For more details on the Fréchet differentiability of the operator F we refer to [Hettlich, 1998, Hettlich, 1999, Potthast, 1996]), where there are also approaches for other types of boundary conditions. The generalization of this Newton method for recovering both the shape of the unknown obstacle and the unknown impedance was also made in [Kress and Rundell, 2001].

5.6.2 Decomposition methods

As an alternative approach appearing on the second half of the 80's, are the **decomposition methods**. These take care of the ill-posedness and the nonlinearity of the inverse scattering problem separately, in the following way (see the works of [Kirsch and Kress, 1986, Kirsch and Kress, 1987a, Kirsch and Kress, 1987b]).

In a first step the total field u is reconstructed from the given far-field pattern u_∞, which is an ill-posed problem. This can be done, for example, by representing the scattered field u^s as a layer potential over an approximate boundary γ, that needs to be considered to be inside of D. Moreover, we will need the following assumption.

Assumption 5.25 (Analytic Continuation Principle). *The solution u^s to the direct problem of scattering by D can be analytically extended to the interior of D as a solution to the Helmholtz equation in a neighbourhood of the boundary Γ of D.*

Remark 5.26. If the boundary Γ is analytic, then assumption 5.25 holds, by a combination of thm.6.19 and lemma 6.37 in [Gilbarg and Trudinger, 1998].

Assuming that γ is sufficiently close to Γ in a way that the solution u^s to the direct problem of scattering by D can be analytically extended up to γ and assuming that k^2 is not an interior Dirichlet eigenvalue of the negative Laplacian for the interior of γ, we can represent the scattered field u^s as a single layer potential over γ (see [Colton and Kress, 1983, thm. 3.30]), that is,

$$u^s(x) = \int_\gamma \Phi(x,y)\,\varphi(y) ds(y), \quad x \in \mathbb{R}^m \backslash \gamma \tag{5.53}$$

with density $\varphi \in C(\gamma)$.

Remark 5.27. We choose a single-layer representation because it leads to less complexity later on in the implementation. However, the additional condition on the wave number k is needed. If we considered a combined single- and double-layer

potential as in section 5.5.1, the condition that k^2 is not an interior eigenvalue would not be needed, leading however to a harder implementation, since we would have to deal with the hypersingular layer operator T in (5.22) to compute the (later appearing) gradient of the scattered field u^s in the linearization step of the hybrid method.

Due to analyticity of the single layer potential in $\mathbb{R}^m \backslash \gamma$, it is clear that if the analytic continuation principle 5.25 does not hold, then the previous representation would not make sense for the cases where $\gamma \cap D \neq \emptyset$. One knows that the exterior trace to the boundary of the previous potential is given by

$$u^s(x) = \big(S_\gamma \varphi\big)(x), \quad x \in \gamma$$

where $S_\gamma : C(\gamma) \to C(\gamma)$ is the single-layer operator (5.19) over γ. By the asymptotics of the single layer potential, the far-field must satisfy equation

$$S_{\gamma,\infty}\, \varphi = u_\infty \text{ in } \Omega_m \tag{5.54}$$

with the far-field operator $S_{\gamma,\infty} : C(\gamma) \to C(\Omega_m)$ given by

$$S_{\gamma,\infty}\, \varphi = \varrho_m \int_\gamma e^{-ik\hat{x}\cdot y}\, \varphi(y) ds(y), \quad \hat{x} \in \Omega_m, \tag{5.55}$$

with ϱ_m given as in (5.15). As mentioned before, the previous operator is compact (since it has a continuous kernel) so (5.54) must be replaced by a regularized equation. In order to show that a regularization scheme is applicable one needs to show that the operator $S_{\gamma,\infty}$ is injective.

Theorem 5.28. *Assume that k^2 is not an interior Dirichlet eigenvalue of the negative Laplacian with respect to the open bounded domain D_γ with boundary γ. Then the operator $S_{\gamma,\infty} : L^2(\gamma) \to L^2(\Omega_m)$ is injective and has dense range.*

Proof. Assume that $\psi \in L^2(\gamma)$ satisfies $S_{\gamma,\infty}\psi = 0$. Then the single-layer potential

$$v(x) = \int_\gamma \Phi(x,y)\, \psi(y) ds(y), \quad x \in \mathbb{R}^m \backslash \gamma$$

has a vanishing far-field. By Rellich's lemma and analyticity, we conclude that v vanishes in $\mathbb{R}^m \backslash \overline{D_\gamma}$. By continuity up to the boundary, we conclude that $S_\gamma \psi = 0$ over γ. As k^2 is not an interior Dirichlet eigenvalue with respect to the open bounded domain D_γ we know that S_γ is injective (see [Colton and Kress, 1983, thm.3.30]) and so we conclude that $\psi = 0$, proving injectivity of S_γ.

To prove denseness, one shows by a similar argument that the adjoint operator S_γ^* is injective. Then, one concludes that S_γ is dense, since for a linear bounded operator A the closure of the range of A is the orthogonal complement of the nullspace of A^* (for details see [Colton and Kress, 2019, thm.5.17]). □

Remark 5.29 (Denseness and noisy data). Again, we recall that in applications' context, far-field data may contain noise due to measurements. Therefore, the fact that the single-layer far-field operator $S_{\gamma,\infty}$ range is dense in L^2 allows to obtain reconstructions even from noisy far-field data u_∞. Nonetheless, due to the ill-posedness of the inversion of this operator (coming from its continuous kernel and thoerem 2.33), a regularized approach must be consideredm, as follows.

Using Tikhonov regularization, we need to replace (5.54) by

$$\left(\alpha I + S^*_{\gamma,\infty} S_{\gamma,\infty}\right) \varphi = S^*_{\gamma,\infty} u_\infty, \tag{5.56}$$

solving it with respect to φ for some regularization parameter $\alpha > 0$. The scattered field u^s can now be approximated by

$$u^s(x) = \int_\gamma \Phi(x,y)\, \varphi ds(y), \quad x \in \mathbb{R}^m \backslash \gamma. \tag{5.57}$$

and using the jump relations we also get the approximations to u^s and its exterior normal derivative $\partial u^s/\partial \nu$ on γ_n given by

$$u^s(x) = (S_\gamma \varphi)(x), \quad x \in \gamma, \tag{5.58}$$

$$\frac{\partial u^s}{\partial \nu}(x) = -\frac{1}{2}\varphi + (K^*_\gamma \varphi)(x), \quad x \in \gamma, \tag{5.59}$$

respectively.

Now, in the second step of the method, one tries to locate the obstacle as the position where the boundary condition holds. For the considered Dirichlet boundary condition, this is the position where the total field $u = u^i + u^s$ vanishes, considering the gicen incident field u^i and the approximated scattered field u^s calculated by (5.57). This step is clearly nonlinear, but it is well-posed. This can be done in a least squares sense (by a iterative method) or in the Dirichlet case just by plotting $|u|$.

Summarizing, in the Kirsch and Kress decomposition method, the requirement that the far-field of the potential coincides with the given far-field u_∞ leads to an ill-posed linear integral equation that can be approximately solved via Tikhonov regularization. Then, in a second step, one tries to find the boundary Γ as the location where the boundary condition (5.7) is satisfied. This second step is clearly nonlinear.

Another decomposition method, is the point source method [Potthast, 1998]. Similarly, an ill-posed integral equation needing regularization also arises. The point source method was afterwards adapted in [Potthast and Schulz, 2007] to reconstruct the obstacle without knowing its boundary condition.

Though these methods do not need forward solvers to determine the solution to direct problems, the reconstructions obtained are not as accurate as those obtained by Newton's iterations. As for the theoretical background, these methods are usually compared with a minimization problem (see[Colton and Kress, 2019, sec.5.4]), but there is a gap between the theory and the implementation of the methods. While the method is applied considering two separate minimization steps, in the theory the minimization is considered as a whole.

5.6.3 Hybrid methods

Several hybrid methods have arised in between, combining the ideas of decomposition methods and Newton-type methods. The idea is to take advantages of both of them by getting good reconstructions without the need of a forward solver at each step. These methods can be revised in [Ivanyshyn et al., 2010] and were motivated by the work [Kress, 2003], which related the connection between the least squares method and the iterative methods for inverse scattering problems.

The **hybrid method** that we will focus on was developed in the series of papers by [Kress and Serranho, 2005, Kress and Serranho, 2007, Serranho, 2006, Serranho, 2007b] and consists basically in iterating the Kirsch and Kress decomposition in the following way.

Suppose that at iteration n we have γ_n, parameterized by $z_n : X \to \mathbb{R}^m$ (with usually $X = [0, 2\pi]$ and $m = 2, 3$), as a curve approximation to the exact boundary Γ, parameterized by z_*, of the obstacle. Then, each iteration of the method is divided in two steps. In the first step, one represents the solution over the boundary γ_n by a layer potential as in (5.53) by

$$u_n^s(x) = \int_{\gamma_n} \Phi(x, y)\, \varphi_n(y) ds(y), \quad x \in \mathbb{R}^m \backslash \gamma_n. \tag{5.60}$$

In this way, as in (5.54), we solve the far-field equation over γ_n

$$S_{\gamma_n,\infty}\, \varphi_n = u_\infty \text{ in } \Omega_m$$

with respect to φ_n, with $S_{\gamma,\infty}$ defined in (5.55).

In a second step of each iteration, we now update the position of the approximation γ_n in the following way. For a fixed analytic field u, we now define the operator G_D that maps the parameterization z of the contour γ to the exterior trace of the Dirichlet boundary condition of that field u over γ, that is,

$$G_D : z \mapsto u \circ z.$$

If the field u is the total field, then in order to find the position of the boundary Γ of the obstacle D as the location where the boundary condition is satisfied, we want to find the solution to

$$G_D(z) = 0.$$

In the spirit of a Newton-type method, we now linearize the previous equation around z_n (which is the paramterization of the current approximation γ_n and solve the linearized equation

$$G_D(z_n) + G'_D(z_n)h = 0 \quad \text{in } X \tag{5.61}$$

with respect to the shift h. In the next theorem, we characterize the Fréchet derivative of G_D.

Theorem 5.30. *The operator $G_D : C^2(X) \to C(X)$ is Fréchet differentiable and the Fréchet derivative is given by*

$$G'_D(z)h = (\operatorname{grad} u \circ z) \cdot h.$$

Proof. By the Taylor formula, the Fréchet differentiability of G_D is a direct consequence of the analyticity of u and the C^2–smoothness of z. Moreover, from the Taylor formula for u, one gets for each $t \in X$ that

$$u\big(z(t) + h(t)\big) = u\big(z(t)\big) + \operatorname{grad} u\big(z(t)\big) \cdot h(t) + O\big(|h(t)|^2\big),$$

as $||h||_\infty \to 0$. Therefore, by definition of G_D we have

$$||G_D(z+h) - G_D(z) - (\operatorname{grad} u \circ z) \cdot h||_\infty = O(||h||_\infty^2)$$

as $||h||_\infty \to 0$ and by definition of the Fréchet derivative one has the result. □

With this characterization, equation (5.61) can be rewritten in the following way

$$(\operatorname{grad}\, u \circ z_n) \cdot h = -u \circ z_n \text{ in } X. \tag{5.62}$$

In this way, at each iteration n we approximate u^s by u_n^s given by (5.60) obtained in the first step of the iteration and solve

$$\big((\operatorname{grad}\, u_n^s + \operatorname{grad}\, u^i) \circ z_n\big) \cdot h = -\big(u_n^s + u^i\big) \circ z_n \quad \text{in } X,$$

with respect to h in a least squares sense, obtaining the new approximation γ_{n+1} parameterized by $z_{n+1} = z_n + h$. Note that we use the jump relations (5.58) and (5.59) to compute the terms involved, through the decomposition

$$\operatorname{grad} u|_{\gamma_n} = \nu \left.\frac{\partial u}{\partial \nu}\right|_{\gamma_n} + \nabla_t\, u, \tag{5.63}$$

where $\nabla_t u$ represents the surface gradient of u, which in $\mathbb{R}^2$ reduces itself to the tangential derivative times the tangential unit vector. We now repeat the two steps until some stopping criteria is fulfilled. The details on the numerical implementation can be checked in [Serranho, 2007a].

Remark 5.31. Note that to show solvability of (5.61) we would need to show that $G'_D(z_n)$ is injective. However this can only be done if we are over the correct boundary Γ, if u is considered to be the exact total field and if there exists an open set of Γ where $h \cdot \nu \neq 0$. In this case, by the boundary condition, we have that if

$$0 = G'_D(z_*)h = h \cdot \operatorname{grad} u \circ z_* = h \cdot \nu \, \frac{\partial u}{\partial \nu}$$

then $h = 0$ everywhere. By contradiction, assume that this is not the case. Then, as there exists an open subset of Γ where $h \cdot \nu \neq 0$, the normal derivative of u would need to vanish on that open subset of Γ. By the boundary condition and Holmgren's theorem we conclude that the total field $u = 0$ in $\mathbb{R}^m \backslash \overline{D}$, which can not happen since the scattered field goes to zero at infinity and the incident field does not. A similar result can be shown for the Neumann and Robin boundary condition (see [Serranho, 2006, thm.5]).

This hybrid method is able to compete with Newton-type methods in terms of the quality of the reconstruction, without needing a forward solver in each step and therefore having less computational cost. In the spirit of decomposition methods, it separates the ill-posedness in the first step from the non-linearity in the second step. This method can also be extended for other types of boundary conditions, namely for the Neumann condition [Kress and Serranho, 2007] an to recover both the shape the obstacle and impedance function [Serranho, 2006]. For details on the hybrid method for reconstructions in three-dimensions, we refer to [Serranho, 2007b].

Numerical Implementation of the Hybrid method in 2D

We will now detail the numerical implementation of the Hybrid method in 2D, since it is easily adapted also to implement the Kirsch and Kress decomposition method described in section 5.6.2. In fact, Kirsck-Kress decomposition method is a simpler case, where the first (ill-posed) step is made just once and the second (non-linear step) is repeated until a good approximation is found.

Also, we are now in a position to present the numerical method for the inverse problem, since we can reuse all the quadrature rules and its ideas that have been already mentioned in section 5.5.1, concerning the direct problem.

For the inverse problem that we will now discuss, we consider star-shaped obstacles, that is, the boundary of the obstacle is given by

$$\gamma_r = \{z(t) = r(\hat{x}(t))\,\hat{x}(t) \;\mid\; r : \Omega \to \mathbb{R}^2, t \in [0, 2\pi]\} \tag{5.64}$$

where $\hat{x}(t)$ is defined in $\mathbb{R}^2$ by

$$\hat{x}(t) = (\cos t, \sin t), \quad t \in X = [0, 2\pi].$$

As for parameterization space for r, we choose trigonometric polynomials, since they are dense in $L^2[0, 2\pi]$ (see [Kress, 1998]). In this way, we consider radius functions r that are linear combinations of trigonometric polynomials of order less than or equal to N_z, that is,

$$r(t) = a_0 + \sum_{j=1}^{N_z} a_j \cos jt + \sum_{j=1}^{N_z} b_j \sin jt \tag{5.65}$$

with $a_j, b_j \in \mathbb{R},\ j = 1, \ldots, N_z$.

Consider γ_n, parameterized by z_n, to be the current approximation to the solution Γ of the inverse problem.

In a first step, the total-field u is reconstructed from the given far-field data u_∞, by representing the scattered field u^s by a single-layer potential over γ_n, that is,

$$u^s(x) = \int_{\gamma_n} \Phi(x, y)\varphi(y)dy.$$

This representation leads to less complexity in the implementation than a combined single-and double-layer potential (see remark 5.27) and can be taken under the assumptions discussed in section 5.5.1. In this way, as referred in section 5.5.1, we have to solve the Tikhonov's regularized far-field equation

$$\left(\alpha_n I + S^*_{\gamma_n,\infty} S_{\gamma_n,\infty}\right) \varphi^{(n)} = S^*_{\gamma_n,\infty} u_\infty, \tag{5.66}$$

where α_n should be decreasing with n (the closer we are to the real boundary, the less we want to alter the exact equation) and

$$(S_{\gamma,\infty}\,\varphi)(\hat{x}) = \frac{e^{i\pi/4}}{\sqrt{8\pi k}} \int_\gamma e^{-ik\hat{x}\cdot y}\,\varphi(y)ds(y), \quad \hat{x} \in \Omega.$$

By the relation (e.g. [Spanier and Oldham, 1987, Ch.53])

$$\pi J_0(|y|) = \int_0^\pi \cos(|y|\cos t)dt = \frac{1}{2}\int_\Omega e^{i\hat{x}\cdot y}d\hat{x}, \quad y \in \mathbb{R}^2$$

one can write (5.66) in the parameterized form

$$\alpha_n\psi^{(n)}(s)+\frac{1}{4k}\int_0^{2\pi}J_0(k|z_n(s)-z_n(t)|)|z_n'(t)|\psi^{(n)}(t)dt=$$

$$=\frac{e^{-i\pi/4}}{\sqrt{8\pi k}}\int_0^{2\pi}e^{ik\hat{x}(t)\cdot z_n(s)}u_\infty(\hat{x}(t))dt$$

where $\psi^{(n)}(t)=\varphi^{(n)}(z_n(t))$. Since all the integral kernels involved in the previous equation are continuous, by the Nyström method associated with the trapezoidal rule (5.45) one gets the linear system

$$\alpha_n\psi_i^{(n)}+\frac{\pi}{4kN}\sum_{j=0}^{2N-1}J_0(k|z_n(t_i)-z_n(t_j)|)|z_n'(t_j)|\psi_j^{(n)}=$$

$$=\frac{e^{-i\pi/4}}{\sqrt{8Nk}}\sum_{j=0}^{2N-1}e^{ik\hat{x}(t_j)\cdot z_n(t_i)}u_\infty(\hat{x}(t_j))$$

for $i=0,\ldots,2N-1$, which is solved in order to obtain the $\psi_i^{(n)}=\psi^{(n)}(t_i)$.

By the jump relations for the single layer operator (see theorem 5.10) given by

$$\begin{aligned}u^s(x) &= S_{\gamma_n}\varphi,\\ \frac{\partial u^s}{\partial\nu}(x) &= -\frac{\varphi}{2}+K_{\gamma_n}^*\varphi,\end{aligned}$$

using the same quadratrure rules as for the forward problem, namely the one to deal with the logarithmic singularity of the kernels involved described in (5.44) and the trapezoidal rule (5.45) to deal with the smooth part, one gets the approximations

$$\begin{aligned}u^s(z_n(t_i)) &\approx u_n^s(z_n(t_i)):=\sum_{j=0}^{2N-1}\left(R_{|i-j|}^{(N)}M_1^S(t_i,t_j)+\frac{\pi}{N}M_2^S(t_i,t_j)\right)\psi_j^{(n)},\\ \frac{\partial u^s}{\partial\nu}(z_n(t_i)) &\approx \frac{\partial u_n^s}{\partial\nu}(z_n(t_i))\\ &:= -\frac{\psi_i^{(n)}}{2}+\sum_{j=0}^{2N-1}\left(R_{|i-j|}^{(N)}M_1^{K^*}(t_i,t_j)+\frac{\pi}{N}M_2^{K^*}(t_i,t_j)\right)\psi_j^{(n)},\end{aligned}$$

for $i=0,\ldots,2N-1$, where the kernels M_1^S, M_2^S and $M_1^{K^*}, M_2^{K^*}$ are given respectively by (5.38)–(5.39) and (5.42)–(5.43) and the quadrature weights are given

by (5.47). One now computes the tangential derivative of the total field $u_n = u_n^s + u^i$ over γ_n by trigonometric differentiation, that is, one takes the tangential derivative of the trigonometric interpolation polynomial of u_n as an approximation to the tangential derivative of the total field u. In this way, one can find an approximation to the gradient of the total field using the decomposition

$$\operatorname{grad} u|_{\gamma_n} \approx \nu \left.\frac{\partial u_n}{\partial \nu}\right|_{\gamma_n} + \tau \left.\frac{\partial u_n}{\partial \tau}\right|_{\gamma_n}.$$

Again, we stress that the normal derivative of u_n^s and computed by the jump relations, while the tangential derivative of u_n^s is computed by trigonometric differentiation.

From the linearized equation (5.62) and the approximation space for the parameterization given by (5.64) and (5.65) one gets

$$\left(a_0^{(h)} + \sum_{j=1}^{N_z} a_j^{(h)} \cos jt_i + \sum_{j=1}^{N_z} b_j^{(h)} \sin jt_i\right) \operatorname{grad} u_n(z_n(t_i)) \cdot (\cos t_i, \sin t_i) = -u_n\big(z_n(t_i)\big)$$

for $i = 0, \ldots, 2N-1$ and so one now fits the coefficients $a_j^{(h)}, b_j^{(h)}$, $j = 0, \ldots, N_z$ by a Levenberg-Marquardt step (note that one must have $N_z < N$) in order to establish the shift

$$h(t) = \left(a_0^{(h)} + \sum_{j=1}^{N_z} a_j^{(h)} \cos jt + \sum_{j=1}^{N_z} b_j^{(h)} \sin jt\right)(\cos t, \sin t), \quad t \in [0, 2\pi],$$

and get a new approximation γ_{n+1} parameterized by $z_{n+1} = z_n + h$. We then repeat the process until some stopping criteria is achieved, for instance, while $||u_n||_{L^2(\gamma_n)}$ is decreasing.

For numerical results of the hybrid method we refer to [Serranho, 2007a], both in 2D and 3D.

5.6.4 Sampling methods

When the previous classes of methods first appeared, they required the *a priori* knowledge of some physical properties of the obstacle, namely the boundary condition imposed and an initial guess for the position and shape of the obstacle. An alternative method for recovering scatterers without this *a priori* knowledge was needed. In the second half of the 90's, a new family of methods arose - the **sampling** or **probe methods** - that could deal with this problem (e.g. the linear sampling method [Colton and Kirsch, 1996], the factorization method [Kirsch, 1998] and the probe algorithm [Ikehata, 1998]). Their idea

is to establish a criterion to distinguish whether a point is inside or outside D, based on the range of some appropriate operator, and then apply it to a grid of sampling points. Though these methods do not need *a priori* knowledge on the boundary condition, they usually just reconstruct the obstacle and not the boundary condition. Recently in [Cakoni and Colton, 2004], after reconstructing the obstacle by the linear sampling method, a procedure was suggested to reconstruct also the unknown impedance λ on the boundary of this reconstructed obstacle. Moreover, a big drawback arises, in general, for this class of methods: they require a huge amount of data, namely the far-field data for many incident directions, in order to get meaningful reconstructions. Recently a sampling method was proposed, that needs only one incident direction [Ma and Hu, 2021].

Since then, several other methods were suggested to solve the inverse scattering problem (see, for instance, [Cakoni and Colton, 2006, Colton and Kress, 2019, Colton and Kress, 2006, Kress, 2007, Potthast, 2005]), always trying to get good reconstructions with small computational cost and needing only as few as possible input data. However, recently a new approach as emerged, namely the use of machine learning. In the following subsection we will address briefly this matter, with its benefits of great optimization quality and adaptability and drawbacks as huge amounts of data needed for training.

5.6.5 Machine Learning approaches

Due to the development of **machine learning** (in particular, deep learning) there have been recent developments in using this technique for inverse scattering problems. The idea is to feed the training of the neural network with the measured or synthetic scattering data as input and a representation of the obstacle as output. In this section, we will just briefly review the main possibilities of this approach without going into detail. In general, machine learning offers the promise of great optimization capacity and adaptability to different settings and problems. On the downside, it needs huge amnounts of data for the training process.

There are different approaches to inverse scattering problems using **neural networks**. The first is to consider direct learning, where no structure of the problem or solution is embedded in the network. In this ways, one finds a proper neural network architecture such that it maps the given input format of the scattering data to the predicted obstacle representation in the output format, training it with existing data [Yang and Liu, 2020, Xu et al., 2020]. Specific neural network architectures have also been developed for inverse scattering problems, as the SwitchNet [Khoo and Ying, 2019]. Another approach is to consider an objective

function that needs to be minimized. In our context, this could, for instance, be made by considering the optimal parameters of the representation of the obstacle that minimize the difference between the measured and the corresponding scattering data of that obstacle [Meng et al., 2020]. In this way, information on the form of the solution must be embedded in the neural network. Other possibilities include iterating the neural network procedure using a cost function towards the global minimum and avoiding local minima [Sanghvi et al., 2020]. Finally, **Physics-informed neural networks** are networks that embed the physics of the problem in an internal layer, forcing the solution to satisfy the governing equations. One example is [Guo et al., 2022], where a forward solver using Green's function is embedded in the layers of the neural network.

For further details in review of deep learning applications to inverse scattering problems, we refer to [Chen et al., 2020].

As a final remark, it is important also to notice that most of the proposed neural networks produce as output an image that should be a mask to the position of the obstacle. In this way, theresult is similar to the one of sampling methods, while decomposition, Newton-type and hybrid methods between both look for the boundary opf the obstacle. Therefore, while the latter three need usually o0nly one incident wave and look for a boundary, they are involved in less dimensionality and complexity than sampling and machine learning approaches.

5.7 Models for inhomogeneous mediums

Until now, we considered the inverse scattering problem for an impenetrable obstacle, but in medical imaging one should assume that the obstacle is penetrable. Therefore we will briefly say some words on this, just to gist the possibility of modelling, and leaving numerical methods and theoretical results out of this text. In this way, instead of considering an obstacle, the goal is now to recover properties of an inhomogeneopus medium.

We consider the Helmholtz equation in a inhomogeneous medium, that is,

$$\Delta u(x) + k^2 n(x) u(x) = 0, \quad n \in \mathbb{R}^m \tag{5.67}$$

where the **refractive index** $n(x)$ at a point $x \in \mathbb{R}^m$ is defined by square of the ratio between the speed of sound c_0 in the background and the at the point x, that is

$$n(x) = \left(\frac{c_0}{c(x)} \right)^2 .$$

and we assume that $1 - n$ has compact support. In the case that n is piecewise continuous and the scattered field u^s satisfies the Sommerfeld radiation condition (5.4), then the model for the total field $u = u^i + u^s$ is given by the **Lippmann-Schwinger equation**

$$u(x) = u^i(x) - k^2 \int_{\mathbb{R}^m} \Phi(x, y)(1 - n(y))u(y)dy. \tag{5.68}$$

For more details on this problem we refer to [Colton and Kress, 2019, Cha.8].

If, on the other hand, the inhomogeneous medium is due to a different homogeneous medium inside the domain D with wave number k_1, then the problem might be modelled by a transmission boundary condition as

$$\begin{aligned} \Delta u + k^2 u = 0 \quad & \text{in } \mathbb{R}^m \backslash \overline{D} \\ \Delta u_1 + k_1^2 u_1 = 0 \quad & \text{in } D \\ Bu = Bu_1 \quad & \text{in } \partial D \end{aligned}$$

where B is an appropriate differential operator related with the boundary condition (usually a vector differential operator with two components, for one Dirichlet- and one Neumann-type boundary condition), the exterior total field u is defined by $u = u^i + u^s$ and u^s satisfies the Sommerfeld radiation condition (5.4). Note that in this case there are two unknown fields, namely the exterior scattered field u^s and the interior field u_1. More details on this topic can be checked, for instance, in [Yan, 2002].

Index

Bibliography

[Alessandrini and Rondi, 2005] Alessandrini, G. and Rondi, L. (2005). Determining a sound-soft polyhedral scatterer by a single far field measurement. *Proc. Amer. Math. Soc.*, 133:1685–1691.

[Alves, 2009] Alves, C. J. (2009). On the choice of source points in the method of fundamental solutions. *Engineering Analysis with Boundary Elements*, 33(12):1348 – 1361. Special Issue on the Method of Fundamental Solutions in honour of Professor Michael Golberg.

[Ammari, 2011] Ammari, H. (2011). *Mathematical Modeling in Biomedical Imaging II: Optical, Ultrasound, and Opto-Acoustic Tomographies*, volume 2035. Springer Science & Business Media.

[Anton, 1999] Anton, H. (1999). *Cálculo: um novo horizonte*. Bookman, 6^aEd.

[António et al., 2008] António, J., Tadeu, A., and Godinho, L. (2008). A three-dimensional acoustics model using the method of fundamental solutions. *Engineering Analysis with Boundary Elements*, 32(6):525 – 531. Meshless MethodsMeshless Methods.

[Antunes, 2022] Antunes, P. R. S. (2022). A well-conditioned method of fundamental solutions for laplace equation. *Numer Algor*, 91:1381–1405.

[Antunes et al., 2024] Antunes, P. R. S., Calunga, H., and Serranho, P. (2024). Improving the conditioning of the method of fundamental solutions for the helmholtz equation on domains in polar or elliptic coordinates. *Applied Mathematics and Computation*, 482:128969.

[Antunes et al., 2025] Antunes, P. R. S., Santos, V., and Serranho, P. (2025). The mfs-svd method for the laplace equation in three dimensions. *SIAM Journal on Scientific Computing*, 47(1):A454–A471.

[Araújo and Serranho, 2019] Araújo, A. and Serranho, P. (2019). On the use of quasi-equidistant source points over the sphere surface for the method of fundamental solutions. *Journal of Computational and Applied Mathematics*, 359:55 – 68.

[Barnett and Betcke, 2008] Barnett, A. and Betcke, T. (2008). Stability and convergence of the method of fundamental solutions for helmholtz problems on analytic domains. *Journal of Computational Physics*, 227(14):7003 – 7026.

[Bass, 2013] Bass, R. F. (2013). *Real Analysis for Graduate students*. second edition edition.

[Cakoni and Colton, 2004] Cakoni, F. and Colton, D. (2004). The determination of the surface impedance of a partially coated obstacle from far-field data. *SIAM J. Appl. Math.*, 64:709–723.

[Cakoni and Colton, 2006] Cakoni, F. and Colton, D. (2006). *Qualitative methods in inverse scattering theory*. Springer, Berlin.

[Chen et al., 2023] Chen, C., Noorizadegan, A., Young, D., and Chen, C.-S. (2023). On the determination of locating the source points of the mfs using effective condition number. *Journal of Computational and Applied Mathematics*, 423:114955.

[Chen et al., 2020] Chen, X., Wei, Z., Li, M., and Rocca, P. (2020). A review of deep learning approaches for inverse scattering problems. *Progress In Electromagnetics Research*, 167:67–81.

[Cheng and Yamamoto, 2003] Cheng, J. and Yamamoto, M. (2003). Uniqueness in inverse scattering problem within non-trapping polygonal obstacles with at most two incoming waves. *Inverse Problems*, 19:1361–1384.

[Colton and Kirsch, 1996] Colton, D. and Kirsch, A. (1996). A simple method for solving inverse scattering problems in the resonance region. *Inverse problems*, 12:383–393.

[Colton and Kress, 1983] Colton, D. and Kress, R. (1983). *Integral Equation Methods in Scattering Theory*. Wiley, Chichester.

[Colton and Kress, 2006] Colton, D. and Kress, R. (2006). Using fundamental solutions in inverse scattering theory. *Inverse Problems*, 22:285–299.

[Colton and Kress, 2013] Colton, D. and Kress, R. (2013). *Integral Equation Methods in Scattering Theory*. Society for Industrial and Applied Mathematics, Philadelphia, PA.

[Colton and Kress, 2019] Colton, D. and Kress, R. (2019). *Inverse Acoustic and Electromagnetic Scattering Theory*. Springer, 4^{th} edition edition.

[Colton and Sleeman, 1983] Colton, D. and Sleeman, B. (1983). Uniqueness theorems for the inverse problem of acoustic scattering. *IMA J. Appl. Math.*, 31:253–259.

[Elschner and Hu, 2011] Elschner, J. and Hu, G. (2011). Uniqueness in inverse transmission scattering problems for multilayered obstacles. *Inverse Problems and Imaging*, 5(4):793–813.

[Fairweather et al., 2003] Fairweather, G., Karageorghis, A., and Martin, P. (2003). The method of fundamental solutions for scattering and radiation problems. *Engineering Analysis with Boundary Elements*, 27(7):759 – 769. Special issue on Acoustics.

[Ferreira, 1995] Ferreira, J. C. (1995). *Introdução à Análise Real*. Fundação Calouste Gulbenkian.

[Gilbarg and Trudinger, 1998] Gilbarg, D. and Trudinger, N. (1998). *Elliptic partial differential equations of second order*. Springer, Berlin, 2^{nd} edition.

[Gintides, 2005] Gintides, D. (2005). Local uniqueness for the inverse scattering problem in acoustics via the faber-krahn inequality. *Inverse Problems*, 21:1195–1205.

[Grinberg, 2004] Grinberg, N. (2004). *Factorization Method in Inverse Obstacle Scattering*. Habilitation Thesis, Karlsruhe.

[Guo et al., 2022] Guo, R., Lin, Z., Shan, T., Song, X., Li, M., Yang, F., Xu, S., and Abubakar, A. (2022). Physics embedded deep neural network for solving full-wave inverse scattering problems. *IEEE Transactions on Antennas and Propagation*, 70(8):6148–6159.

[Hadamard, 1952] Hadamard, J. (1952). *Lectures on Cauchy's Problems in Linear Partial Differential Equations*. Dover, New York.

[Hettlich, 1998] Hettlich, F. (1995, (erratum, Inverse Problems 14, 204-210, 1998)). Fréchet derivatives in inverse obstacle scattering. *Inverse problems*, 11:371–382.

[Hettlich, 1999] Hettlich, F. (1999). *The Domain derivative in Inverse Obstacle Problems*. Habilitation Thesis.

[Hohage, 1997] Hohage, T. (1997). Logarithmic convergence rates of the iteratively regularized Gauss-Newton method for an inverse potential and an inverse scattering problem. *Inverse Problems*, 13:1279–1299.

[Hohage, 1998] Hohage, T. (1998). Convergence rates of a regularized newton method in sound-hard inverse scattering. *SIAM J. Numer. Anal.*, 36:125–142.

[Hohage, 1999] Hohage, T. (1999). *Iterative Methods in Inverse Obstacle Scattering: Regularization Theory of Linear and Non-Linear Exponentially Ill-posed Problems*. Dissertation, Linz.

[Ikehata, 1998] Ikehata, M. (1998). Reconstruction of an obstacle from the scattering amplitude at a fixed frequency. *Inverse Problems*, 14:949–954.

[Isakov, 1998] Isakov, V. (1998). *Inverse Problems for Partial Differential Equations*. Springer-Verlag, New York.

[Ivanyshyn et al., 2010] Ivanyshyn, O., Kress, R., and Serranho, P. (2010). Huygens' principle and iterative methods in inverse obstacle scattering. *Advances in Computational Mathematics*, 3:413–429.

[Khoo and Ying, 2019] Khoo, Y. and Ying, L. (2019). Switchnet: A neural network model for forward and inverse scattering problems. *SIAM Journal on Scientific Computing*, 41(5):A3182–A3201.

[Kincaid and Cheney, 2009] Kincaid, D. and Cheney, W. (2009). *Numerical analysis - Mathematics of Scientific Computing*, volume 2 of *Pure and Mathematics Undergraduate Texts*. American Mathemtics Society, 3^{rd} ed.

[Kirsch, 1989] Kirsch, A. (1989). Surface gradients and continuity properties for some integral operators in classical scattering theory. *Math. Methods Appl. Sci.*, 11 (no. 6):789–804.

[Kirsch, 1998] Kirsch, A. (1998). Characterization of the scattering obstacle by the spectral data of the far field operator. *Inverse Problems*, 14:1489–1512.

[Kirsch and Kress, 1986] Kirsch, A. and Kress, R. (1986). On an integral equation of the first kind in inverse acoustic scattering. *Inverse Problems (Cannon and Hornung, eds.), ISNM*, 77:93–102.

[Kirsch and Kress, 1987a] Kirsch, A. and Kress, R. (1987a). A numerical method for an inverse scattering problem. *(Engl and Groetsch, eds.), Academic Press, Orlando,*, pages 279–290.

[Kirsch and Kress, 1987b] Kirsch, A. and Kress, R. (1987b). An optimization method in inverse acoustic scattering. *Boundary Elements IX, Vol.3 Fluid Flow and Potential Applications (Brebbia et al., eds), Springer Verlag, Berlin Heidelberg New York*, pages 3–18.

[Kirsch and Kress, 1993] Kirsch, A. and Kress, R. (1993). Uniqueness in inverse obstacle scattering. *Inverse Problems*, 9:285–299.

[Kress, 1985] Kress, R. (1985). Minimizing the condition number of boundary integral operators in acoustic and electromagnetic scattering. *Quart. J. Mech. Appl. Math.*, 38:323–341.

[Kress, 1995] Kress, R. (1995). On the numerical solution of a hypersingular integral equation in scattering theory. *J. Comp. Appl. Math.*, 61:345–360.

[Kress, 1998] Kress, R. (1998). *Numerical Analysis*. Springer.

[Kress, 1999] Kress, R. (1999). *Linear Integral Equations*. Springer.

[Kress, 2003] Kress, R. (2003). Newton's method for inverse obstacle scattering meets the method of least squares. *Inverse Problems*, 19:91–104.

[Kress, 2005] Kress, R. (2005). Tomographie. Lecture Notes.

[Kress, 2007] Kress, R. (2007). Uniqueness and numerical methods in inverse obstacle scattering. *Journal of Physics: Conference Series*, 73(1):012003.

[Kress and Rundell, 2001] Kress, R. and Rundell, W. (2001). Inverse scattering for shape and impedance. *Inverse problems*, 17:1075–1085.

[Kress and Serranho, 2005] Kress, R. and Serranho, P. (2005). A hybrid method for two-dimensional crack reconstruction. *Inverse Problems*, 21:773–784.

[Kress and Serranho, 2007] Kress, R. and Serranho, P. (2007). A hybrid method for sound-hard obstacle reconstruction. *Journal of Computational and Applied Mathematics*, 204:418–427.

[Kussmaul, 1969] Kussmaul, R. (1969). Ein numerisches Verfahren zur Lösung des Neumannschen Aussenraumproblems für die Helmholtzsche Schwingungsgleichung. *Computing*, 4:246–273.

[Lax and Philips, 1967] Lax, P. and Philips, L. (1967). *Scattering Theory*. Academic Press, London.

[Leis, 1986] Leis, R. (1986). *Initial Boundary Value Problems in Mathematical Physics*. John Wiley, New York.

[Levine, 1964] Levine, L. (1964). A uniqueness theorem for the reduced wave equation. *Comm. Pure Appl. Math.*, 17:147–176.

[Liu, 1997] Liu, C. (1997). Inverse obstacle problem: local uniqueness for rougher obstacles ans the identification of a ball. *Inverse Problems*, 13:1063–1069.

[Louis, 2006] Louis, A. K. (2006). Developments of algorithms in computerized tomography. In *Proceedings of Symposia in Applied Mathematics*, volume 63, pages 25–42.

[Ma and Hu, 2021] Ma, G. and Hu, G. (2021). Factorization method with one plane wave: from model-driven and data-driven perspectives. *Inverse Problems*, 38(1):015003.

[Magalhães, 1997] Magalhães, L. T. (1997). *Álgebra linear como introdução a Matemática Aplicada*. Texto editora, 7^a ed.

[Martensen, 1963] Martensen, E. (1963). Über eine Methode zum räumlichen Neumannschen Problem mit einer Anwendung für torursartige Berandungen. *Acta Math.*, 109:75–135.

[McLean, 2000] McLean, W. (2000). *Strongly Elliptic Systems and Boundary Integral Equations*. Cambridge University Press.

[Meng et al., 2020] Meng, P., Su, L., Yin, W., and Zhang, S. (2020). Solving a kind of inverse scattering problem of acoustic waves based on linear sampling method and neural network. *Alexandria Engineering Journal*, 59(3):1451–1462. A Special Section on: Computational Methods in Engineering and Artificial Intelligence.

[Natterer, 2001] Natterer, F. (2001). *The Mathematics of Computerized Tomography*. Classics in Applied Mathematics. SIAM.

[Potthast, 1996] Potthast, R. (1996). Fréchet differentiability of the solution to the acoustic neumann scattering problem with respect to the domain. *J. Inverse Ill-posed Prob.*, 4:67–84.

[Potthast, 1998] Potthast, R. (1998). A point source method for inverse acoustic and electromagnetic obstacle scattering problems. *IMA J. Appl. Math.*, 61, no.2:119–140.

[Potthast, 2001] Potthast, R. (2001). On the convergence of a new newton-type method in inverse scattering. *Inverse Problems*, 17:1419–1434.

[Potthast, 2005] Potthast, R. (2005). Sampling and probe methods - an algorithmical review. *Computing*, 75:215–235.

[Potthast and Schulz, 2007] Potthast, R. and Schulz, J. (2007). A multiwave range test for obstacle reconstructions with unknown physical properties. *Journal of Computational and Applied Mathematics*, 205:53–71.

[Sanghvi et al., 2020] Sanghvi, Y., Kalepu, Y., and Khankhoje, U. K. (2020). Embedding deep learning in inverse scattering problems. *IEEE Transactions on Computational Imaging*, 6:46–56.

[Schaback, 1995] Schaback, R. (1995). Error estimates and condition numbers for radial basis function interpolation. *Adv Comput Math*, 3:251–264.

[Schechter, 2001] Schechter, M. (2001). *Principles of Functional Analysis*, volume 36 of *Graduate Studies in Mathematics*. American Mathematics Society, 2^{nd} ed.

[Serranho, 2006] Serranho, P. (2006). A hybrid method for inverse scattering for shape and impedance. *Inverse Problems*, 22:663–680.

[Serranho, 2007a] Serranho, P. (2007a). *A hybrid method for inverse obstacle scattering problems*. PhD thesis, Georg-August Universität, Göttingen, Germany.

[Serranho, 2007b] Serranho, P. (2007b). A hybrid method for inverse scattering for sound-soft obstacles in 3D. *Inverse Problems and Imaging*, 4:691–712.

[Smyrlis, 2009] Smyrlis, Y.-S. (2009). Applicability and applications of the method of fundamental solutions. *Mathematics of Computation*, 78(267):1399–1434.

[Smyrlis and Karageorghis, 2009] Smyrlis, Y.-S. and Karageorghis, A. (2009). Efficient implementation of the mfs: The three scenarios. *Journal of Computational and Applied Mathematics*, 227(1):83 – 92. Special Issue of Proceedings of {NUMAN} 2007 Conference: Recent Approaches to Numerical Analysis: Theory, Methods and Applications.

[Sommerfeld, 1967] Sommerfeld, A. (1949 (fifth printing, 1967)). *Partial Differential Equations in Physics*. Academic Press, New York.

[Spanier and Oldham, 1987] Spanier, J. and Oldham, K. B. (1987). *An Atlas of Functions*. Washington, DC: Hemisphere.

[Sun et al., 2019] Sun, F., Zhang, D., and Guo, Y. (2019). Uniqueness in phaseless inverse scattering problems with known superposition of incident point sources. *Inverse Problems*, 35(10):105007.

[Xu et al., 2020] Xu, K., Wu, L., Ye, X., and Chen, X. (2020). Deep learning-based inversion methods for solving inverse scattering problems with phaseless data. *IEEE Transactions on Antennas and Propagation*, 68(11):7457–7470.

[Yan, 2002] Yan, G. (2002). Inverse scattering for transmission problem. *Computers & Mathematics with Applications*, 44(3-4):439 – 444.

[Yang and Liu, 2020] Yang, H. and Liu, J. (2020). A qualitative deep learning method for inverse scattering problems. *The Applied Computational Electromagnetics Society Journal (ACES)*, 35(2):153–160.